THE UNIVERSITY OF CALGARY

THE RATES AND REGULATION OF INSENSIBLE PERSPIRATION

by

Darren Wai-hong Koon

A THESIS

SUBMITTED TO THE FACULTY OF GRADUATE STUDIES

IN PARTIAL FULFILLMENT OF THE REQUIREMENTS FOR THE

DEGREE OF MASTER OF SCIENCE

DEPARTMENT OF CHEMICAL AND PETROLEUM ENGINEERING

CALGARY, ALBERTA

AUGUST, 1987

ISBN 0-315-38019-5

THE UNIVERSITY OF CALGARY

FACULTY OF GRADUATE STUDIES

The undersigned certify that they have read, and recommend to the Faculty of Graduate Studies for acceptance, a thesis entitled,

THE RATES AND REGULATION OF INSENSIBLE PERSPIRATION

submitted by Darren Wai-Hong Koon in partial fulfillment of the requirements for the degree of Master of Science in Engineering

Dr. A.A. Jeje, Supervisor/Committee Chairman
Department of Chemical and Petroleum Engineering

Dr. L.A. Behie
Department of Chemical and Petroleum Engineering

Dr. A. Hastaoglu
Department of Chemical & Petroleum Engineering

Dr. C. Frank
Department of Surgery, Faculty of Medicine

26 August 1987

date

ABSTRACT

A human being comfortably at rest loses water continuously to the ambient through the skin which is dry to the eye and to touch. This phenomenon is termed "insensible perspiration". Such water withdrawn from the body could traverse the skin along two possible pathways. In one scheme, liquid water diffuses across the avascular epidermis and evaporates from the scaly outer layers of the stratum corneum. Such migration would encounter very high diffusional resistances (D_{AB} $\approx 5\times10^{-14} m^2/s$) but the surface area available for moisture exchange with the ambient is large, $\approx 1.8\ m^2$. In the second scheme, water is evaporated from the free surfaces of columns of sweat liquids perpetually present in the ducts of eccrine glands. Such sweat is retracted below the skin surface in the normal resting state. The flux of water vapor encounters low diffusional resistances ($D_{AB} \approx 3\times10^{-4} m^2/s$) but the total cross-sectional area available in the pores is small, $\approx 0.01\ m^2$. The rates of water loss by this scheme would be regulated by conditions external and internal to the skin. Anatomical and physiological data have been introduced into a mathematical analysis to determine that insensible perspiration occurs primarily by the second scheme. Anatomical features of the eccrine sweat duct are found to participate in the regulation of cutaneous water loss. The water loss rates were calculated to be between 1 and 150 g/hr ($\approx 2.8\times10^{-7}$ to 4.2×10^{-5} kg/s) and this compares favorably with experimental values reported in the literature normally in the 1 to 90 g/hr ($\approx 2.8\times10^{-7}$ to 2.5×10^{-5} kg/s) range.

ACKNOWLEDGEMENTS

The author wishes to acknowledge and express his gratitude to the many individuals who have contributed to his work, namely:

His supervisor, Dr. A.A. Jeje, for his continuous support, guidance, encouragement and supervision throughout the entire course of this study without which the author could not have finished.

Mr. Wladyslaw Wozniak for some invaluable discussions throughout the course of this work.

Mr. Andrew Ji for providing technical assistance in some of the drawings in this thesis.

The Natural Sciences and Engineering Research Council of Canada and the Department of Chemical and Petroleum Engineering at the University of Calgary for providing grants to this study.

The author wishes to dedicate this thesis to his parents and Winnie, for their continuous support, confidence, patience, encouragement and understanding throughout the entire course of this study.

TABLE OF CONTENTS

Chapter	Description	Page
	Abstract	iii
	Acknowledgements	iv
	Table of Contents	v
	List of Figures	vii
	List of Tables	ix
	List of Symbols	x
1	INTRODUCTION	1
1.1	Scope of work	5
2	ANATOMY AND PHYSIOLOGY OF THE HUMAN SKIN	6
2.1	Introduction	6
2.2	The Epidermis	9
2.3	The Dermis	11
2.4	Eccrine Sweat Glands	12
2.5	Sweat Composition	18
2.6	The Skin Blood Circulation	20
2.6.1	Tissue Temperature Profiles	21
3	LITERATURE REVIEW	25
3.1	Rates of Insensible Perspiration	26
3.1.1	Methods and Apparatus	26
3.1.2	Total Rates	28
3.1.3	Site Variation	30
3.2	Contributing Factors	34
3.2.1	Internal Factors	34

3.2.2	External Factors	36
3.3	Insensible Sweating vs Transepidermal Water Loss	40
3.4	Characteristics of the Stratum Corneum	44
4	MODELLING AND ANALYSIS	48
4.1	Introduction	48
4.2	Anatomic and Physiological Considerations	50
4.3	Material Balances	54
4.3.1	Case with meniscus retracted but microvilli submerged in liquid	54
4.3.2	Case with microvilli exposed to gases	58
4.4	The Temperature Profile along the Eccrine Duct	60
4.5	Case with meniscus displaced to the skin surface	64
4.5.1	Boundary condition at the surface of the stratum corneum	69
5	RESULTS	76
5.1	Case of sweat liquid withdrawn below the skin surface	76
5.1.1	The basis for elevated temperatures and vapor pressures at retracted meniscus surface	85
5.2	Case for meniscus at pore rim	91
6	DISCUSSION	100
7	CONCLUSIONS	107
8	RECOMMENDATIONS	109
	REFERENCES	111
	APPENDIX A	127
	APPENDIX B	139

LIST OF FIGURES

Figure	Description	Page
2.1	A Three-dimensional Illustration of Human Skin Layers	7
2.2	Schematic diagram of an eccrine sweat gland in the cutaneous layers	13
2.3	Local tissue temperature minus skin surface temperature in the superficial 10 mm layer of the forearm	22
2.4	Temperature profiles from the skin surface into the core for the forearm and the thigh	24
4.1	Schematic diagram showing the model for the case when the meniscus is retracted into the ecrine duct with microvilli submerged	55
4.2	Comparison between an experimental data curve of Bazett and McGlone (1927) and its best fit curve using polynomial regression	63
4.3	Schematic diagram showing the model for the case when the meniscus is displaced to the skin surface	65
4.4	Density of stratum corneum vs. mass fraction of water in stratum corneum	71
4.5	Diffusivity of water in stratum corneum vs. mass fraction of water in stratum corneum	72
4.6	Mass fraction of water in stratum corneum vs. mole fraction of water vapor in ambient	75
5.1	Concentration profiles for water vapor in the helical duct of an eccrine gland	77

5.2	Estimated rates of water loss from 3 million eccrine sweat glands vs. the location of meniscus along the helical duct from the dermo-epidermal boundary	80
5.3	Estimated rates of water loss from 3 million eccrine sweat glands vs. mole fraction of water vapor in ambient	81
5.4	Estimated rates of water loss from 3 million eccrine sweat glands vs. straight duct radius	83
5.5	Estimated rates of water loss from 3 million eccrine sweat glands vs. pore mouth radius	84
5.6	Profiles of mix-cup temperatures of the blood flowing through a 50 μm diameter arteriole adjacent to the straight intradermal eccrine sweat duct in the forearm	89
5.7	Estimated rates of water loss from 3 million eccrine sweat glands vs. mole fraction of water vapor in ambient when the meniscus is displaced to the skin surface	95
5.8	Estimated rates of water loss from 3 million eccrine sweat glands vs. skin surface temperature when the meniscus is displaced to the skin surface	96
5.9	Estimated rates of water loss from 3 million eccrine sweat glands vs. pore mouth radius when the meniscus is displaced to the skin surface	98
5.10	Estimated rates of water loss from 3 million eccrine sweat glands vs. stratum corneum thickness when the meniscus is displaced to the skin surface	99
6.1	Radial concentration profiles of water in stratum corneum	104
B.1	Schematic diagram illustrating the treatment of irregular boundaries in discretization	142

LIST OF TABLES

Table	Description	Page
2.1	A comparison of the average chemical compositions of blood plasma and sweat	19
5.1	Comparison of results using different mesh sizes for the temperature profile along an eccrine duct	88
5.2	Comparison of results using different mesh sizes for the case when the meniscus is at pore rim	93
A.1	Vapor pressure of liquid water	138

LIST OF SYMBOLS

Symbol	Description
A	Area, m^2
Bi	Biot number ($h_w r_w$/k), dimensionless
Cp	Heat capacity, kJ/kgK
D	Diffusivity, m^2/s
Fx	Function as defined in equation (4.11)
H	Height, m
L	Length of intra-epidermal eccrine duct, m
MW	Molecular weight, g/mole
N	Molar flux, mole/m^2s
P	Pressure, mmHg
Pr	Prandtl number (μCp/k), dimensionless
Q	Mass rate, g/hr
R	Universal gas constant, mmHg-m^3/K
Re	Reynolds' number ($2r_w$ρu/μ), dimensionless
S	Surface area, m^2

T	Temperature, °C
V	Volume, m^3
X	Discretized form of mole fraction x, dimensionless
Z	Stratum corneum thickness, m
c	Concentration, mole/m^3
h	Heat transfer coefficient, W/m^2K
k	Thermal conductivity, W/mK
n	Molar flux, mole/m^2s
r	Radius, m
u	Velocity, m/s
x	Mole fraction, dimensionless
z	Distance, m

Subscripts

A	Water
B	Air
L	Liquid
b	Bulk

e	Entrance
m	Microvilli
o	Initial
pr	Pore
s	Skin surface
sc	Stratum corneum
t	Tissue
v	Vapor
w	Wall

Greek Symbols

Θ	Dimensionless temperature as defined in equation (4.17)
Ψ	Transformed variable as defined in equation (4.6)
Γ	Transformed variable as defined in equation (4.7)
α	Transformed co-ordinate as defined in equation (4.27)
β	Transformed co-ordinate as defined in equation (4.26)
γ	Lumen divergence ratio (r_s/r_o), dimensionless
κ	Relaxation factor, dimensionless

μ	Viscosity, cp
ν	Thermal diffusivity, m^2/s
ρ	Density, g/m^3
σ	Surface tension, N/m
ω	Mass fraction, dimensionless

CHAPTER ONE

INTRODUCTION

A human being comfortably at rest loses water continuously at low but measurable rates to the ambient through the skin which is dry to the eye and to touch. This phenomenon has been termed "insensible perspiration". The rates are quoted by different investigators at between 100 and 700 g/day (Kuno, 1956; Lamke et al., 1977; Grice, 1980). Quantitative measurements of such water loss rates date back to 1614 when Sanctorius made records of his own loss of weight over a period of 30 years (Benedict and Root, 1926)! The continuous efflux of water through the skin and in exhalations contributes to the regulation of heat exchange between an individual and the environment. The regulation of water and heat losses through the skin is important, especially for newborn infants, such that the body core temperature is maintained (Hammarlund et al., 1977; Stromberg et al., 1983; Fitch and Korones, 1984). Losses from the palms and soles are significantly higher than from the other surfaces of the skin and the moistness may enhance gripping to surfaces during locomotion and in holding objects. Measurements of the water loss rates have been applied to predict basal metabolic rates (Wiley and Newburgh, 1931; Hardy et al., 1941).

There are two possible pathways by which the water lost in insensible perspiration could traverse the cutaneous layers. Liquid water could diffuse across the

layers of the skin with varying degrees of consolidation and permeability and evaporate from the surfaces exposed to the ambient air. This process is termed "transepidermal water loss". Such migrating water would be bound within tissues. Free liquid water is not expected to infiltrate any pore spaces between these cells. The diffusive resistances are high since D_{AB} has been estimated at $\approx 5\times10^{-14} m^2/s$ (Blank et al., 1984) across the skin layers but the surface area available is large ($\approx 1.8 m^2$). The principal barrier has been suggested to be at the inner layer of the stratum corneum. Considerably more water is lost when this barrier is disrupted such as observed for burn victims or when the skin has diseases (Sodeman and Burch, 1944; Moserova and Behounkova-Houskova, 1979a, 1979b). The second pathway involves the direct evaporation of water or sweat which is retracted into the eccrine sweat ducts below the skin surface. Low resistances are encountered for vapor fluxes in air ($D_{AB} \approx 5\times10^{-4} m^2/s$) but the total cross-sectional area available for diffusion through all such glands at the skin surface is small ($\approx 0.01 m^2$). Kuno (1956) speculated that, since the total of the pore mouth cross-sectional area of all the eccrine glands is so small ($\leq 1\%$ of the total body surface), the water fluxes through would be insignificant. Consequently, this pathway is often discounted even though the rates of diffusion of water within the eccrine ducts may be orders of magnitude higher than through the "solid" tissues, because of the vastly different diffusional resistances.

Experimental studies have generally been focused on measuring rates of water loss from small areas of skin, both *in vivo* (Albert and Palmes, 1951; Nilsson, 1977),

and *in vitro* (Berenson and Burch, 1951; Blank, 1953; Buettner, 1959), or from the entire body surface (Benedict and Root, 1926; Kuno, 1956) under various ambient conditions. Empirical expressions have been derived in an effort to relate water loss fluxes with parameters such as skin surface temperature, ambient water vapor concentration, or ambient temperature (Goodman and Wolf, 1969; Kerslake, 1972). In addition, lumped or bulk transport properties for the multi-layered skin such as diffusion coefficients or permeability constants are reported (Scheuplein, 1978; Blank et al., 1984). Such correlations however, do not shed light on the actual mechanisms for insensible water loss. An argument often advanced by proponents of transepidermal perspiration is that subjects afflicted with "hereditary anhidrotic ectodermal dysplasia", the congenital absence of sweat glands, continue to lose water at rates comparable to normal subjects (Sunderman, 1941; Upshaw and Montgomery, 1949). Similar water loss rates were also observed for subjects with their sweat glands "inactivated" by a cholinergic agent (Pinson, 1942). For such observations, it was neither established that the skin anatomy for subjects without the glands were similar to those for normal subjects, nor was it demonstrated that the activity of the secretory part of sweat glands were suppressed by chemical agents to rates below that required to sustain insensible water loss. Variations in the anatomy of the skin could accompany different genetic expressions for the rare cases of the absence of sweat glands.

Sweat secretion by eccrine glands has primarily been investigated for the frequencies of faradic stimulation required and the response times for sweat droplets to

appear at the skin surface. The changes in the electrical conductance of the skin during stimulation has also been of interest (Lloyd, 1961; Adams and Vaughan, 1965; Adams, 1966; Bullard, 1971; Holmes and Adams, 1975). The electrical conductance would be proportional to the water content of the stratum corneum since water is the carrier for ions within the tissue. The water content of the layer changes as it absorbs some of the sweat liquids secreted to the skin surface.

Many apparently normally-formed eccrine glands are unable to produce sweat droplets when thermal, faradic, pharmaceutical or mental stress stimuli are applied (Kuno, 1956). These may constitute half of all the glands (Montagna and Parakkal, 1974). Such glands may have limited secretory ability but would be able to participate in insensible water loss. Some other anatomical and physiological observations on the skin tissues and the eccrine glands have also yet to be related to insensible perspiration (Jeje and Koon, 1987). These include the gradients of temperature within the skin (Bazett and McGlone, 1927), and the endowment of the straight (dermal) portion of the eccrine duct with a special arteriolar plexus, the presence of microvillous processes on the periductal surface of the intra-epidermal coil within the stratum spinosum, and the increase in the diameter and the cross-sectional area of the lumen of the intra-epidermal coil towards the skin surface.

1.1. Scope of Work

The present investigation is on the contribution of eccrine sweat glands to insensible perspiration. A physical model which involves direct evaporation of sweat from a meniscus retracted below the skin surface, lateral dispersion of water within the duct into the keratinized cells of the stratum corneum, and generation of super-saturated vapor in the duct unit in the neighbourhood of microvilli on the periductal wall has been proposed to describe water vapor transport through an eccrine sweat duct unit (Jeje, 1987; Jeje and Koon, 1987). The effects of changes in ambient conditions such as the air humidity and the temperature on the loss of water vapor from the eccrine duct are incorporated. The aim is to provide generalizations on the significance of the various structural and physiological factors of the skin and the ambient conditions on the rate of insensible water loss. Results from the analysis are used to evaluate gross insensible loss rates for all the eccrine sweat glands in the skin such that comparisons can be made with the overall rates reported in the literature.

In the following, the anatomy and physiology of the human skin will be briefly reviewed, the literature on insensible water loss discussed and the model for the current work presented.

CHAPTER TWO

ANATOMY AND PHYSIOLOGY OF THE HUMAN SKIN

2.1. Introduction

The skin constitutes the body's outer protective covering against microbial invasion and serves as a physical barrier to a rapid loss of water and heat from the body into the environment. Its epithelium is continuous with that of external orifices, i.e. the digestive, respiratory, urinogenital systems, the smaller-scale pilary system and the microscopic sebaceous and sweat glands. The skin is highly vascularized, innervated and endowed with glands for the secretion of sweat, sebum, salts and organic substances. The sweat producing organs are uniquely adapted to the thermoregulatory demands of the organism. Part of the extensive neuroreceptor network serves in transducing the sensations of hot and cold which result in copious production of visible sweat or alter the microvascular flows of blood to regulate the body temperature. A 1.7 m tall adult weighing 70 kg has a skin with a surface area, weight, and volume of approximately 1.8 m^2, 4 kg, and 3.6 litres respectively (Dubois and Dubois, 1916; Leider and Buncke, 1954).

A three-dimensional illustration of the human skin layers is presented in Figure 2.1 with almost all the normal features shown. The skin is typically divided into two parts, the epidermis and the dermis. The epidermis is a thin stratified epithelium. This avascular layer is about 50 to 150 μm thick, and the thickness

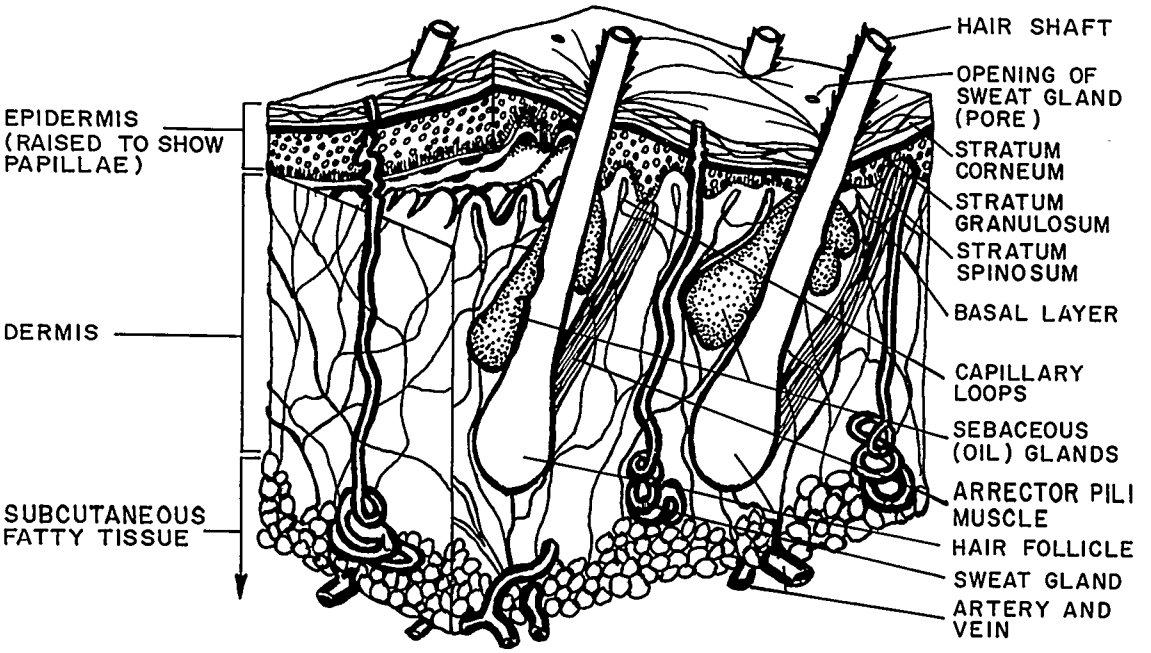

Figure 2.1 : A three-dimensional illustration of the human skin layers. The thickness of the epidermis and the dermis is usually less than 5 mm.

varies relatively little over most of the body except at the palms and soles where it is typically 0.4 to 0.6 mm. Underlying the epidermis is the much thicker layer of dense fibroelastic connective tissue called the dermis. The thickness varies between 1 mm at the palms to 4 mm at the dorsal surfaces of the trunk (Odland, 1983). The dermis has extensive vascular and nerve networks. Specialized secretory and excretory glands, and keratinized appendage structures (hair and nail) are embedded or supported in this tissue. Beneath the skin is the subcutaneous tissue, or hypodermis, which is composed of fatty connective tissue. Skeletal muscles are next in the sequence (Solomon and Davis, 1983).

The following brief description of the anatomy and physiology of skin layers is not exhaustive. It is primarily intended to provide the relevant details necessary for a description of the mechanisms by which water would be continuously lost by a human being at rest to the surrounding.

2.2. The Epidermis

The cells of the epithelial tissues originate primarily from the basal layer apposed to the dermis. After division, these cells migrate towards the surface and undergo physical and metabolic changes. The epidermis may be divided into an inner layer of viable cells, the stratum malpighii, and an outer layer of enucleate, dehydrated and dead horny cells, the stratum corneum. The stratum malpighii is further divided into several sub-layers : the one-cell deep cuboidal or columnar basal layer (stratum basale, or stratum germinativum), the prickle cell layer (stratum spinosum), the granular layer (stratum granulosum), and the stratum lucidum (Jarrett, 1973). The latter is not readily visible except in palmar and plantar epidermis. These sub-layers are not sharply demarcated anatomical entities and they tend to gradually merge into one another.

The columnal basal cells are arranged with their long axis perpendicular to the dermo-epidermal interface or junction. The cells are linked by intercellular cytoplasmic strands called "desmosomes" and are supported on a basement membrane which is only 0.5 to 1.0 μm thick. A tissue-free gap of 35 to 45 nm width, the basal lamina, lies between the membrane and the dermis (Lever and Lever, 1949).

The cells migrating away from the basal layer assume a polyhedral shape in the stratum spinosum of 5 to 10 cells layers. The cells differ from the basal cells both morphologically and histochemically. The morphological changes involve the flattening of the cell.

The one to two layers of cells of the stratum granulosum are anucleate and the cytoplasm contain particles of a basophilic material called "keratohyalin granules". The cells are flattened and exhibit hydrolytic activity consistent with a degradation of the cytoplasmic contents (Montagna and Parakkal, 1974).

The stratum corneum is the outermost layer of dead cells which continuously exfoliate at the surface. The flattened or squamous cells are keratinized to water-proof the body surface. The interstices between cells become progressively smaller at the deeper parts, and the intercellular space near the stratum granulosum is lipid filled. Each cell resembles a thin hexagonal plate, measuring approximately 25 μm in width and 0.5 μm in thickness (Treager, 1966). That is, in transit from the basal layer to surface, each cell increases its projected area by 25 times. The tangential stack of lamina has between 15 to 25 layers except in the palms and soles. The thickness of the stratum corneum varies over the body surface. It depends both on the number of cell layers and the degree of hydration. Estimates give an average thickness of 8 to 13 μm for the forearm, thigh, abdomen, and back (Holbrook and Odland, 1974). In the palms and soles, the thickness can range from 400 to 600 μm (Scheuplein, 1978).

2.3 The Dermis

The dermis is an irregular dense connective tissue composed mainly of fibrous proteins, namely collagen, elastin and reticulin embedded in an amorphous ground substance or interfibrillar gel. Fibroblasts are dispersed in this matrix. The ground substance is semi-fluid, and contains glycosaminoglycans, neutral heteropolysaccharides, proteins, soluble collagen, glycoproteins, inorganic salts, and water amongst other compounds and macromolecules.

The dermis may be divided into a superficial papillary layer and a deep reticular layer. The papillary layer is molded against the overlying epidermis and accordingly has surface contours of papillae and folds conforming to the basal epithelial ridges and grooves of the epidermis. The papillary dermis consists of loosely distributed fibres within the interfibrillar gel. Extensive networks of arterioles and capillaries in the papillae deliver oxygen and nutrients to the cells of the avascular epidermis. The reticular layer has more fibrillar matter densely arranged parallel to the skin surface.

2.4. Eccrine Sweat Glands

The eccrine sweat glands of man are widely distributed over the body surface. They are most numerous on the palm and sole, next on the head, and much less on the trunk and extremities (Kuno, 1956). Man has 2 to 5 million glands over the entire body surface, at an average of 145 to 339 per cm^2 (Kuno,1956). New ones are not formed after birth. The total number of glands differs among races (Montagna and Parakkal, 1974) but there is no significant variation between sexes (Szabo, 1962). The number that can be thermally activated is about 2.3 million, or 125 to 130 per cm^2 (Kuno, 1956).

An isolated eccrine sweat gland is schematically illustrated in Figure 2.2. Anatomically, eccrine sweat glands are simple tubes which extend from the surface of the skin to midway into the dermis or down to the hypodermis. Each tubule consists of an irregular and tightly coiled basal portion, a straight segment that extends from the coil to the epidermis, and a proximal coiled or spiral segment that lies within the epidermis. Half to two-thirds of the basal coil is involved with secretion and the remaining portion is part of the duct which is made up of 3 segments : a helical portion in the epidermis which is termed "the epidermal sweat duct unit", a straight portion traversing the dermis approximately normal to the skin surface, and the coiled basal portion (Montagna et al., 1962).

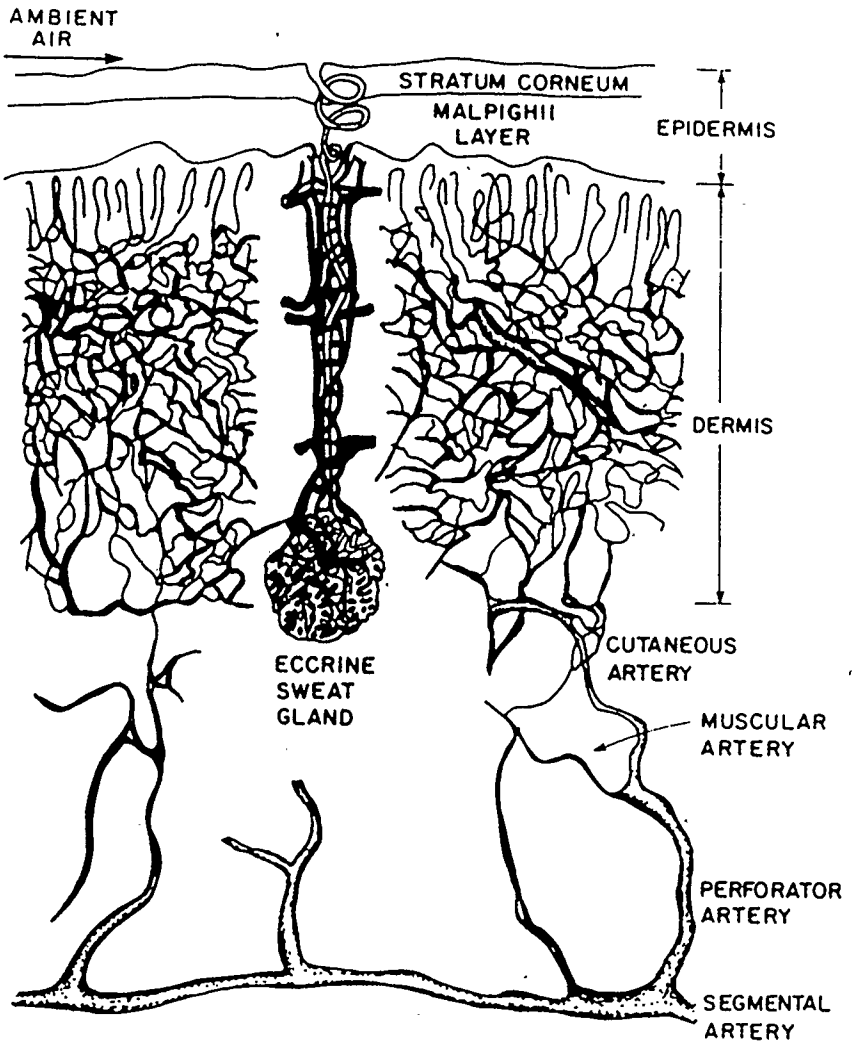

Figure 2.2 : Schematic diagram of an eccrine sweat gland in the cutaneous layers. The dermis is highly vascularized and surrounded by a plexus in the dermis only. The intraepidermal helical coil has a lumen lined with microvilli (not shown) near the dermo-epidermal boundary. The Malpighii layer includes the stratum spinosum, the basal cell layer, the stratum granulosum and the stratum lucidum.

The secretory coil is a blind sac composing of 3 distinct cell types : secretory (clear,serous), dark (mucoid), and myoepithelial cells. The length of the coil averages 3.3 mm, with an outer diameter of 47 μm (Sato and Sato, 1983) and a lumen diameter of 20 μm (Lever and Lever, 1949). It is enveloped by a basement membrane, which is a basal lamina with fine filaments and thin collagen fibres. The dark (mucous) cells contain cytoplasmic granules with a strong affinity for basic dyes (Montagna and Parakkal, 1974). They are small and their nuclei are frequently more towards the lumen (Hibbs, 1958). The dark cells may generate the glycoproteins in sweat.

The clear cells are larger and more abundant than the dark cells. They stain faintly or not at all with basic dyes and their nuclei are usually basally located. Where two or more serous cells abut, intercellular canaliculi are formed, averaging 1.5 μm in diameter (Hibbs, 1958). The canaliculi open directly into the lumen. The lateral borders of these serous cells are frequently infolded. Numerous villi projections from two neighbouring cells form an intercellular channel, which is open to the basal lamina. Desmosomes, gap junctions, and tight junctions occupy the luminal end. The serous cells contain abundant mitochondria and because of their resemblance to transporting epithelial cells, it is generally believed that the clear cells are responsible for the secretion of the sweat fluid and electrolytes into the coil lumen (Hashimoto, 1978).

Both serous and mucous cells rest upon an incomplete layer of myoepithelial cells which in turn rest upon the thick hyalin basement membrane. The myoepithelial cells are spindle shaped and filled with irregularly arranged bundles of myofilaments (Sato et al., 1979). Due to their contractile nature, myoepithelial cells are thought to supply the force which expels the sweat fluids into the lumen (Nicolaidis and Sivadjian, 1972; Randall, 1946). Sato et al.(1979), however, proposed that the myoepithelial cells provide only structural support for the secretory epithelium. This suggestion has been supported by Montgomery et al. (1984).

A short transitional zone lies between the single-layered secretory coil and the double-layered duct. The basement membrane becomes abruptly thin, remains inconspicous along the entire duct, and is continuous with the epidermal basal lamina (Sato and Sato, 1983). Myoepithelial cells are absent. Small, flat cells are often seen along the periphery and they are suspected to be the precursors of the basal cells in the duct (Hashimoto, 1978).

The coiled duct, or the proximal segment of the sweat duct, is composed of two layers: an inner layer of luminal cells and an outer layer of basal cells. The luminal cells have a hyalin cuticular border and bear numerous short microvilli on the luminal surface. The basal cells are cuboidal and its cytoplasm is usually slightly denser, and the mitochondria are larger and more numerous than the luminal cells (Hibbs, 1958). The lateral borders are frequently infolded, with desmosomes, gap junctions, and tight junctions present throughout the intercellular chan-

nels. The lumen of the duct varies between 10 to 20 μm in diameter (Holyoke and Lobitz, 1952) and the outer diameter averages 30 μm (Kuno, 1956). It is believed that reabsorption of components of the precursor sweat, primarily electrolytes, occurs mostly in this region of the duct.

The straight duct, or the distal portion of the sweat duct, is narrower than at any other location. It is composed of essentially the same cell types as in the coiled duct, namely a single layer of luminal cells and one or two layers of basal cells. The luminal cells are cuboidal and highly cuticularized. They contain fewer mitochondria and show less enzymatic (Na-K-ATPase) activity (Sato et al., 1971). These suggest that there is less active reabsorption than in the proximal or coiled duct.

The last segment of the eccrine sweat duct is the epidermal sweat duct unit. It consists of a spiral coil from the dermo-epidermal boundary to the skin surface. The spiral diameter and the lumen cross-sectional area increase outwards. The tightness of the helical coil appears inversely correlated to the thickness of the epidermis. Thus a thick epidermis contains widely spaced coils of near uniform radius while a thin epidermis may have 2 to 3 coils closely spaced but with increasingly larger loops. Essentially, the total length of the helical duct at any site may be independent of the epidermal thickness (Pinkus, 1939).

In the palms and soles, the duct opens to the surface through the ridges of the epidermis. The average diameter at the outlet of the ducts and the short region of funnel-like expansion at the surface are 15 μm and 72 μm respectively (Kuno,

1956). The duct is composed of a single inner layer of luminal cells and two or three rows of outer cells. These cells are derived from dermal duct cells through mitosis and upward migration (Lever and Lever, 1949). At the lower level of the epidermis, short microvilli cover the luminal surface of inner cells (Zelickson, 1961). The ductal cells begin to keratinize at a lower level than the cells of the surrounding epidermis and are fully keratinized at the level of the granular layer of the surrounding epidermis (Lever and Lever, 1949). This recessed keratinization of the ductal wall cells is advantageous to prevent a collapse of the terminal portion of the gland and the drying out of the glands under low humidity conditions (Lobitz et al., 1954).

2.5. Sweat Composition

Normal sweat collected at the skin surface is a clear aqueous solution containing 99.0 to 99.5 % by weight water and 0.5 to 1.0 % solids. The solids include inorganic salts, organic acids and carbohydrates, nitrogenous substances, vitamin related compounds, hormones, and enzymes, amongst other substances (Altman and Dittmer, 1971). The inorganic salts consist mainly of sodium and chloride ions, and small quantities of calcium, potassium, sulfur, sulfate, and bicarbonate ions. Other ions are in very small amounts. Specific gravity of the sweat is normally between 1.001 to 1.006. Normal surface sweat is hypotonic with the plasma but during profuse sweating, it may approach isotonic concentrations (Rothman, 1954). Sweat in the secretory part is isotonic or slightly hypertonic to plasma. Reabsorption of salts and water occurs primarily in the coiled duct as indicated earlier.

A comparison of the compositions of sweat and plasma in Table 2.1 shows that sodium and chloride ions concentrations are usually lower in sweat, while calcium and potassium ions do not differ appreciably between the two fluids. Concentration of urea can be twice as high as that of blood. Glucose is almost absent in sweat, while the amount of lactic acid is more than 20 times of that in blood.

Constituent	Plasma	Sweat
Na^+ (mEq/L)	138	23.3
K^+ (mEq/L)	4.7	2.7
Ca^{2+} (mEq/L)	5.2	5.5
Cl^- (mEq/L)	102.4	25.9
Glucose (mg/L)	700-1000	0-30
Urea-N (mg/L)	120-150	300-600
Lactic Acid (mg/L)	50-200	2850-3360

Table 2.1: A comparison of the average chemical compositions of blood plasma and sweat (Rothman, 1954; Altman and Dittmer, 1971) Only the major constituents are listed.

2.6. The Skin Blood Circulation

A schematic diagram of the cutaneous vascular system is also presented in Figure 2.2. The blood supply to the skin is derived from the branches of the subcutaneous arteries. Dividing arteries of about 100 μm in diameter (Ryan, 1973) enter the reticular dermis vertically or obliquely before dividing again into approximately 50 μm diameter arterioles in the mid-dermis. A horizontal plexus deep in the subpapillary dermis is sometimes recognized. Interconnections exist between plexuses such that the network is integrated into a unit (Montagna and Parakkal, 1974). The straight portion of eccrine duct is accompanied by its own plexus of arterioles approximately parallel to the duct (Ryan, 1973). On reaching the papillary dermis, the ascending branches develop a horizontal network of interconnecting and looping micro-circulatory elements parallel to the skin surface. Usually there is one capillary loop per papilla. Each loop supplies 0.04 to 0.27 mm^2 of skin surface and the average distance between loops is 50 to 100 μm (Rothman, 1954). The repeated sub-division of arteries, arterioles, and capillaries forms a candelabra pattern of network. The capillaries drain into small venules which descend and connect with more branches from the deep dermis and drain into the subcutaneous venule system. The venous system is more disposed to be horizontally oriented than the arterial system (Ryan, 1973). Arteriovenous anastomoses (AVA), which are shunts or channels connecting the arterial and venous sides of the circulation, are found throughout the vascular network.

2.6.1. Tissue Temperature Profiles

It is important to consider the temperature profiles through the superficial layers of the skin in which eccrine glands are normally fully embedded. Exchange of materials and heat occurs between the blood vessels and the connective tissues. The temperature profile along the eccrine duct, especially the intradermal straight portion which is closely associated with a plexus of arterioles and capillaries, would therefore be highly dependent on the corresponding tissue temperature profile. The steady temperature profiles through the peripheral 2 to 4 mm layer of the human skin at rest are not normally monotonic with distance from the skin surface as would be predicted from the theory of heat conduction without heat generation across a multi-layered solid. Such irregular profiles were originally observed by Bazett and McGlone (1927) and later confirmed by Mendelson (1936). These investigators threaded thermocouples into the skin to varying depths to achieve good spatial resolution. They reported incidences of hyperemia or inflammations whenever such incidents occurred. Some of their results for conditions without inflammations in the forearm and deltoid of resting subjects are reproduced in Figure 2.3. This figure shows the difference between the local tissue temperature and the value at the skin surface versus the distance into the skin. In the cases of interest vaso-constriction or dilatation are absent for the cutaneous blood supply. The profiles vary considerably with the ambient conditions and from one individual to another. Yet the general pattern remains the same. For all the curves, a maximum is observed at distances of between 0.8 to 1.2 mm into body from the skin

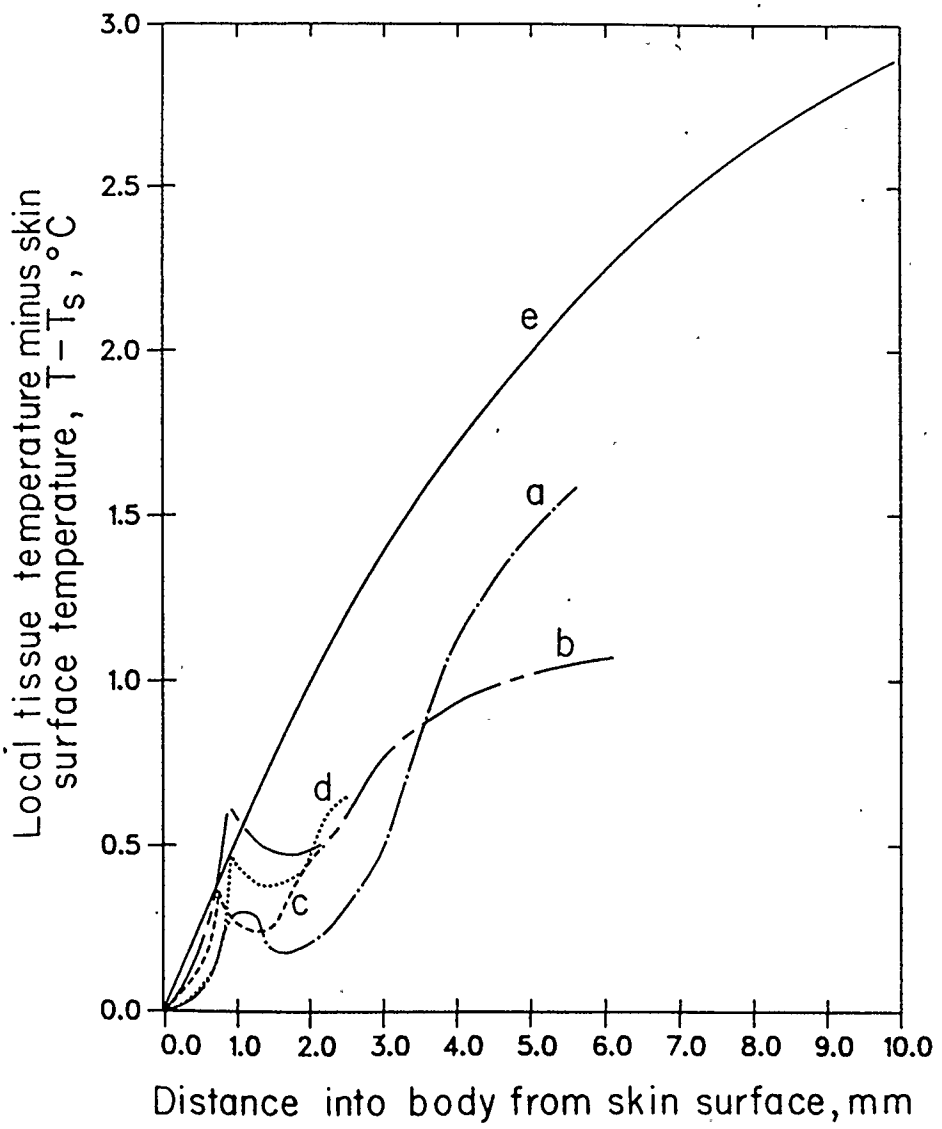

Figure 2.3 : Local tissue temperature minus skin surface temperature in the superficial 10 mm layer of the forearm as measured by Bazett and McGlone (1927). Subject feels cool (a) and subject is comfortable (b); the forearm (c) and deltoid (d) by Mendelson (1936); and the lumbar region (e) by Reader and Whyte (1951).

surface. The validity of the data has come under criticism as whether bulk tissue temperatures were being determined by thermocouple junctions which might be adjacent to or have punctured arterioles or capillaries in the skin (Hardy, 1934). The repeatability of the measurements and consistency of the data, however, suggest that such profiles are truly representative of the local bulk tissue temperatures of interest. Presented in Figure 2.4 are representative temperature measurements at different distances into the skin (Reader and Whyte, 1951; Nielson, 1969). The spatial resolution of this data is not as high as for Figure 2.3.

The column of liquid within the eccrine duct would have an axial temperature profile similar to the vascular plexus immediately surrounding the gland. This temperature pattern would be determined in part by heat exchange with and the temperature gradients through the layers of the skin as illustrated in Figure 2.3. The free surface of the column retracted, in the resting state, below the surface of the skin would therefore be at a temperature higher than at the skin surface. Hence the vapor pressure and rate of evaporation at the meniscus would be elevated above corresponding values at the skin surface temperature. That is, the temperature distribution in the skin would affect the rates at which water would be lost to the ambient as would be further explained later on. This issue is important because many investigators have erroneously based their analysis on evaporation at the skin surface temperature.

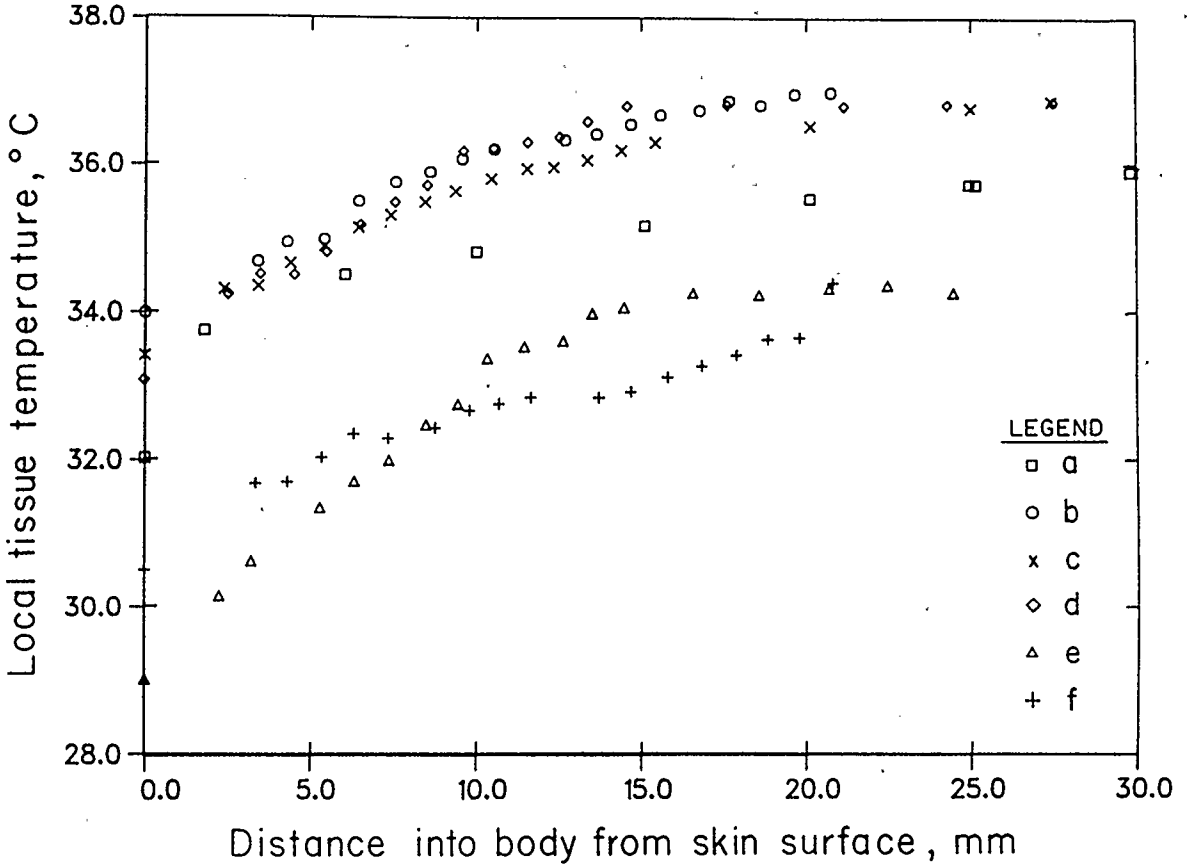

Figure 2.4 : Temperature profiles from the skin surface into the core for the forearm and thigh. For the lower two curves, the subjects felt cool. The uppermost curves are for comfortable subjects at different ambient conditions. Similar patterns are observed for the forearm, deltoid, thighs and lumbar regions. (curve a - forearm with ambient temperature T_∞ of 24°C (Reader and Whyte, 1951); curve b - forearm with $T_\infty \approx 31.6$°C and relative humidity RH of 15% (Bazett and McGlone, 1927); curve c - forearm with $T_\infty = 22.8$°C and RH = 86% (B.& M.,1927); curve d - thigh under same condition (B.& M., 1927); curve e - forearm with $T_\infty \approx 18.4$°C and RH = 19% (B.& M., 1927); curve f - forearm with $T_\infty = 18.5$°C and RH = 14% B.& M., 1927))

CHAPTER THREE

LITERATURE REVIEW

The literature on insensible perspiration is extensive. Most of the reported studies involve accumulation of experimental facts on the rates of water loss from the entire human body at rest, regional variations of the rates and the influence of ambient temperature and relative humidity. Excised strips from the skin have also been used to determine the tissue moisture contents in equilibrium with air at varying relative humidities. Diffusion coefficients for water through the skin and the electrical conductivities and mechanical properties of the tissues have also been of interest. The present review is not exhaustive and is intended to provide an overview for commenting on the interpretations of such data.

In order to avoid confusion in terminologies, "insensible water loss" would denote the total loss of water due to the lungs (respiratory) and out of the skin (cutaneous). "Insensible perspiration" would denote the cutaneous water loss through sweat glands (insensible sweating) and across the epidermis (transepidermal water loss).

3.1. Rates of Insensible Perspiration

3.1.1. Methods and Apparatus

Early determinations of insensible perspiration rates involved measuring the changes in weight of individuals over a period of time (Benedict and Root, 1926; Wiley and Newburgh, 1931). Average values are thus obtained. Such measurements are primitive and are affected by ingestion, excretion, ambient conditions and changes in emotional state. The accuracy of the mass balances used must be high or the time elapsed from the start of measurement must be long before significant moisture loss is noted. This method is still popular and insensible perspiration is estimated as the difference between total water loss and respiratory water loss which is determined with a breathing apparatus simultaneously.

In more recent investigations, measurements have been confined to small patches of intact or excised human skins. Total insensible perspiration can be estimated if measurements are made at representative sites of the body. The techniques are varied. Air (or nitrogen) with known water content has been used as a carrier passed through a cuvette attached to the skin surface. The flow rates and the water content of the exit gas are monitored and the moisture added to the stream calculated (Burch and Winsor, 1944; Goodman and Wolf, 1969; Spruit and Malten, 1969; Lamke and Wedin, 1971). Such a procedure is called a ventilated chamber method. Precautions must be taken to minimize condensation of water on the confining walls and leaks should be avoided. The water content of the gas has been

measured with gravimetric methods (Pinson, 1942; Burch and Winsor, 1944; Grice and Bettley, 1967; Grice et al., 1972), electrolytic methods (Baker and Kligman, 1967; Mathias et al., 1981), and infrared gas analyzer (Goodman and Wolf, 1969).

There are drawbacks to the application of the ventilated chamber method. The temperatures of enclosed skin patches are elevated at low gas flow rates. At higher rates, the convection currents and turbulence may lead to enhanced mass transfer rates and abnormal water loss rates. In the unventilated chamber method, the water exchange is determined by measuring the change in weight of a hygroscopic salt placed inside the chamber (Felsher and Rothman, 1945; Hattingh, 1972). The micro-environment at the skin surface could be thus altered.

More recently, an indirect method has been developed whereby an unventilated chamber or cup is mounted onto the skin surface. The moisture gradients are determined with highly sensitive humidity sensors (Nilsson, 1977; Lamke et al., 1977; Miller et al., 1981). Both open and closed cups have been used. This method circumvents the problems associated with forced convection and there is little interference with the conditions at the site of measurement. The main difficulty has been with estimating the vapor loss rates. Since only one or two humidity sensors could be used, a linear water concentration profile, normal to the skin surface, can only be drawn. Such a profile is inappropriate even at steady state. For this situation the governing equation giving the mole fraction of water (x_A) is (Bird, Stewart and Lightfoot, 1960):

$$\left(\frac{1-x_A}{1-x_{Ao}}\right)=\left(\frac{1-x_{A\infty}}{1-x_{Ao}}\right)^{(z/H)} \tag{3.1}$$

where x_{Ao} and $x_{A\infty}$ are the mole fraction of water at skin surface and top of the cup, and H is the height of the cup. An examination of the equation shows that the gradient dx_A/dz is not constant with respect to z. Nevertheless, the simplicity of the apparatus and its minimal interference with the test site has made it attractive to physiologists.

3.1.2. Total Rates

As early as 1831 Sanctorius measured the change in his own weight and estimated that 35 ounces (≈1000 g) of water was lost in a night. Other similar measurements were in the range of 31 to 50 ounces (900 to 1500 g) for a 24 hour period (Kuno, 1956). The ambient conditions were, however, not stated. Such losses would include the contributions from respiration. Kuno (1956) reported an amount of 23 g/hr-m^2 as an average value for total insensible water loss. This corresponds to a loss of ≈1000 g/day. Grice (1980) also reported an average insensible water loss of 1000 g/day. Lamke and Wedin (1971) measured an average insensible water loss of ≈1300 g/day at an ambient temperature of 28°C and 40% relative humidity (RH). The average value of water loss due to the skin has been variously quoted as 50 (Kuno, 1956) and 60% (Rothman, 1954; Grice, 1980) of the total insensible water loss, which amounts approximately to between 500 to 700 g/day. Lamke et al. (1977) measured rates of water loss in different regions by mounting humidity

sensors on an open-end cylindrical capsule. He estimated the average rate of insensible perspiration to be 380, 530 and 700 g/day at 22, 27 and 30°C respectively with a 30% RH. This compares favorably with the range cited above.

The total insensible water loss shows an almost linear relationship to the basal metabolic rate (Wiley and Newburgh, 1931; Rothman, 1954). It was estimated that the evaporative heat loss was, on the average, about 24% of the total heat loss (Soderstrom and Dubois, 1917). The cutaneous heat loss is especially significant in newborn infants as they have a relatively larger body surface per unit volume and higher sweat gland density. The situation is even more severe in premature infants (Sauer et al., 1984). It was estimated that preterm infants weighing less than 1 kg had mean evaporative water losses of 64.2 ml/kg-day, while those weighing 1.7 to 2.0 kg lost 16.7 ml/kg-day (Wu and Hodgman, 1974). In cases of immature infants careful monitoring of the radiant heat supply is therefore required. The cutaneous component shows a definite decline with age (Rothman, 1954) and is slightly lower in women than in men (Hardy et al., 1941).

3.1.3. Site Variation

It is generally agreed that the palms and soles lose more water to the ambient relative to the other regions of the body. On other surfaces, the loss is fairly equally distributed. Burch and Sodeman (1943) found that the rate of insensible perspiration varied regionally. In the descending order of water loss rates per unit area are the surfaces of the hands, feet, head, arms, legs, and the trunk. Kuno (1956) classified the general body surface into three zones. Zone 1 consists of the palm and sole which produce the highest rates despite their much thicker stratum corneum layers (400 to 600 μm thick as compared to 10 μm of the general body surface). The keratinocytes found in these regions do not differ from those in other regions. The measured rates vary between 50 to 100 g/hr-m^2. The high rate is most likely due to the high density of sweat glands, as suggested by Mali (1956). Szabo (1962) determined that the average density of sweat glands at the sole is 620 per cm^2. The density is 150 to 250 per cm^2 in most other surfaces. Zone 2 consists of the forehead, the cheek, the neck and the dorsal region of hand. Water loss rates vary between 25 to 45 g/hr-m^2. These regions are usually uncovered. These results indicate that exposed regions show higher rates of insensible perspiration. Zone 3 consists of the abdomen, the back, the arms and the legs, and probably all the other parts usually covered with clothes. The rates vary between 7 to 17 g/hr-m^2.

Kuno's findings on regional variations have been supported by Baker and Kligmna's experiments (1967). Using a ventilated chamber and humidity sensors,

they reported a mean loss of 11.4 and 8.5 g/hr-m^2 in the palm (zone 1) and forehead (zone 2), and an average mean loss of 3 g/hr-m^2 in the abdomen and back (zone 3). Losses on the forearm and shin (zone 2) were reported to be ≈3.5 g/hr-m^2 which are lower than anticipated. It should be noted that the losses measured by these investigators are lower than those suggested by Kuno (1956) but the trends are similar. The discrepancy may be ascribed to the fact that, before measurements, each site was treated with a solution of benzoyl ester of scopolamine to inhibit sweat gland activity. *In vivo* determination by Lamke and Wedin (1971) using a technique similar to those of Baker and Kligman (1967) indicated mean rates of 17.3, 21.4, 15.5 and 16.5 g/hr-m^2 for the regions back, chest, forearm, and thigh respectively at an ambient temperature of 28°C and 40% RH. The skin surface temperature was measured at ≈35°C. With no pretreatment of the skin, the values reported by these investigators are similar to those quoted by Kuno (1956). Similar results were reported by Lamke et al. (1977).

Numerous measurements have been done on the rates of insensible perspiration using dead human skin patches (Winsor and Burch, 1944; Burch and Winsor, 1944, 1946; Berenson and Burch, 1951; Blank, 1952, 1953; Mali, 1956). Such measurements are now rarely undertaken because dead tissues have different properties from live ones. The usual procedure was to mount a piece of excised skin, free of subcutaneous fat, tightly over the surface of a water-filled cylinder (Blank, 1952). The change in weight of the cylinder would be taken as the loss of water through the skin. In some cases a ventilated chamber was used to measure the

amount of water loss (Onken and Moyer, 1963). In addition, the cylinder can be enclosed in a temperature-controlled bath so that the lower end of the excised skin would be maintained at a warmer temperature. Saline solution such as sodium chloride has been used in place of pure water (Burch and Winsor, 1944). It was claimed that rates of water loss as obtained in excised skin patches were of the same magnitude to those in living skin (Burch and Winsor, 1944), thus insensible perspiration would mainly be a passive process and solely due to transepidermal water loss as active sweating would be absent. Such *in vitro* studies, however, need to be examined carefully. Eccrine pores and hair follicles interspersed within the skin patch may provide alternative pathways for water diffusion. Considerable vapor efflux would occur through such openings and transepidermal water loss may be insignificant. Burch and Winsor (1944) obtained average values of 49 and 48 g/hr-m^2 for living and dead abdomen skins respectively. No specific conditions were reported. Their values are consistently higher than those found for *in vivo* situations (e.g. Lamke et al., 1977, reported an average loss of 9 g/hr-m^2 at 27°C ambient temperature and 30% RH in the same region). Burch and Winsor (1944) passed dry oxygen through the skin site and measured the outlet gas water content by condensation using solid carbon dioxide. Apparently a 10 minute duration was used for each measurement as the rates were reported in mg/10min-5cm^2. The high values may be due to the short duration of time, a high gas flow rate, inaccuracy of the balance, leakage of moisture from the outside into the chamber, or measurement errors. For the same region Blank (1953) and Onken and Moyer (1963) reported fluxes of 1

to 2 and about 3 g/hr-m^2 respectively, both for *in vitro* conditions. Again relevant data such as ambient temperature and relative humidity were not reported. These values, however, are considerably lower than normal *in vivo* cutaneous water loss. It should be recognized that the conditions on the inner side of the skin strips for *in vitro* studies are vastly different from *in vivo* situations with intact skin. The mapping of an *in vivo* temperature gradient across a skin patch has been difficult but undertaken. The temperature at which water is vaporized is important as it determines the vapor pressure at site of evaporation. In most cases excised skins were at ambient temperatures while in other cases solutions bathing the lower layers were maintained at warmer temperatures. The usage of pure water or saline solution would not resemble conditions in the dermis. Such efforts to imitate *in vivo* conditions may be futile and lead to a misinterpretation of results.

3.2. Contributing Factors

It has been shown that the rate of insensible perspiration does not remain constant even for an individual, as it depends on various internal and external factors. For the sake of arguments the rate of insensible perspiration is represented by the following simplified expression:

$$Q_A = C\ (x_{Ao} - x_{A\infty}) \tag{3.2}$$

where C is a constant of proportionality and x_{Ao}-$x_{A\infty}$ represents the diffusional driving force between the skin surface and the ambient air. C can be treated as constant only when the internal and external conditions remain unchanged. x_{Ao} is the equilibrium water vapor mole fraction at site of evaporation and is therefore dependent on physiological conditions. $x_{A\infty}$, on the other hand, represents the ambient vapor mole fraction and consequently depends on the ambient conditions. The importance of both the internal and external factors should be obvious.

3.2.1. Internal Factors

Physiological factors include the mental state of the subject, the amount of cutaneous blood supply, and the level of metabolic activity. The pattern of sweating induced mentally as opposed to thermal stimulation is quite different. It has been demonstrated that subjects performing mental arithmetic produced sweat on the palms and soles, and less profusely on the axilla (Kuno, 1956). No trace of sweat was detected on other surfaces. The forehead also sweats during mental

exercises (Kuno, 1956). In contrast, sweat induced thermally was found on the general body surface (Kuno, 1956).

The effects of vascular changes are two fold. A change in the vascular supply may mean a change in heat-transfer areas at surfaces of arterioles and capillaries, as a result of vaso-constriction or dilatation. It could also mean a change in the heat flux as the blood flow rate changes. These affect or determine the temperature profiles along the intradermal straight eccrine duct. Such an effect may not only cause the value x_{Ao} in equation (3.2) to be different, but may induce a change in the amount of secretory activity. Consequently C would be a variable parameter and not a constant. The second effect is on the rate of exchange of materials between the straight eccrine duct and the accompanying arterioles and the connective tissues. Skin temperature variations would cause a change in the rates of secretion or reabsorption of ions, water and other substances. Studies on such vascular changes are few. Kuno (1956) noticed an increase in water loss after one leg was immersed into water at 40 to 42°C. He suggested that the cause was mainly due to an increase in temperature. Other studies on vaso-constriction or dilatation include those of Pinson (1942), Grice and Bettley (1966; 1967), and Baker and Kligman (1967). These investigators reported that vascular changes had little effects on rates of water loss. Their studies, however, were performed with sweat glands activity inhibited by anodal cataphoresis (Pinson, 1942), topical application of anticholinergic substances such as poldine methosulphate (Grice and Bettley, 1966) or benzoyl ester of scopoamine (Baker and Kligman, 1967). Physiological conditions may be vastly

changed as a consequence.

3.2.2. External Factors

Important variables external to the body include the ambient temperature, relative humidity and air velocity. The effect of air velocity is complex but in general the presence of air currents near a skin surface would increase the rate of water loss from such a region. The enhancement is caused by convective currents which modify the concentration profiles at the surface. This has yet to be thoroughly studied.

On the influence of ambient temperature and relative humidity, results in the literature and their corresponding interpretations are diverse and contradictory. Kuno (1956) claimed that insensible perspiration varied only slightly with changes in the ambient temperature. Temperature fluctuations however induce changes in the temperatures of the superficial skin layers and in the cutaneous circulation. Experimental results were not cited. Berenson and Burch (1951) examined the influence of such environmental conditions on water evaporation through excised skin. They found an almost linear, direct variation with ambient temperature. Their studies, however, were done with progressively decreasing relative humidity as the ambient temperature was raised. Kligman (1964) found an inverse linear relationship between relative humidity and water diffusion for excised skin. Water loss was negligible above 90% RH. This could be expected as the excised skin would be at

essentially the same temperature as the ambient. Such *in vitro* studies, as mentioned earlier, do not represent the true physiological situation. Grice et al. (1972) studied the effect of relative humidity on living skin treated with poldine methosulphate. The purpose was to measure only the transepidermal water loss. They found that at low humidity, the rate of water loss was actually increased by an increase in relative humidity. The trend was reversed at higher humidity. The phenomenon as observed at low humidity was suggested (Grice, 1980) to be due to an increase in water content in the stratum corneum (Spencer et al., 1975) and consequently a greater water permeability in the layer. The explanation may not be applicable since at low relative humidity (below 60%) between 20 to 35°C ambient temperature the water content in stratum corneum has been demonstrated (Spencer et al., 1975) to change very little with relative humidity for *in vitro* conditions. The change would even be smaller for *in vivo* situations since stratum corneum would then be at a higher temperature. At present no alternative explanation can be suggested for their observations. The interference of sweat gland activity using a cholinergic agent, however, may be undesirable.

Variations in relative humidity reflect in changes of the ambient water content and temperature. The driving force term in equation (3.2) would be reduced as the value $x_{A\infty}$ increases. This results in a decrease in the rate of cutaneous water loss. Such a relationship was confirmed by Goodman and Wolf (1969) in their *in vivo* studies on the forearm using a ventilated chamber method. The ambient temperature was at 25°C while the skin surface temperature was not reported. The exit gas

was analyzed using an infra-red gas analyzer. They, however, reported that the relationship between humidity and cutaneous water loss was non-linear. The result appears inconclusive as the measurements were only taken at four different ambient water vapor concentrations.

Changes in ambient temperature have two major effects. x_{Ao} may be increased due to an altered skin blood flow. The change in the cutaneous temperature pattern could enhance the secretory activity of the sweat glands. Lamke and Wedin (1971) reported an average increase in the rate of cutaneous water loss from 10.1 to 17.5 g/hr-m^2 when the ambient temperature was raised from 15 to 28°C for *in vivo* studies on the back, chest, forearm and thigh. It was suspected that below 15°C the blood vessels of the skin were constricted. Dwelling on results involving such extreme temperatures may not be appropriate here. The *in vivo* studies by Lamke et al. (1977) provides a more accurate picture. Using an open cup with humidity sensors mounted on the inside wall, these investigators estimated rates of water loss for various regions of the body surface at 22.1, 26.9, and 30.3°C respectively. The corresponding total insensible perspiration rates were estimated at 381, 526 and 695 g/day. It was also shown (Lamke et al., 1977) that the percentage contribution from different regions was fairly equal, irrespective of the change in the ambient temperature. It was suggested that the increase in water loss was due mainly to higher secretory activity.

In an effort to relate rates of water loss with a driving force term such as x_{Ao}-

$x_{A\infty}$ in equation (3.2), Kerslake (1972) correlated data from various measurements and obtained the following expression:

$$Q_A = 6.0 + 1.75\,(P_{As} - P_{A\infty}) \tag{3.3}$$

where P_{As} and $P_{A\infty}$ represent vapor pressures of water at skin surface temperature and ambient temperature respectively. While the expression implies a linear relationship, it predicts a rate of 6 g/hr-m^2 as $P_{A\infty} \rightarrow P_{As}$. Kerslake (1972) suggested that this steady rate could be attributed to sweating. The use of the term P_{As} suggests that pure water would be evaporating from the skin surface. Such would not be the case if transepidermal perspiration were the mechanism for water loss. Water is bound in the stratum corneum and thus cannot be treated as pure. As for water evaporating from sweat ducts, the temperature at the local site of evaporation (the meniscus) may be higher than the skin surface temperature, depending on the level of sweat inside the duct.

3.3. Insensible Sweating vs. Transepidermal Water loss

Whether insensible perspiration is mainly due to water loss from sweat pores or through the epidermal skin layer has been an issue of contention. Kuno (1956) suggested that even when the rate of evaporation from the sweat pores is high, their total surface area ($\approx 0.01 m^2$) is too small for them to be a contributing factor. Numerous but inconclusive experimental studies have been done in the attempt to determine the major pathway. The claim that sweat glands do not participate during insensible perspiration has been based on some observations that individuals who lack sweat glands completely or almost completely, a syndrome called "hereditary anhidrotic ectodermal dysplasia", eliminate normal quantities of water through the skin (Richardson, 1926; Sunderman, 1941; Upshaw and Montgomery, 1949). The skin of these individuals is unususally soft, thin and feminine (Upshaw and Montgomery, 1949), and may therefore be less water resistant than normal skin. The mechanism of water loss may subsequently be different for these relatively rare individuals.

Hancock et al. (1929) analyzed the constituents of bath water from individuals who had not washed or visibly sweated for one week. Salts recovered were mainly potassium chloride (≥90%) and sodium chloride. They concluded that the potassium was derived from the epidermis, particularly from sebaceous gland secretions, and insensible perspiration was largely transepidermal. While the sodium content was low, it may be suggested that sweat liquids normally retracted into the sweat

duct would not cause salt or any other substances to precipitate on the skin surface upon evaporation. Their method may introduce large errors of measurement. The primitive nature of their procedure may cause a substantial variation in the results.

In the palms and soles, sweat glands have been determined to produce water continuously. At other body surfaces, such a phenomenon has not been demonstrated conclusively. Rothman (1954) reported that sweat droplets could be observed over the general body surface with a light microscope. Randall (1946) measured the amount of sweat secreted on the extensor surface of the forearm by applying dilute iodine solution and subsequently pressing lightly a starch containing paper onto the test site. The appearance of a blue-black spot on the paper denotes the activity of an individual gland. The size of each spot would be a quantitative measure of the amount of sweat secretion. The procedure of painting iodine on the skin has been criticized (Dole and Thaysen, 1953) for two reasons. Iodine may irritate the tissue being studied and it washes away irregularly as sweating proceeds. Dole and Thaysen (1953) modified the method by introducing iodine into the starch paper by sublimation. The test sites include the forearm, thigh, back and abdomen. Both Randall (1946) and Dole and Thaysen (1953) reported similar findings in that sweat glands show periodic activity in secreting sweat onto the cutaneous surface. Moreover, upon thermal stimulation, the sweating rate is first increased by an increase in the number of functional glands, followed by an increase in output of individual glands. Nicolaidis and Sivadjian (1972), using a hygrophotographic recording technique whereby a hygrosensitive film was placed in contact with the

forehead, observed high-frequency (12 to 21 Hz) pulsatile expulsion of sweat onto the skin surface. The degree of discoloration of the originally dark film is an indication of water being absorbed, and the area of discoloration indicates quantitatively the amount absorbed. The aforementioned experiments on the sweat gland activity seem to indicate the participation of sweat glands during insensible perspiration.

Qualitative measurements on the filling of eccrine ducts with sweat and hydration of the stratum corneum have been made by analyzing the time delays required for sweat emergence after electrical stimulation of eccrine glands. Such measurements are commonly done using the footpad of cat (Lloyd, 1959; Adams, 1966; Holmes and Adams, 1975) because the pad has a high density of sweat glands. Bullard (1971), upon stimulating the eccrine glands of human forearm, distinguished two latency periods. He reported a time delay of one to two minutes between stimulation and the emergence of sweat, and several more minutes before the sweating level achieved a steady state. Both time lags were greatly reduced in consecutive stimulations. The first latency was suggested to be the time required to fill the duct with sweat, and the second latency to be the time needed for epidermal hydration. From the correlation between the two latency periods and the time between each successive stimulus, Bullard (1971) estimated a time of ≈20 minutes for a duct to completely empty itself. The estimation is based on the assumption that the ducts are normally empty for a person at rest. Lloyd (1959) , using the footpad of cat, reported a time of ≈75 minutes for complete sweat reabsorption. There is no evidence that the ducts are actually ever emptied of liquids. The latency may be due

to physiological factors.

Attempts to measure quantitatively the transepidermal water loss have generally been performed by some sort of sweat gland activity inhibition. These include iontophoresis of formaldehyde (Pinson, 1942), and topical application of anticholinergic compounds such as poldine methosulphate (Grice and Bettley, 1966; Bettley et al., 1967; Grice et al., 1971; 1972) or benzoyl ester of scopolamine (Baker and Kligman, 1967). Pinson (1942), using anodal cataphoresis of formaldehyde, reported no differences in the rate of insensible perspiration before or after the treatment. Hence he concluded that sweat glands were not involved in cutaneous water loss. The use of iontophoresis, however, may damage the tissue, as is evidenced by the fact that upon enhanced treatment the skin became dry and scaly, and the rate of water loss was increased (Pinson, 1942). Grice and Bettley (1966), applying poldine methosulphate, reported an average water loss of 151 g/day, ≈25% of the total cutaneous water loss. They attributed the amount to transepidermal water migration. While the use of such an anticholinergic substance may impair the secretory activity at the basal portion of the coiled duct, there may be other pathways by which water migrates into the duct lumen and be evaporated into the ambient. The existence of such pathways would be discussed in chapter 4. It should be recognized, at this point, that results obtained using the aforementioned method may not be a true indication of the process of transepidermal water loss.

3.4. Characteristics of the stratum corneum

It has been generally accepted that the principal diffusional barrier of the skin resides in the most superficial layer of the epidermis, the stratum corneum. This is shown by the fact that on removing the layer, water loss rates are greatly enhanced. At the same time, sebum which is usually present on most skin surfaces apparently does not function as a barrier, as no significant reduction in water loss was found until the amount of sebum added (30μ thickness) was more than 10 times the usual amount (0.4 to 4 μm thickness) (Tregear, 1966). The precise nature of the barrier, however, still remains unresolved. Blank (1953), using a serial stripping technique, found that the rate of water diffusion was unaltered until the whole stratum corneum layer has been removed, at which time the diffusion rate was dramatically increased. He therefore concluded that the barrier was located in the innermost layers of the stratum corneum. This view was confirmed by Kligman (1964) and Scheuplein and Blank (1971) who argued that if the stratum corneum were a uniform barrier, it would not be until the last layers were removed that there would be a sudden and marked increase in water loss. Some investigators (Jarrett, 1980) however maintained that the barrier nature of the stratum corneum is uniform and homogeneous. This view appears doubtful since the degree of consolidation of the stratum corneum decreases outward. With adhesive tape stripping, each succeeding strip removed less than the previous one (Kligman, 1964). This has been suggested as evidence that the cells are more tightly bonded with increasing depth. The cohesion gradient is gradual and continuous. Serial stripping is a primitive method with

inconsistent and low reproducibility results. Skin surface contours may also lead to uneven sampling for each strip. The method, however, is simple and direct. In addition to the variation in packing and cohesiveness, cells in the inner layers have a finer keratin matrix (Tregear, 1966). Therefore even though the stratum corneum acts as a diffusional barrier on the whole, its resistance is expected to increase with increasing depth into the skin.

There are two possible routes by which water can traverse in the stratum corneum. It can either penetrate through the cells (Kligman, 1964) or along the narrow and tortuous intercellular channels (Tregear, 1966) which are ≈4 μm wide. The latter route seems improbable since the water present in the stratum corneum would be "bound" (Walkley, 1972; Andeson et al., 1973). Rothman (1954) has also suggested that the transepidermal water loss is mainly a result of keratinization of the cells advancing to the surface. While this process may provide part of the loss, the amount is too small for it to account for insensible perspiration.

The question remains as to which component (or components) in the stratum corneum inhibits water migration through the skin. Each cell in the stratum corneum consists of basically three components: the keratin itself, a non-keratinous shell surrounding it, and inter-cellular desmosomes. In addition, lipids are present in the intercellular spaces. The lipids are in the form of triglycerides, free fatty acids, free sterols and sterol esters. It has been suggested that this mixture of lipids is responsible for the low water permeability of the skin (Grice, 1980). *In vitro* stu-

dies (Grice, 1980) showed that soaking stratum corneum in acetone or chloroform alone did not alter the diffusion rate. However, when a mixture of chloroform and methanol was used, the rate of water loss was greatly enhanced (change from 2 to $\approx$30 g/m^2-hr). Similar results were obtained by El-Shimi and Princen (1977) on guinea pig and Imokawa and Hattori (1985) on human corneum. It was suggested that lipids complexed with proteins or carbohydrates in the stratum corneum are usually insoluble in solvents such as acetone or chloroform. But a chloroform-methanol mixture is both a polar and non-polar solvent and is thus able to remove the hydrophilic complex lipids (Grice, 1980). Another study of interest is that rats fed on a diet deficient in essential fatty acids had an impaired water barrier and consequently an increased water loss rate (Prottey, 1977). Though these studies seem to indicate that lipids play an important role in preventing water efflux, more work has yet to be done before the precise nature of this barrier is elucidated.

Studies on the characteristics of the stratum corneum have generally been concentrated on the sorption-desorption behavior of water (El-Shimi and Princen, 1977, 1978; Wurster and Yang, 1982) in excised human or guinea pig skin. Such isolated pieces not only contain stratum corneum layers but also other structures such as eccrine glands and hair follicles, which might provide alternative routes for water movement. Nevertheless, values for the diffusion coefficient are obtained from such sorption-desorption isotherms. In general the diffusion coefficient increases with the water content of stratum corneum, taking into account its swelling behaviour. Blank et al.'s (1984) measurements of tritiated water migration

through pieces of stratum corneum showed that the flux decreases as the water content of stratum corneum increases. The unexpected result could be explained by their method of evaluating the diffusivity. The molar flux of water (N_A) in a binary system is given by (Bird, Stewart and Lightfoot, 1960),

$$N_A = -D_{AB}\, c\, \frac{\partial x_A}{\partial z} + x_A\,(N_A + N_B) \tag{3.4}$$

where D_{AB} is the diffusion coefficient of A in B and c is the concentration of the gas mixture. In stratum corneum water is the only moving component and therefore $N_B = 0$ and hence,

$$N_A = \frac{-c\, D_{AB}}{1 - x_A}\, \frac{\partial x_A}{\partial z} \tag{3.5}$$

Blank et al. (1984) assumed that the mole fraction of water, x_A, was small and therefore $1-x_A \approx 1$. This is not true since the water content of stratum corneum can become considerably large. Both the gradients and absolute values of moisture content would have to be determined in order to evaluate D_{AB} given that N_A in equation (3.5) can be measured.

CHAPTER FOUR

MODELLING AND ANALYSIS

In this chapter, the formulation of the problem is presented. Detailed mathematics and computational schemes are described in Appendix A and B. Results from the analysis will be presented in the next chapter.

4.1. Introduction

The analysis is based on the premises that eccrine glands are always filled with sweat to various levels at any time, and the lumena of eccrine ducts open to the ambient and therefore offer low diffusional resistance to water vapor fluxes. An evidence in support of the continuous presence of aqueous solutions in the ducts is that the palms and soles are normally always moist. On these surfaces, the eccrine gland density is high, sweat gland secretion is known to be continuous yet liquid droplets are not apparent on the surfaces (Montagna, Ellis and Silver, 1962). Measured rates of insensible perspiration are also high (Kuno, 1956). It is here suggested that the glands on other surfaces of the body have similar characteristics though the rates of secretion of the glands would be lower than on the palmar surface. The continuous secretion would be the primary source for replenishing the water evaporated and contributions may be made by other tissues.

The "empty duct" theory, as proposed by Lloyd (1959; 1961), was based on

the observation that a latency period was required between electrical stimulation and appearance of observable sweat droplets on the surfaces of cat foot pads. Such delay, however, may be due to other reasons. The local capillary blood flows would require time for readjustment. The glomerular secretory coil response to the stimuli may be slow and an increase in the migration rates of fluids across the connective tissues between the blood vessels and the sweat glands may not occur the instant the stimuli are applied. The method of detection is subjective and errors of time measurement could be significant.

Another evidence is that a significant amount of water loss occurs when the ambient water vapor concentration is equivalent to that of pure water at skin surface temperature (Rothman, 1954; Buettner, 1953; 1959; Bettley and Grice, 1967; Goodman and Wolf, 1969; Kerslake, 1972). The appreciable water loss suggests that the primary vapor source is at a higher temperature than the skin surface temperature. This is consistent with the model that sweat liquids retracted into the skin would evaporate at a temperature attained by the luminal cells adjacent to the free liquid surface.

4.2. Anatomic and Physiological Considerations

The rates of water loss through the eccrine glands and the significance of the various anatomical features of these organs are of primary interest. The focus is on the upper portion of the duct, the "epidermal eccrine sweat duct unit". Complex processes of secretion and reabsorption of various ions and organic substances take place in the coiled and straight portion of the duct (Cage and Dobson, 1965; Sato and Dobson, 1970; Sato, Dobson and Mali, 1971; Mangos, 1973; Odland, 1983; Schwarz and Simpson, 1985). These processes are not included in the current analysis since the absorption rate of solutes is inversely correlated to the sweat secretion rates when the sweat appears at the skin surface. At low sweat liquid secretion rates, all solutes are expected to be re-absorbed. Only the evaporative process for water is considered.

Under the conditions chosen, a meniscus of the sweat liquid column in the duct is assumed maintained at a constant position. That is, a continuous slow basal rate of liquid influx into the lumen of the secretory coil occurs (Jurgensen, 1924; Vasti, 1932) and this is balanced by the reabsorption of part of the liquid in the duct (Mangos, 1973), evaporative losses to the ambient, condensation of the vapor onto the luminal lining of the periductal surface, and lateral dispersion into the stratum corneum. If the sweat liquids are secreted into the duct lumen in a periodic manner (Randall, 1946; Nicolaidis and Sivadjian, 1972), the time constant is considered to be much shorter than for the evaporative process that the meniscus location is con-

sidered unchanged over an interval of interest. Over a long time, the meniscus position would not be fixed. It may rise or fall in the duct.

The dilute sweat solution is assumed to have colligative properties of pure water. Normal surface sweat contains 99 to 99.5% water, the balance being salts and organic substances. Solute concentrations have been found to increase with sweat production rates and the current assumption is equivalent to stipulating negligible solute concentrations when the liquid does not flow to the skin surface. Surface active agents are also assumed absent at the meniscus as these would lower the liquid vapor pressure. Otherwise the vapor pressure of water would be reduced.

Electron micrographs of eccrine ducts show non-circular cross-sections. This may be due to the tissue handling techniques. The circularity is in itself not important except at the location of the meniscus where variable curvature of the free liquid surface could result in spatially dependent evaporation rates.

Conditions which induce vaso-constriction or dilatation of the cutaneous plexus are assumed absent. That is, a normal blood supply to the dermal tissues as well as the intradermal portion of the straight eccrine duct is assumed. Thus the temperature profiles through the skin and the thickness of the layers would remain unchanged.

The analysis presented is for two limiting cases of insensible perspiration. The first case involves the meniscus being retracted into the duct to the neighbourhood

of the dermo-epidermal junction. Microvilli in the duct would be exposed to gases under this condition. For the second case, the meniscus is located at the pore rim. Lateral dispersion of liquid into the stratum corneum would then occur and the surface area for water evaporation is increased. Gross rates for the two cases will be compared with typical values quoted in the literature.

When the meniscus is retracted into the duct, its position is important in determining the water loss rate. The intra-epidermal eccrine duct is a helix with a radius which is 1 to 2 orders of magnitude greater then the luminar diameter. Straightening the duct effectively at an oblique angle through the epidermis would not change the physics of the problem. The cross-sectional area of the channel is also assumed to increase uniformly from the dermo-epidermal boundary to the skin surface. The hydraulic diameter of the duct at the dermo-epidermal junction is usually between 3 to 5 μm, while that at the pore rim is about 15 μm before it rapidly enlarges to about 72 μm. Therefore a divergence ratio of 3 to 5 is prescribed. The abrupt, funnel shape enlargement at the pore rim is ignored in the analysis.

The surface of the duct above the meniscus may act as a sink or a source of water vapor to modify the concentration gradients within the lumen. Luminal cells of the stratum granulosum have characteristics of the stratum corneum and can thus absorb the vapor. Vapor diffusing outward may also condense on this surface which is a little colder than the site of evaporation. Closer to the pore mouth, vapor may be absorbed by the keratinized cells and dispersed into the stratum corneum.

This water ultimately evaporates into the ambient. The dispersion of water into the stratum corneum is, however, not expected to be significant except when the meniscus is displaced close to the skin surface.

To simplify the analysis, the periductal surface above the meniscus is assumed to be in chemical equilibrium with respect to water vapor at local conditions. Thus lateral processes such as absorption, adsorption, condensation or evaporation are assumed negligible. Finally, the narrowness of the duct (3 to 15 μm) as compared to the total length (≈800 μm) suggests that a one-dimensional analysis would be adequate.

4.3. Material Balances

For the analysis, the heat and mass exchange between the skin and the ambient gases have been decoupled. The coupling makes the problem significantly more difficult without accurate data on the thermal conductivities of the different layers of the skin, and the permeation rates of aqueous solutions within the connective tissues. In any case, what is being examined is a rational way of describing insensible perspiration. As indicated earlier, only about 24% of the metabolic energy release can be attributed to evaporative losses from the skin. The balance occcurs by conduction over the large surface area of the skin. The sweat glands are microscopic organs which would withdraw the energy required for vaporization from the massive surrounding tissues without significantly altering the cutaneous temperature field.

4.3.1. Case with meniscus retracted but microvilli submerged in liquid

This state is schematically illustrated in Figure 4.1. The one-dimensional steady transport of water vapor in the narrow but divergent helical coil by molecular diffusion, with the vapor source at a meniscus below the skin surface, satisfies the diffusion equation :

$$S\,N_A|_z - S\,N_A|_{z+\Delta z} = 0 \qquad (4.1)$$

in the region excluding the vapor evolution sites. For stagnant air the molar flux (N_{Az}) of the vapor is given as (Bird, Stewart, and Lightfoot, 1960):

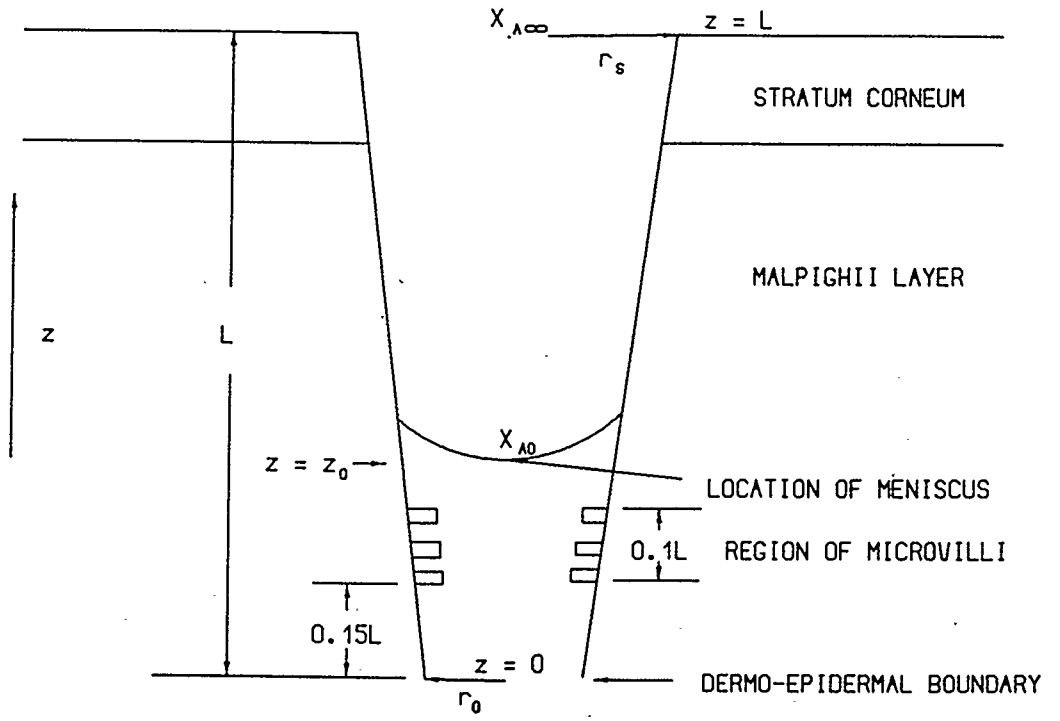

Figure 4.1 : Schematic diagram showing the model for the case when the meniscus is retracted into the eccrine duct with microvilli submerged.

$$N_{Az} = \frac{-c\, D_{AB}}{1 - x_A} \frac{dx_A}{dz} \tag{4.2}$$

where c is the molar concentration of the gas mixture, x_A is the mole fraction of water vapor, and D_{AB} is the diffusion coefficient for water vapor in air. The local cross-sectional area (S_z) is given as:

$$S_z = \pi r^2 \tag{4.3}$$

and r, the local hydraulic radius of the duct, is given as:

$$r = r_o \left[1 + (\gamma - 1) \frac{z}{L} \right] \tag{4.4}$$

where r_o is the radius of the duct at dermo-epidermal junction, L is the total length of the helical duct, and γ is the ratio between the pore mouth radius (r_s) and the straight duct radius (r_o).

On substituting expressions (4.2), (4.3) and (4.4) into equation (4.1) and simplifying, with the assumption of constant c and D_{AB}, the following ordinary differential equation with transformed variables is obtained:

$$\left[\frac{\gamma - 1}{L} \right]^2 \left[\Psi^2 \frac{d^2\Gamma}{d\Psi^2} + 2\Psi \frac{d\Gamma}{d\Psi} \right] = 0 \tag{4.5}$$

where

$$\Psi = 1 + (\gamma - 1) \left[\frac{z}{L} \right] \tag{4.6}$$

and

$$\Gamma = \ln (1 - x_A) \tag{4.7}$$

The solution to (4.5) is of the form

$$\Gamma = \frac{C_1}{\Psi} + C_2 \tag{4.8}$$

where C_1 and C_2 are integration constants to be determined from the boundary conditions.

The relevant boundary conditions are prescribed at the outlet of the pore and at the source of vapor generation, the meniscus. The former is dependent on the ambient temperature, relative humidity and air velocity. A slow, yet sufficient air stream above the mouth would be assumed so that the mole fraction of water vapor in ambient air is the same as that at the pore mouth. The second boundary condition depends on the local skin temperature at which the vapor is generated. The temperature at the free surface location determines the vapor pressure and consequently the local evaporation rates. It is therefore necessary to determine the temperature profile along the eccrine duct. Since experimental data are unavailable, the temperature profile along the helical duct in the avascular epidermis is assumed to be the same as for the neighbouring epidermal cells. The temperature profile for the intradermal straight duct would be prescribed by the arteriole plexus surrounding it. The latter will be calculated.

On incorporating the two boundary conditions into equation (4.8) and simplifying, the following expression is obtained:

$$(1-x_A)^{\gamma^{-1}-\gamma_o^{-1}} = \frac{(1-x_{A\infty})^{\Psi^{-1}-\gamma_o^{-1}}}{(1-x_{Ao})^{\Psi^{-1}-\gamma^{-1}}} \tag{4.9}$$

where γ_o is the ratio of the radius of the channel at which the meniscus is located to the radius of the duct at dermo-epidemal junction, x_{Ao} is the mole fraction of water vapor in equilibrium with local liquid interface, and $x_{A\infty}$ is the mole fraction of water vapor at pore mouth. On rearranging equation (4.9), the mole fraction of water vapor at any position along the duct lumen is given as:

$$x_A = 1 - exp\,(Fx) \tag{4.10}$$

where

$$Fx = \frac{(\Psi^{-1}-\gamma_o^{-1})\ln(1-x_{A\infty}) - (\Psi^{-1}-\gamma^{-1})\ln(1-x_{Ao})}{(\gamma^{-1}-\gamma_o^{-1})} \tag{4.11}$$

The gradient at any location is given by:

$$\frac{dx_A}{dz} = \exp(Fx)\,\frac{\Psi^{-2}}{\gamma^{-1}-\gamma_o^{-1}}\,\frac{(\gamma-1)}{L}\ln\frac{(1-x_{A\infty})}{(1-x_{Ao})} \tag{4.12}$$

The molar flux (N_{Az}) as prescribed by equation (4.2) can thus be evaluated from equations (4.11) and (4.12). Further details on the derivation of equations are given in Appendix A.

4.3.2. Case with microvilli exposed to gases

In the foregoing, the microvilli were submerged in the liquid and do not affect vapor loss from the body. However, when the meniscus is retracted below the microvilli, these moist convex surfaces with high curvature are exposed to gases

and the water vapor in the region they occupy may be supersaturated (Thomson, 1871; Thoma, 1933). Bi-directional movement of vapor, out of the skin and down towards the meniscus, could then occur from this zone. At the meniscus, such vapor would condense to maintain the meniscus at a relatively stable position. The vapor pressure in equilibrium with the microvilli would be given by (Thompson, 1871; Keenan, 1970):

$$P_m = P_v \exp\left[\frac{2\,\sigma\,V_L}{r_m\,R\,T_m}\right] \tag{4.13}$$

where P_v is the vapor pressure above a flat surface of the solution, σ and V_L are the surface tension and the molar volume of the liquid, r_m is the radius of curvature of the curved surface, R is the universal gas constant, and T_m is the local temperature in the region of microvilli. The nature and source of the water evaporating at the site, whether it is intercellular or intracellular, is important since both P_v and V_L decrease in the presence of solutes while σ may either rise or fall (Hammel and Scholander, 1976). At 25°C, the water vapor pressure in equilibrium with connective tissue has been reported to be around 24.6 mmHg. The corresponding vapor pressure in equilibrium with a flat surface is ≈26.7 mmHg. Consequently, pure water is assumed to be vaporized from the microvilli. The ions and other solutes are assumed totally re-absorbed. A dense population of microvilli is required for supersaturated vapor to fill the duct segment. This appears to be the case from studying Zelickson's electron micrographs (1961).

4.4. The Temperature Profile Along The Eccrine Duct

The temperature at which water would evaporate from the meniscus retracted into the eccrine duct depends on the distance into the skin to which the meniscus is withdrawn. The temperature would be prescribed by the temperature profiles for the arterioles that enveloped the duct. These profiles would in turn be determined by the spatially dependent temperature patterns in the skin tissues, and properties of the blood and the vessels. It is required to obtain the temperature profile in the eccrine duct since a 1°C rise in temperature would correspond to a 6% increase in vapor pressure. For the present analysis, the intradermal duct temperature profile would be assumed equivalent to that for an adjacent 50 μm diameter arteriole.

The steady energy equation for blood flow in an arteriole traversing the dermis, in cylindrical co-ordinates, is given as (Kays and Crawford, 1980):

$$\frac{\partial^2 T}{\partial r^2} + \frac{1}{r}\frac{\partial T}{\partial r} = \frac{u}{\nu}\frac{\partial T}{\partial z} \tag{4.14}$$

where u and ν are the velocity and thermal diffusivity of blood. A two-dimensional domain is considered due to azimuthal symmetry. Equation (4.14) is non-dimensionalized as follows:

$$r^+ = \frac{r}{r_w} \tag{4.15}$$

$$z^+ = \frac{z/r_w}{\mathrm{Re}\,Pr} \tag{4.16}$$

$$\Theta = \frac{T - T_t(z)}{T_e - T_t(z)} \tag{4.17}$$

where Re and Pr are the Reynolds' and Prandtl numbers, r_w is the radius of the vessel, T_e is the blood entrance temperature, and T_t is the local tissue temperature. With the assumption of a parabolic velocity profile in the arteriole, the following equation is obtained:

$$\frac{\partial^2\Theta}{\partial r^{+2}} + \frac{1}{r^+}\frac{\partial\Theta}{\partial r^+} = (1 - r^{+2})\left[\frac{\partial\Theta}{\partial z^+} + \frac{1-\Theta}{T_e - T_t}\frac{\partial T_t}{\partial z^+}\right] \tag{4.18}$$

The boundary conditions are:

(i) at the wall, convective condition

$$-k\,\frac{\partial T}{\partial r}|_{r=r_w} = h_w\,(T_w - T_t) \tag{4.19}$$

or

$$-\frac{\partial T}{\partial r}|_{r=r_w} = \frac{Bi}{r_s}\,(T_w - T_t) \tag{4.20}$$

where the Biot number, Bi, is the ratio of actual heat conductance outside the channel to the conductance due to molecular transport alone.

(ii) at centre-line, symmetry condition

$$\frac{\partial T}{\partial r}|_{r=0} = 0 \tag{4.21}$$

(iii) at entrance, constant entrance temperature

$$T|_{z=0} = T_e \tag{4.22}$$

where k is the thermal conductivity of blood and h_w is the heat transfer coefficient of arteriole wall. Equation (4.18) is solved by a finite difference numerical technique. Details are presented in Appendix A.

The tissue temperature profile, $T_t(z)$, remains to be specified. As noted in Chapter 2, such profiles depend on both external and physiological conditions of an individual. Thus there is no universal profile. The data of Bazett and McGlone (1927) (Figure 2.3) would be assumed as representative and one of his curves was fitted by polynomial regression using the method of least squares. The experimental curve was for the forearm region when the subject was comfortable with the environment. A regression curve to the sixteenth order was found to fit the more than 20 experimental data points best. The experimental and the polynomial regression curve fit are shown in Figure 4.2 for comparison. The regression curve was applied so that numerical solutions could be compared to analytic solutions of a less involved problem. The maximum for the polynomial fit is about 3.8% lower than for the experimental data, the cusp has been rounded and the locus of the maximum has been shifted by ≈200 μm deeper into the skin. The application of the regression equation has been restricted to a distance of 3.6 mm into the skin which normally would include all of the epidermis and dermis.

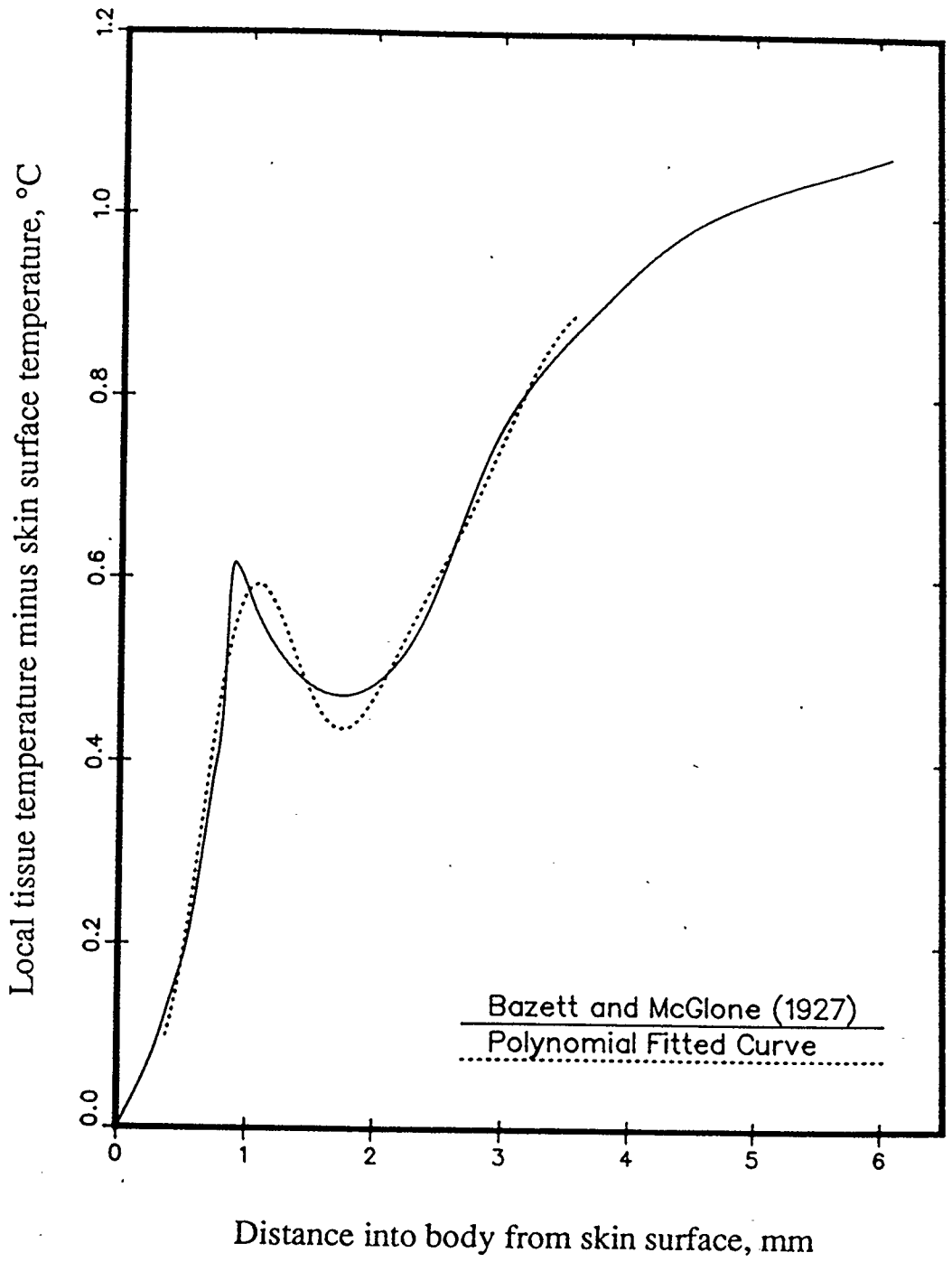

Figure 4.2 : Comparison between an experimental data curve of Bazett and McGlone (1927) and its best fit using polynomial regression. The experimental curve is for forearm and was plotted as curve b in Figure 2.3.

4.5. Case with meniscus displaced to the skin surface

When the meniscus is displaced to the skin surface, the upper limiting case of insensible perspiration, the lateral dispersion of liquid into the stratum corneum becomes significant. The stratum corneum is anisotropic, and the squamous cells from which this layer is constituted has a diameter which is approximately 50 times the thickness. These are stacked as scales and lateral migration of water should be easier than in the vertical direction normal to the skin. The water dispersed into the stratum corneum would ultimately be evaporated from the skin surface. Thus a larger surface area is made available for evaporation.

A schematic diagram of the geometry is shown in Figure 4.3. The meniscus is assumed to have a hemispherical surface and the contact angle at the wall is zero. At this limiting position, the meniscus is assumed maintained by a higher rate of secretion at the coil. The steady two-dimensional molecular diffusion of water vapor into the ambient, in cylindrical co-ordinates, may be described with the following equation:

$$\frac{1}{r}\frac{\partial(r\,N_{Ar})}{\partial r}+\frac{\partial N_{Az}}{\partial z}=0 \qquad (4.23)$$

The molar fluxes (N_{Ar} and N_{Az}) are given by expressions similar to equation (4.2), for stationary air, component B. On substituting the appropriate flux expressions into equation (4.23) and assuming constant c and D_{AB}, the following non-linear partial differential equation is obtained:

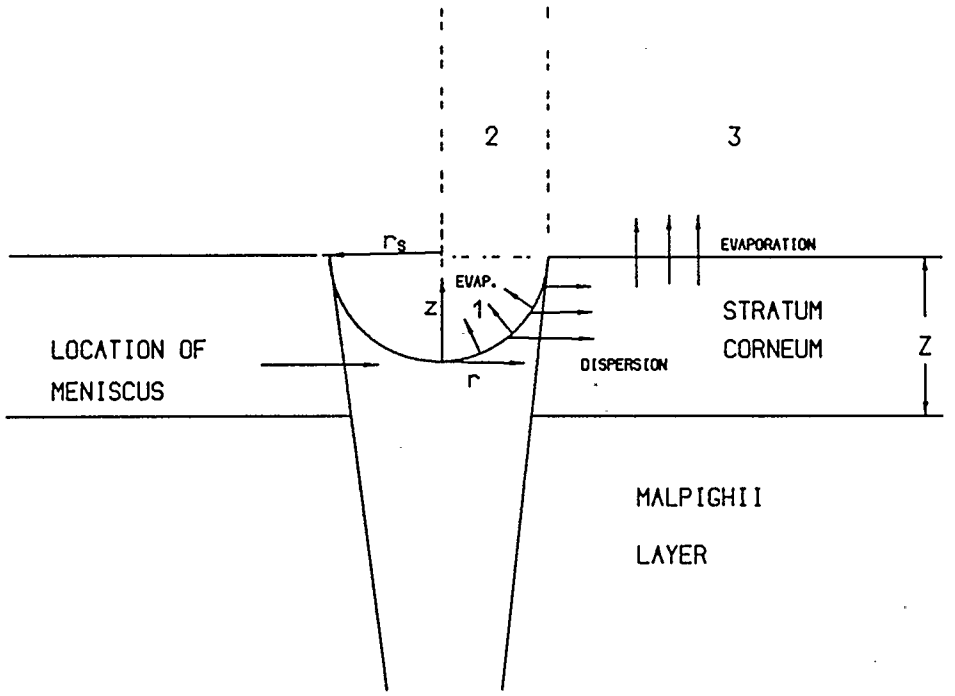

Figure 4.3 : Schematic diagram showing the model for the case when the meniscus is displaced to the skin surface. The domain of interest is divided into 3 regions as shown.

$$\frac{1}{r\,(x_A-1)}\frac{\partial x_A}{\partial r}+\frac{1}{(x_A-1)}\frac{\partial^2 x_A}{\partial r^2}-\frac{1}{(x_A-1)^2}\left[\frac{\partial x_A}{\partial r}\right]^2$$
$$+\frac{1}{(x_A-1)}\frac{\partial^2 x_A}{\partial z^2}-\frac{1}{(x_A-1)^2}\left[\frac{\partial x_A}{\partial z}\right]^2=0 \qquad (4.24)$$

Due to the microscopic size of the pore, diffusion of water vapor is treated as occurring in a semi-infinite domain. On average, the distance separating two adjacent sweat glands is ≈800 μm. Even in the palms and soles with the highest density of sweat glands (≈ $620/cm^2$; Szabo, 1962), the average distance is greater than ≈400 μm, which is more than 20 times the size of a pore. Interference between neighbouring glands is considered absent. Specialized structures such as hair follicles or sebaceous glands are assumed to present no barriers to water migration in the stratum corneum.

Equation (4.24) is solved numerically. As indicated in Figure 4.2 the domain has been divided into 3 regions. The following co-ordinate system has been applied to each:

(1) r- and z-, $0 \le r \le f_r, f_z \le z \le r_s$;

where f_r and f_z describe the distances at any point on the curved meniscus surface from the origin and they are related by:

$$f_r^2+(r_s-f_z)^2=r_s^2 \qquad (4.25)$$

The treatment for this curved boundary is shown in appendix B.

(2) In this region the z- co-ordinate goes to infinity. This co-ordinate is transformed using the following expression (Vrentas et al., 1966; Wagner, 1975):

$$\beta = \tanh(bz) \tag{4.26}$$

where "b" is a stretching parameter. Therefore the co-ordinate system in this region is given by:

$$r- \text{ and } \beta-,\ 0 \le r \le r_s,\ \ tanh(br_s) \le \beta \le 1;$$

(3) In this region both the r- and z- co-ordinates have to be transformed. The z-transformation is given by equation (4.26) and for r-, it is given by:

$$\alpha = \tanh(ar) \tag{4.27}$$

where "a" is again a stretching parameter. With a proper choice of a and b, the region near to the pore can be amplified. The co-ordinate system in this region is given by:

$$\alpha \text{ and } \beta-,\ tanh(ar_s) \le \alpha \le 1,\ tanh(br_s) \le \beta \le 1;$$

Explicit expression of (4.23) applying to each region is given in Appendix B. The appropriate boundary conditions for the whole domain would now be described:

(i) at $r = 0,\ 0 \le z \le \infty$, centre-line symmetry;

$$\frac{\partial x_A}{\partial r} = 0 \tag{4.28}$$

(ii) at r = f_r, z = f_z, constant vapor mole fraction in equilibrium with liquid interface;

$$x_A = x_{Ao} \tag{4.29}$$

(iii) at r = ∞, $r_s \leq z \leq \infty$, constant ambient vapor mole fraction;

$$x_A = x_{A\infty} \tag{4.30}$$

(iv) at z = ∞, $0 \leq r \leq \infty$, constant ambient vapor mole fraction;

$$x_A = x_{A\infty} \tag{4.31}$$

The assumption of constant $x_{A\infty}$ at r = ∞ and z = ∞ implies a large uniform reservoir surrounds the body. Air currents which would have the effect of modifying the concentration field have been neglected.

4.5.1 Boundary condition at the surface of the stratum corneum

The boundary conditions described above (4.28 - 4.31) are necessary but insufficient for the solution to equation (4.23) to be obtained. The condition at the surface of stratum corneum is required. Water is expected to infiltrate laterally from the pore into the keratinized cells of stratum corneum and be evaporated at the surface. Thus the stratum corneum acts as an extended surface for evaporation.

An important characteristic of the stratum corneum is its ability to swell upon absorbing water. The swelling may cause the duct lumen diameter to decrease. *In vitro* studies on stratum corneum from abdominal skins by Robbins and Fernee (1983) showed that the swelling is anisotropic. The surface area of the stratum corneum increases up to ≈20%, while the thickness changes by as much as 200%. This effect has not been included in this analysis. The wrinkled appearance of the palm of a hand soaked in water for a long time is a consequence of such swelling.

In vivo concentration profiles of water across the stratum corneum are unavailable. Since the layers are relatively thin (≈10 μm) in most parts of the body surfaces, the migration of water through the layer is treated as one-dimensional. The steady, one-dimensional diffusion equation governing the lateral migration of water in the stratum corneum, in conjunction with the evaporative loss into the ambient from the surface of which evaporation occurs in the neighbourhood of the eccrine pore is given as:

$$\frac{1}{r}\frac{\partial(rn_{Ar})}{\partial r}+\frac{n_{Az}}{Z}=0 \tag{4.32}$$

where Z is the thickness of stratum corneum. Mass fluxes (n_{Ar} and n_{Az}) are used in place of molar fluxes in this formulation. The mass flux terms are given by:

$$n_{Ar}=\frac{-\rho_s D_s}{1-\omega_{As}}\frac{\partial\omega_{As}}{\partial r} \tag{4.33}$$

and

$$n_{Az}=\frac{-MW_A\, c\, D_{AB}}{1-x_A}\frac{\partial x_A}{\partial z} \tag{4.34}$$

where ρ_s is the density of stratum corneum, D_s and ω_{As} are the diffusivity and mass fraction of water in stratum corneum, and MW_A is the molecular weight of water. Both ρ_s and D_s are strong functions of ω_{As} and therefore could not be treated as constants. Data on abdominal skin patches reported by Blank et al. (1984) would be used. Figure 4.4 shows the correlation between the density of stratum corneum (ρ_s) and the mass fraction of water bound in the stratum corneum (ω_{As}) at 31°C. Blank et al. (1984) assumed that the volume of the wet stratum corneum is the sum of its dry volume and the volume of the absorbed water. Absorption compression of the bound water makes this assumption improbable. Blank et al. (1984) also assumed implicitly that equimolar counter-diffusion occurred in the tissues, i.e., n_A = -n_B. Water is the only component in transit. Thus the calculated diffusion coefficient values, D_s, have to be modified. Diffusivity values of water in stratum corneum corrected for the mass fraction are presented in Figure 4.5. These values were obtained by dividing the original values with (1-ω_A). A further adjustment to these

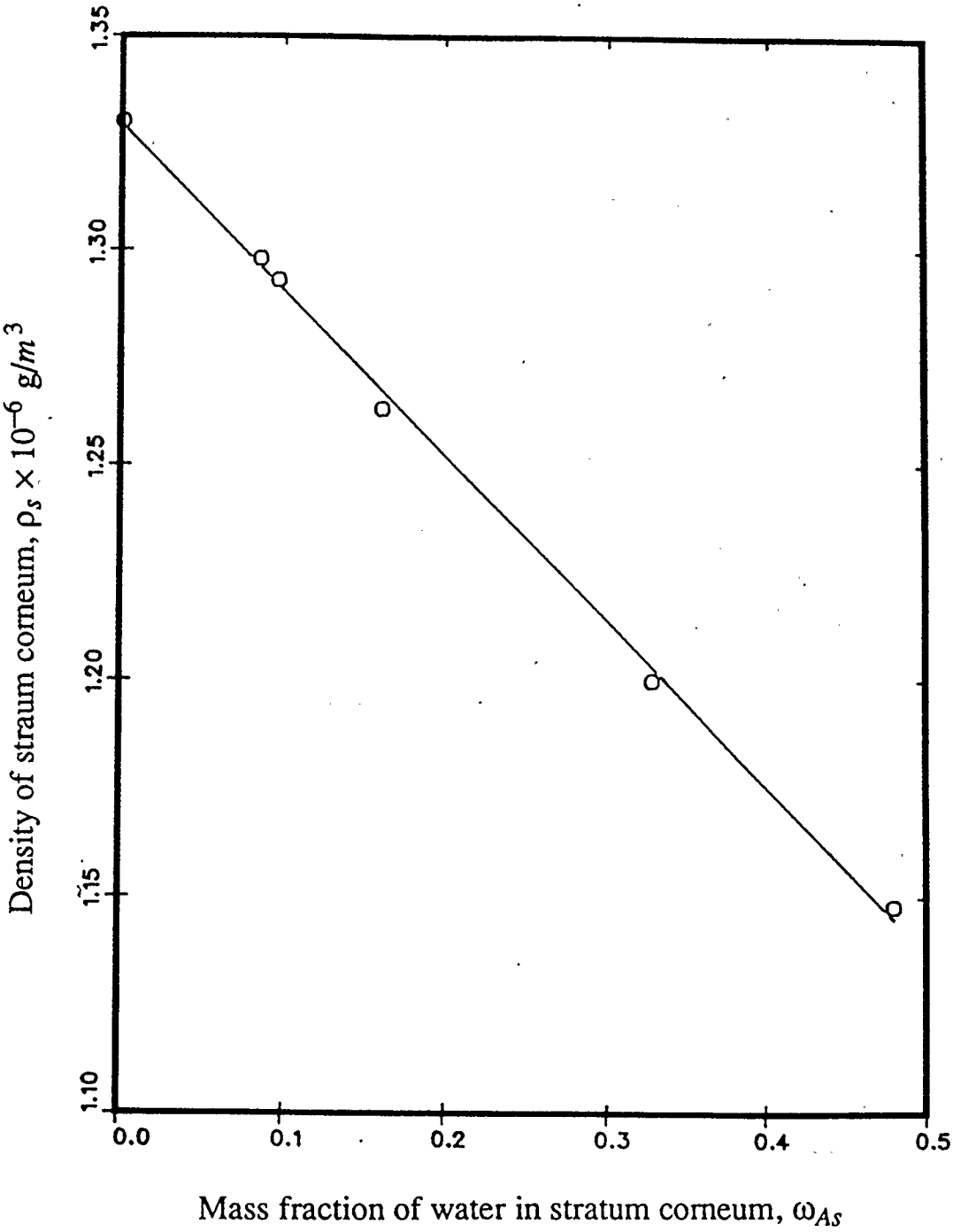

Figure 4.4 : Density of stratum corneum vs. mass fraction of water in stratum corneum. Data from *in vitro* studies of Blank et al. (1984).

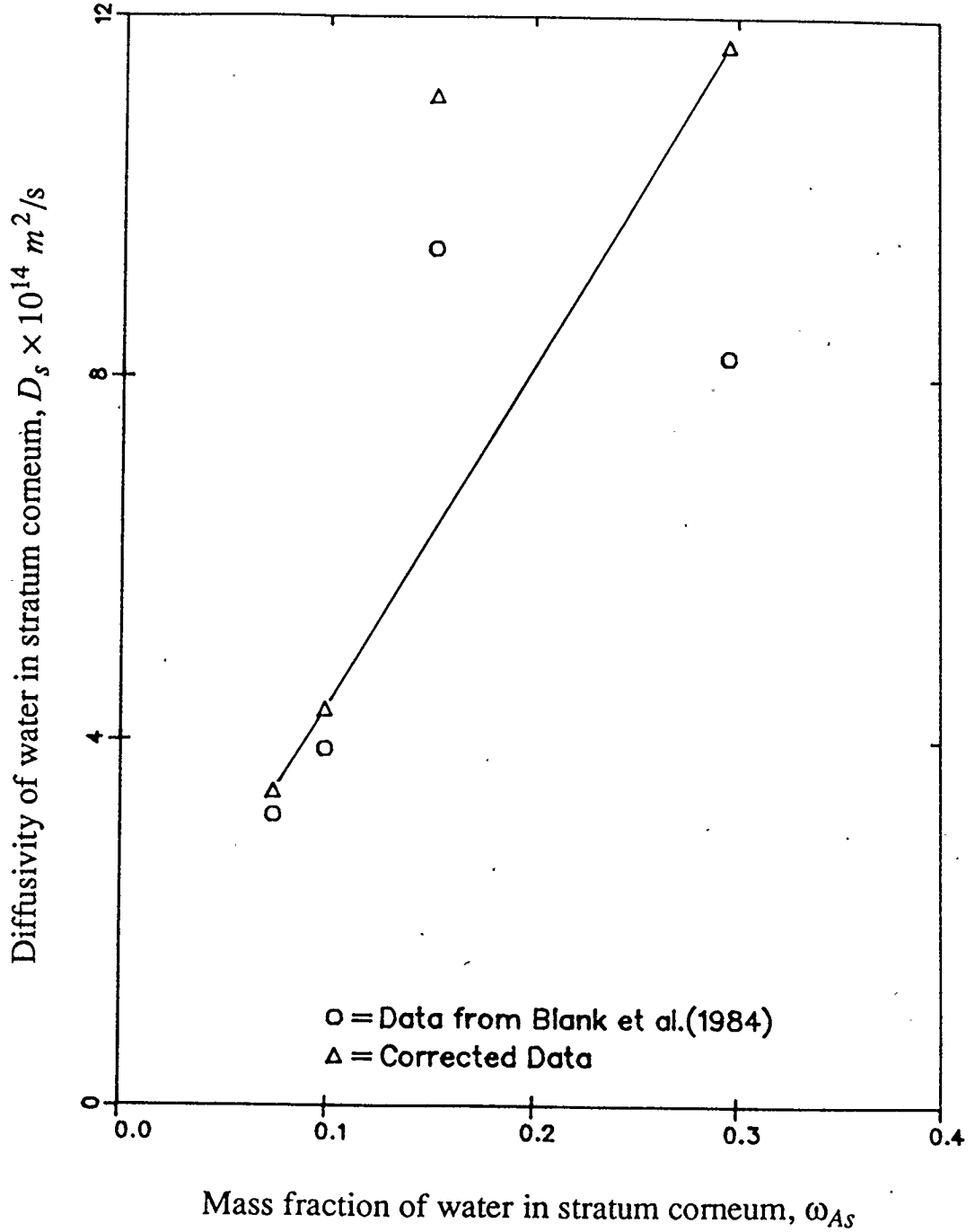

Figure 4.5 : Diffusivity of water in stratum corneum vs. mass fraction of water in stratum corneum. The original data by Blank et al. (1984) and their corrected terms are shown.

values was made because migration of water in the lateral direction of interest is not as restricted as in the direction normal to the layer for which the data was collected. The coefficient in any direction is assumed to be inversely proportional to the corresponding length of a dead keratinocyte cell in that direction. This adjustment, on geometrical considerations, is based on the premise that major resistances to diffusion reside inter-cellularly rather than intra-cellularly. A typical cell is 25 μm wide and 0.5 μm thick (Tregear, 1972). Value for the diffusion coefficient in the lateral direction is therefore taken to be 50 times the value in the vertical direction.

The r- and z- co-ordinates are transformed into the α- and β- co-ordinates using expressions (4.26) and (4.27), to be consistent with the co-ordinates used in region 3 of the domain. The boundary conditions prescribing (4.32) are:

(i) at $z = r_s$, $r = r_s$, constant mass fraction in stratum corneum in equilibrium with sweat liquid interface;

$$\omega_{As} = \omega_{Aso} \tag{4.35}$$

(ii) at $z = \infty$, $r = r_s$, constant mass fraction in stratum corneum in equilibrium with ambient vapor mole fraction;

$$\omega_{As} = \omega_{As\infty} \tag{4.36}$$

Both conditions are evaluated at skin surface temperatures. The first boundary condition corresponds theoretically to maximal hydration in stratum corneum. It has, however, been demonstrated that a piece of stratum corneum, if left alone for

days, can absorb water to many times its own weight before disintegrating. Such conditions are not expected to be encountered for living skin. The data reported by Spencer et al. (1975) were used. The equilibrium data were obtained at 20, 30 and 35°C ambient temperatures. The data has been re-plotted in terms of the mass fraction of water in stratum corneum versus the mole fraction of water in ambient gases. The results are presented in Figure 4.6. At other temperatures, interpolation was applied.

Equation (4.23) with the appropriate boundary conditions is solved using finite difference numerical technique involving the Newton-Raphson method. The Jacobian matrix were evaluated each time by the iterative method of Gauss-Seidel with Successive-Over-Relaxation (Smith, 1965). The results are presented in the following chapter.

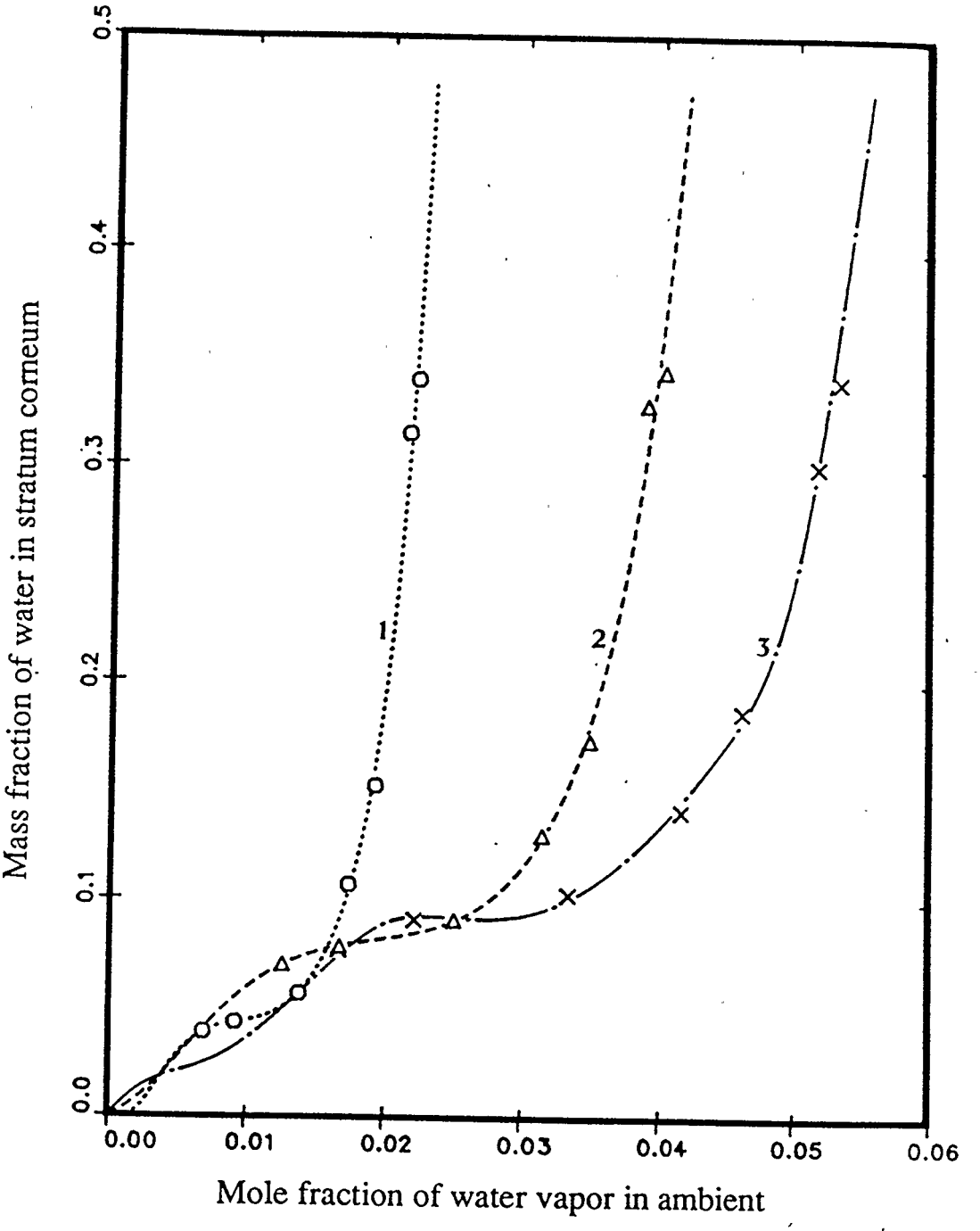

Figure 4.6 : Mass fraction of water in stratum corneum vs. mole fraction of water vapor in ambient. Data from *in vitro* studies of Spencer et al. (1975) at 20 (curve 1), 30 (2) and 35 (3) °C.

CHAPTER FIVE

RESULTS

The concentration profiles in and rates of water loss from single eccrine glands with characteristic dimensions are presented in this chapter. Total insensible water loss rates (Q_A) for the three million glands indicated to be in the skin were then estimated on an assumption of equal physiological performance and similar anatomy. Such rates could then be compared to experimental results in the literature. The effects of variations in internal and external factors are also examined.

5.1. Case of sweat liquid withdrawn below the skin surface

The water vapor concentration profiles within the helical duct for four boundary conditions are shown in Figure 5.1. The concentration profiles are non-linear along the duct lumen. The conditions chosen for the calculations were an ambient temperature (T_∞) of 25°C, the pore mouth radius (r_s) of 7.5 μm and the duct radius (r_o) at dermo-epidermal boundary of 1.5 μm. The latter two figures indicate a divergence ratio (γ) of 5. The diffusivity of water vapor in air at 25°C was found (Perry and Chilton, 1973) to be $\approx 2.62 \times 10^{-4}$ m^2/s and the concentration of the gas mixture was calculated to be 40.87 gmol/m^3. The overall length of the duct was taken as 800 μm.

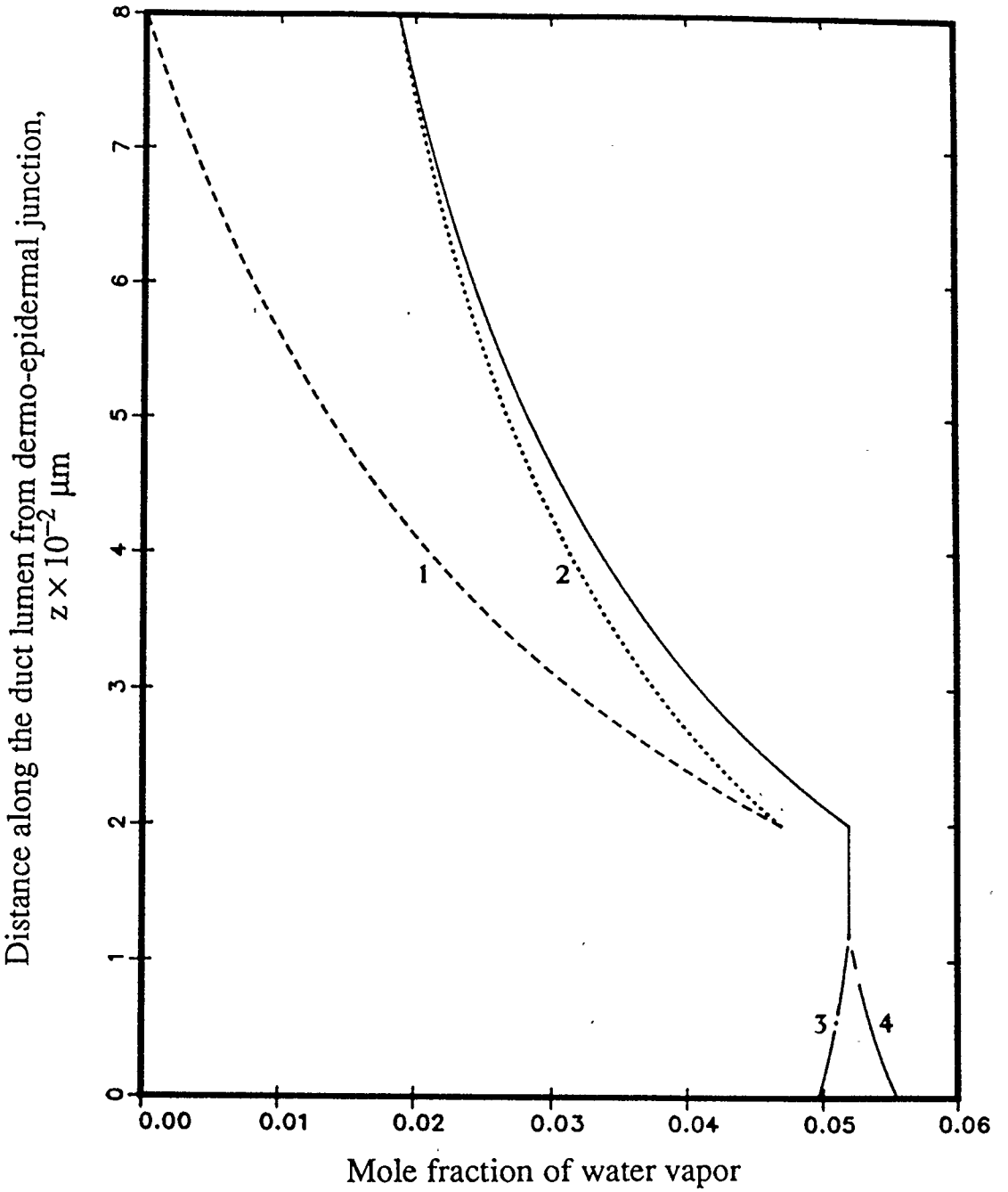

Figure 5.1 : Concentration profiles for water vapor in the helical duct of an eccrine gland. For curves 1 and 2, the meniscus was located at a linear distance (z_o) in the duct of 200 μm from the dermo-epidermal boundary. The vapor would diffuse through a distance of 600 μm in the epidermis which may only be 50 μm thick. The microvilli are assumed submerged in sweat liquids. For curves 3 and 4, the meniscus is retracted to the dermo-epidermal junction. The conditions for the curves are : 1 - meniscus temperature (T_o) = 32°C, ambient temperature (T_∞) = 25°C and ambient relative humidity (RH) = 0%; 2 - T_o = 32°C, T_∞ = 25°C and RH = 60%; 3 - T_o = 33°C, T_∞ = 25°C, RH = 60%; 4 - T_o = 35°C, T_∞ = 25°C and RH = 60%. For all the curves, the lumen divergence ratio (γ) was 5 along the length of duct.

For curve 1 in Figure 5.1, the meniscus was located at 200 μm along the duct lumen from the dermo-epidermal junction, i.e., such that the microvilli are just submerged in the liquid. The temperature at the location of meniscus (T_o) was 32°C and the ambient relative humidity (RH) was taken at the extreme value of 0%. The water loss rate (Q_A) estimate is ≈1.2 g/hr for 3 million glands at these conditions. Curve 2 is for similar conditions but at a relative humidity of 60%. For this case Q_A is ≈0.7 g/hr, or 58% of the value for curve 1.

For curves 3 and 4, the meniscus was located at the dermo-epidermal junction. Thus the microvilli are now exposed to the gases. The microvilli are assumed to occupy 10% of the total length of the duct and the base is 15% above the dermo-epidermal boundary. For the calculations, the microvilli had a 0.01 μm radii (r_m) and were at 32°C. At this temperature, the surface tension (σ) and molar volume (V_L) of liquid water are 0.071 N/m (Weast, 1976) and 1.81 x 10^{-5} m^3/gmol respectively. Using equation (4.13) the supersaturated vapor pressure in the region of microvilli (P_m) is ≈1.106 P_v. This is ≈1.71 mmHg higher than at the meniscus at 33°C. Thus the flux of vapor for curve 3 is both out of the skin and towards the meniscus where condensation would occur. The inward flux would effectively regulate the position of the meniscus while the rate of flux out of the skin would be constant irrespective of the position of the meniscus as long as other conditions remain unchanged. Q_A was calculated to be ≈0.84 g/hr, or 20% higher than that for curve 2. The conditions for both cases (2 and 3) are otherwise identical. For curve 4, the temperature at the location of the meniscus (T_o) was 35°C. In this case water

evaporates from the meniscus. Part of the vapor would condense on the microvilli, with the rest diffusing outward.

The effect of the location of the meniscus along the duct lumen from the dermo-epidermal boundary is shown in Figure 5.2. The meniscus position was varied from 200 to 750 μm along the duct lumen from the dermo-epidermal junction. Other conditions are : T_o = 32°C; T_∞ = 25°C; RH = 60%; γ = 5. The curve shows that the water loss rate increases slowly and almost linearly in the first 250 μm, after which the increment is exponential and rapid. Therefore when the meniscus is normally retracted into the duct below the stratum corneum, Q_A would vary between 1 to above 20 g/hr, for the specified ambient comditions.

The effect of the ambient water vapor content on the rate of water loss is shown in Figure 5.3. The two curves presented are for the meniscus at 32 and 34°C respectively, other conditions being as follows : T_∞ = 25°C; Z_o = 200 μm; γ = 5. As expected, the vapor loss varies linearly with the ambient water vapor concentration. For the conditions given, a 10% increase in relative humidity reduces Q_A by about 0.08 g/hr. The higher water loss for T_m at 34°C corresponds with the increase in vapor pressure, which is about 12%.

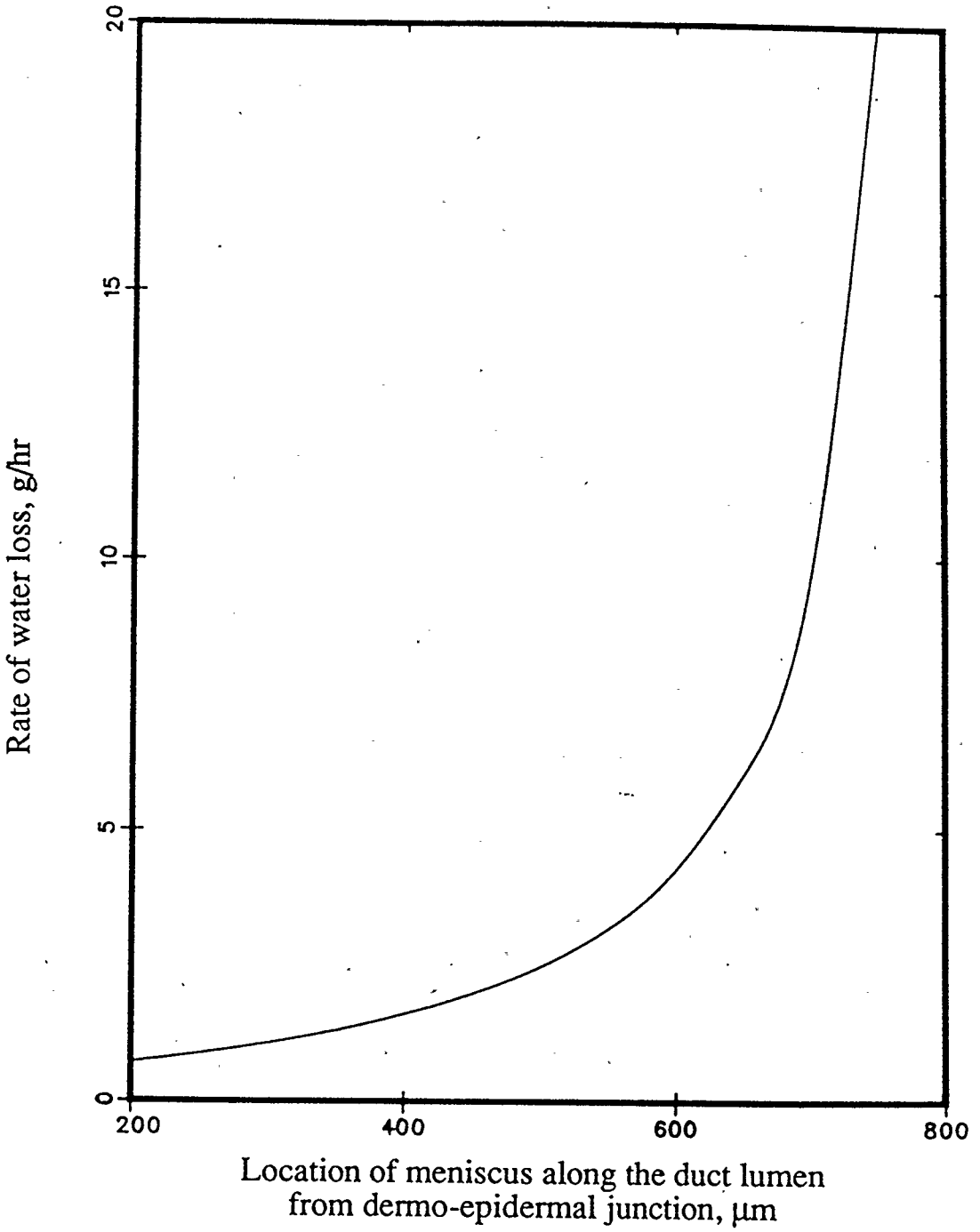

Figure 5.2 : Estimated rates of water loss from 3 million eccrine sweat glands vs. the location of meniscus along the helical duct lumen from the dermo-epidermal boundary. The helical duct diameter increased from 3 to 15 μm from the boundary to the pore mouth. The meniscus was within the epidermis at 32°C, the ambient temperature and relative humidity were 25°C and 60% respectively. The rates of water loss were essentially constant at ~1 g/hr for the menisci retracted below the dermo-epidermal boundary.

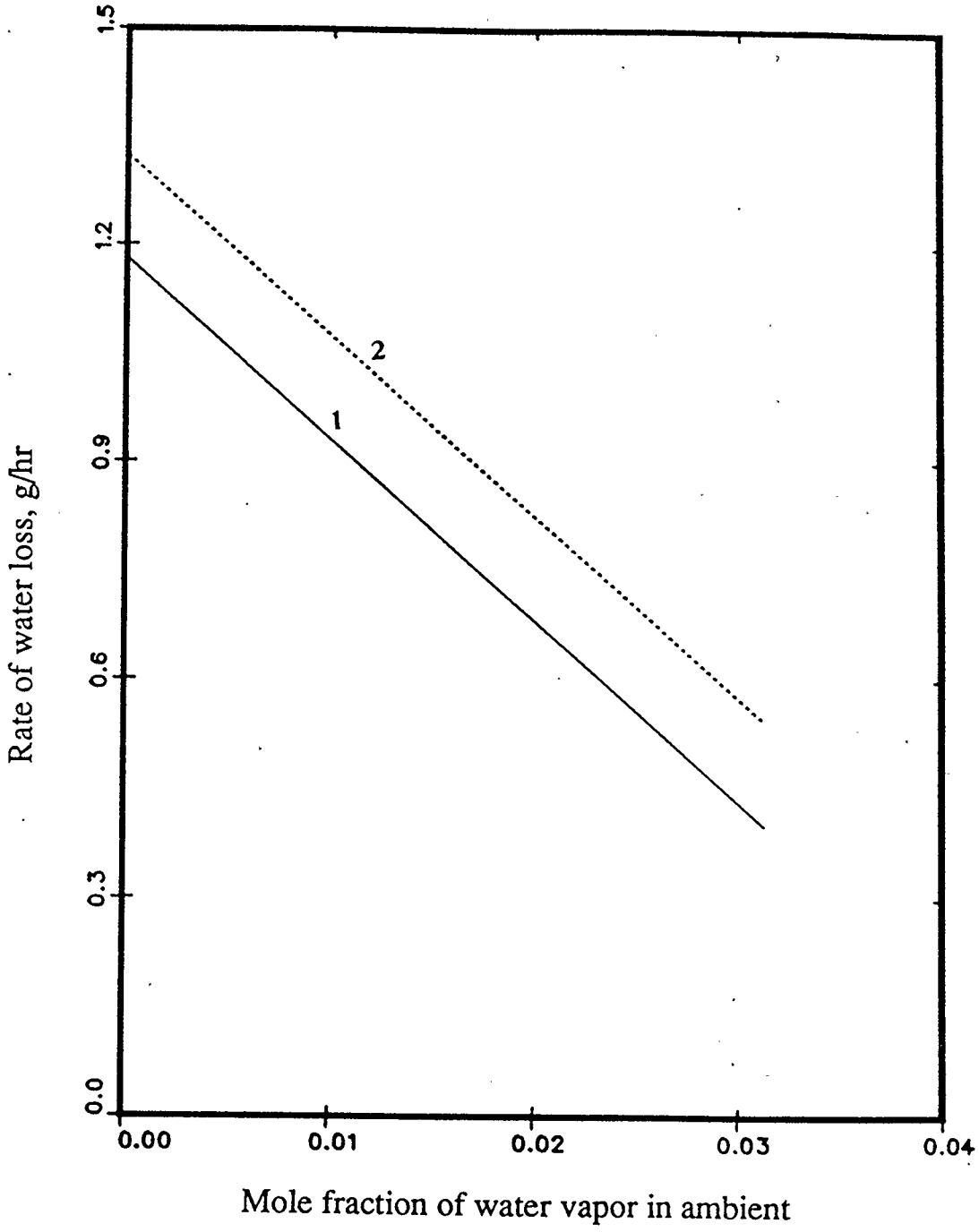

Figure 5.3 : Estimated rates of water loss from 3 million eccrine sweat glands vs. mole fraction of water vapor in ambient. The two curves are for meniscus temperatures of 32 (curve 1) and 34°C (curve 2) respectively. For both curves, z_o = 200 μm, $\gamma = 5$, and $T_\infty = 25$°C.

The effect of the change in divergence ratio (γ) was also examined. This change can be accomplished by either a change in the straight duct diameter (r_o) or the pore rim diameter (r_s). Figures 5.4 and 5.5 show respectively the effects of variations in r_o and r_s on Q_A. The conditions are : T_o = 32°C; T_∞ = 25°C; RH = 60%. For the former graph r_o was varied from 0.5 to 3 μm, equivalent to a change in γ from 15 to 2.5, For the latter r_s was varied from 4.5 to 15 μm, corresponding to a change in γ from 3 to 10. From Figure 5.4 it is observed that Q_A increases linearly with r_o. Extrapolating the curve towards the y-intercept indicates that a water loss of ≈0.4 g/hr exists when $r_o \rightarrow 0$. Equation (4.4) is not valid at this extreme since γ also approaches infinity. The results, nonetheless, indicates that even when the straight duct lumen is highly constricted, appreciable water loss persists. A widening of the pore mouth indicates a more complex relationship between Q_A and r_s. The curve is not linear but passes through the origin when extrapolated.

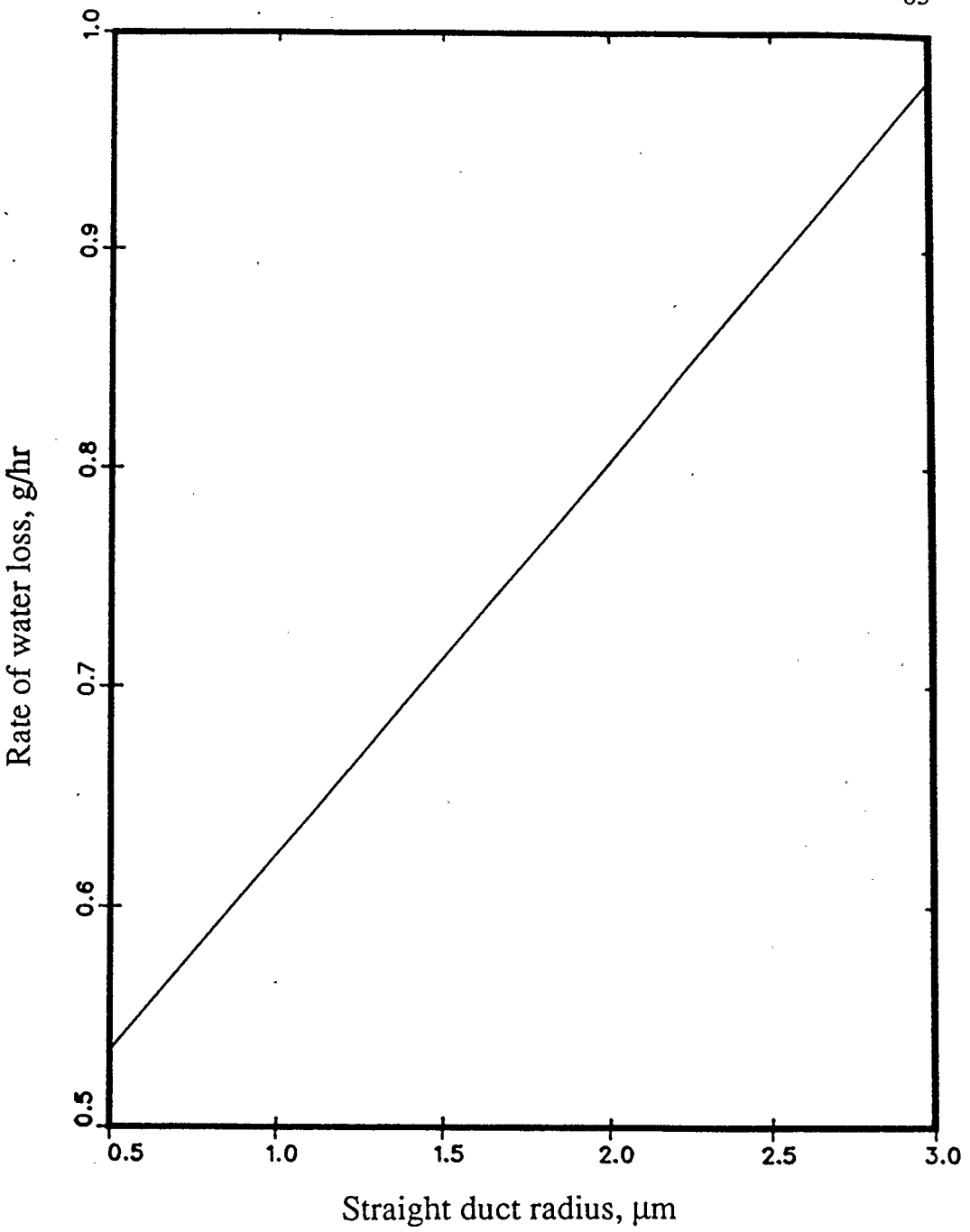

Figure 5.4 : Estimated rates of water loss from 3 million eccrine sweat glands vs. straight duct radius (r_o). The straight duct radius was varied from 0.5 to 3 μm, equivalent to a change in lumen divergence ratio (z_o) from 15 to 2.5. Other conditions are : z_o = 200 μm, T_o = 32°C, T_∞ = 32°C and RH = 60%.

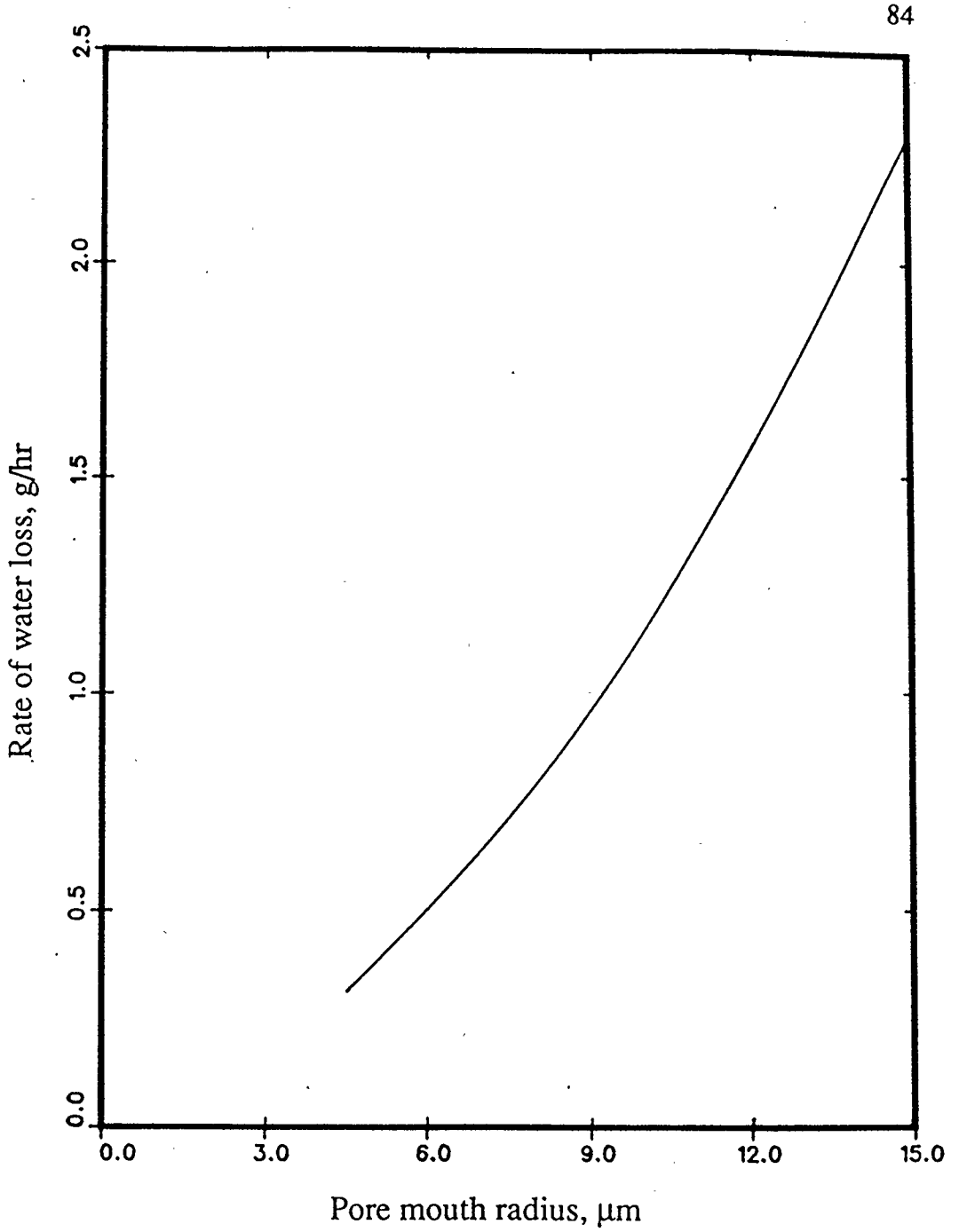

Figure 5.5 : Estimated rates of water loss from 3 million eccrine sweat glands vs. pore mouth radius (r_s). The pore mouth radius was varied from 4.5 to 15 μm, equivalent to a change in lumen divergence ratio (z_o) from 3 to 10. Other conditions are the same for Figure 5.4.

5.1.1. The basis for elevated temperatures and vapor pressures at retracted meniscus surface

The temperature at the site of evaporation is higher than at the skin surface because of the vascular arrangement. As earlier noted, to determine the temperature profile along the straight intradermal eccrine duct, equation (4.18) was solved using the finite difference numerical scheme. The equations were solved by the method of Newton-Raphson, with the linearized equations in the Jacobian matrix calculated iteratively by the Gauss-Seidel scheme and with successive-over-relaxation (SOR).

The question remains as to whether the solution given by the finite difference method approximates the exact solution of the partial differential equation. Two problems are always posed, the convergence and the stability of the approximated solution. (A set of finite difference equations is said to be convergent when the exact solution of the difference equations approaches to the exact solution of the partial differential equation as the grid sizes tend to zero. The difference between the two solutions is often referred to as the discretization error (Smith, 1965).) The investigation of convergence is difficult since the expression for the discretization error is often in terms of unknown derivatives for which no upper or lower bounds can be estimated. In practice, the use of finite number of digits also introduces round-off errors to the finite difference equations. A set of finite difference equations is therefore said to be convergent when the cumulative effect of all the rounding errors is negligible (Smith, 1965). Standard methods of investigating stability

mainly study the growth of an isolated error or a single row of errors (Crank, 1979). Due to the rigor involved in analyzing the problem of convergence and stability, the conditions for the two issues were not studied. The solutions to simpler formulations were compared with the corresponding analytic solutions. Efforts were made to minimize round-off and discretization errors.

The convergence requirement for successful Newton-Raphson operation at any mesh point ($i\Delta r, j\Delta x$) is defined as:

$$\varepsilon_N = \left| \frac{d\Theta_{i,j}}{d\Theta_{i,j} + \Theta_{i,j}} \right| \tag{5.1}$$

where $d\Theta$ is the solution vector for the Jacobian matrix. ε_N was set at $1x10^{-6}$ throughout the calculations. Using $\varepsilon_N = 1x10^{-5}$ apparently did not change the results, up to 5 significant figures. Relaxation factor (κ) for SOR ranged between 1 to 1.5, depending on the values of Biot Number (Bi) and blood velocity (u). Criterion for terminating the Gauss-Seidel iteration is given as:

$$\varepsilon_I = \left| d\Theta^*_{i,j} - d\Theta_{i,j} \right| \tag{5.2}$$

where the superscript * refers to a newly updated value. For successful convergence, the above criterion must be satisifed for every mesh point. Value of $\varepsilon_I = 1x10^{-8}$ was used throughout. This limit is more rigorous than that for ε_N since the accuracy in Newton-Raphson operation depends highly on the accuracy of the solution vector in the Jacobian matrix. Results using $\varepsilon_I = 1x10^{-7}$ were the same up to 4 significant figures.

Double precision storage was used throughout to reduce round-off errors. Discretization errors were minimized by selectively choosing a large mesh size, while keeping the computational time to a reasonable level. An 11x501 mesh size was used. This is so chosen since the primary objective is to obtain profiles of the bulk or mixed-cup temperatures (T_b) along the duct. Hence the variation in the longitudinal (z-) direction is more important than that in the radial (r-) direction. A comparison of results using 3 different mesh sizes is shown in Table 5.1.

The results from the foregoing analysis are shown in Figure 5.6 for the arteriolar flow of 1 and 5 cm/s, and Biot numbers (Bi) between 0.1 to infinity. The blood temperature was 36.25°C as it entered the dermis, 3.12 mm into the body from the skin surface. For the calculations, the blood density was set at 1.06 g/cm^3, the blood viscosity at 2.19 cp, and the blood heat capacity at 3.8 kJ/kgK (Altman and Dittmer, 1971). Thermal conductivity of 0.63 W/mK was used for the dermal tissues, giving a Prandtl number (Pr) of 13.21. Reynolds' number corresponding to blood velocity of 1 and 5 cm/s are 0.24 and 1.21 respectively. These numbers compare favorably with values tabulated for dogs (Caro et al., 1978) although the canine blood viscosity would be about 5 times higher (Altman and Dittmer, 1971).

z (mm)	r^+	11x101		11x501		21x501	
		Θ	T (°C)	Θ	T (°C)	Θ	T (°C)
0.031	0	0.9547	36.158	0.9666	36.182	0.9673	36.184
0.031	1	0.7263	35.696	0.7157	35.675	0.7172	35.678
0.780	0	0.07546	34.178	0.07510	34.177	0.07511	34.177
0.780	1	0.05433	34.131	0.05407	34.130	0.05416	34.131
1.560	0	0.002886	33.913	0.002868	33.913	0.002863	33.913
1.560	1	0.001801	33.911	0.001788	33.911	0.001785	33.911
2.090	0	-0.01946	33.997	-0.01941	33.997	-0.01942	33.997
2.090	1	-0.01380	34.009	-0.01377	34.009	-0.01379	34.009
3.120	0	0.04038	33.563	0.04061	33.564	0.04063	33.564
3.120	1	0.02972	33.533	0.02989	33.534	0.02995	33.534

Table 5.1 : Comparison of results using different mesh sizes for the temperature profile along an eccrine duct. Conditions for the calculations are : Re = 1.21; Pr = 13.21; Bi = 1; u = 5 cm/s.

Note : z = distance from dermo-subcutaneous boundary towards skin surface, $r^+ = r/r_w$ and $\Theta = (T - T_t(z))/(T_e - T_t(z))$.

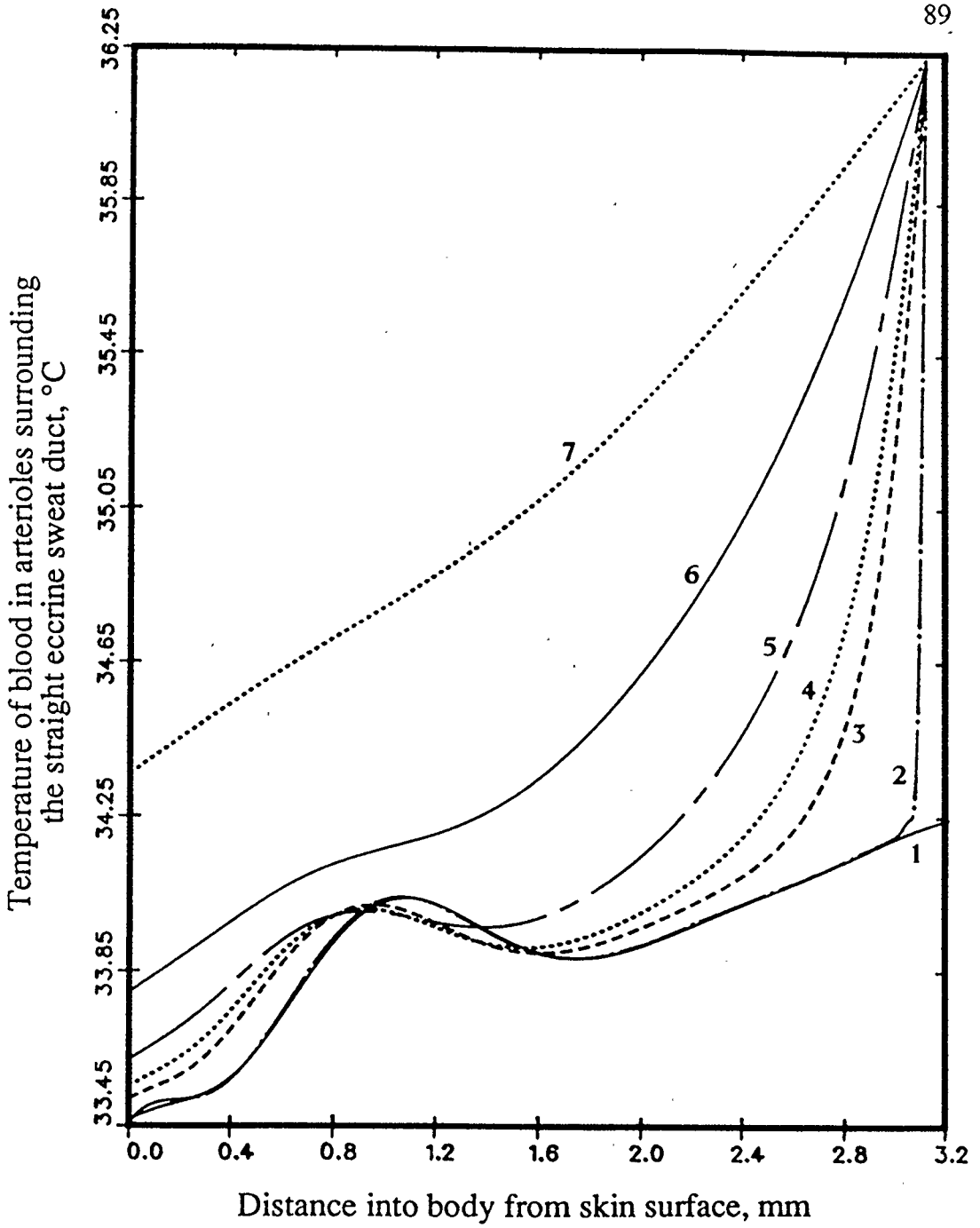

Figure 5.6 : Profiles of mix-cup temperatures of the blood flowing through a 50 μm diameter arteriole adjacent to the straight intradermal eccrine sweat duct in the forearm. The duct is surrounded by such arterioles and is thus heat-stationed. The blood entered the dermis at 36.25°C. The epidermal thickness fro the forearm is ≈0.05 mm and a discontinuous temperature jump would be anticipated at this location. Curve 1 is the regression fitted profile. The conditions for the other curves are as follows: curve 2 - Biot number (Bi) = ∞, velocity of blood in arteriole (u) = 1cm/s; 3 - Bi = 0.25, u = 1cm/s; 4 - Bi = 1.0, u = 5 cm/s; 6 - Bi = 0.25, u = 5cm/s, 7 - Bi = 0.1, u = 5cm/s.

The Biot number value cannot be readily prescribed since the displacement rates of plasma fluids into the connective tissues are unavailable. Consequently a range of Bi was used. For Bi = ∞ the arteriole wall temperature would become identical to the local tissue temperature. An infinite Bi was approximated by imposing a sufficiently large value ($1x10^{10}$).

The profiles indicate that the sweat duct would be warmer than the surrounding tissues and liquid retracted to this region would have a higher vapor pressure than that at the skin surface temperature. A discontinuous temperature jump at the dermo-epidermal junction located at $\approx$100 μm below the skin surface, except in palms and soles where the epidermis is thick, is suggested by the fact that the epidermis is avascular. Hence the helical coil in the epidermis would have essentially the same temperature as the corresponding tissue.

5.2. Case for meniscus at pore rim

The results for the case when the meniscus is situated at the pore rim are now presented. Equation (4.23) for the different regions of the domain, coupled with the appropriate boundary conditions, was solved by the method of Newton-Raphson with Gauss-Seidel iteration and with SOR. Value of 1.65 was used for the relaxation factor κ and double precision storage was maintained throughout the computations. The necessary convergence criterion for Newton-Raphson operation at any mesh point ($i\Delta r$ or $i\Delta\alpha$, $j\Delta z$ or $j\Delta\beta$) is given as:

$$\varepsilon_N = \left| \frac{dx_{Ai,j}}{dx_{Ai,j} + x_{Ai,j}} \right| \tag{5.3}$$

where dx_A is the solution vector for the Jacobian matrix. ε_N was set at $1\text{x}10^{-6}$. Results using $\varepsilon_N = 1\text{x}10^{-5}$ are identical. For the iteration of the linear equations in the Jacobian matrix, the convergence for any point (i,j) is defined as:

$$\varepsilon_I = \left| dx^*_{Ai,j} - dx_{Ai,j} \right| \tag{5.4}$$

where the superscript * stands for a newly iterated value. ε_I was set at $1\text{x}10^{-8}$. Results using $\varepsilon_I = 1\text{x}10^{-9}$ are the same up to 4 significant figures.

A 61x61 mesh size was used in the calculations. The mesh is divided as follows:

$$For\ 0 \le r \le r_s,\quad i = 0,...,20$$

$$For\ r_s \le r \le \infty,\quad i = 20,...,60$$

$$For\ 0 \le z \le r_s,\quad j = 0,...,20$$

$$For\ r_s \le z \le \infty,\quad j = 20,...,60$$

Values of the two constants a and b in equations (4.27) and (4.26) were set at 4.95×10^4. They were so chosen such that the regions 2 and 3 in Figure 4.3 would be close to the pore, and the discretization error due to a change in the co-ordinates, as going from region 1 to 2 or region 2 to 3, would be minimized. That is, the grid sizes from i = 20 to 21 and i = 21 to 22 are the same. A similar situation occurs from j = 20 to 21 and j = 21 to 22. Table 5.2 shows a comparison of results using 2 other different mesh sizes, 51x51 and 71x71. For both of these cases, the mesh size in region 1, i.e., the spaces above the meniscus but below the skin surface, was maintained at 21x21.

r^+	z^+	51x51 x_A	61x61 x_A	71x71 x_A
0.0	0.5	0.03691	0.03711	0.03722
0.5	0.5	0.03944	0.03958	0.03967
0.0	1.0	0.03547	0.03569	0.03582
0.25	1.0	0.03577	0.03599	0.03612
0.5	1.0	0.03680	0.03700	0.03712
0.75	1.0	0.03911	0.03926	0.03935
1.0	1.05	0.04182	0.04193	0.04199
1.05	1.0	0.04218	0.04229	0.04236
1.05	1.05	0.03990	0.04005	0.04014
q_{Apr}		9.371×10^{-9}	9.183×10^{-9}	9.069×10^{-9}
q_{Asc}		6.085×10^{-9}	5.977×10^{-9}	5.912×10^{-9}

Table 5.2 : Comparison of results using different mesh sizes for the case when the meniscus is at pore rim. Conditions for the calculations are : T_∞ = 25 °C, RH = 60%, T_s = 32 °C, r_s = 7.5 μm, Z = 10 μm.

Note : $r^+ = r/r_s$; $z^+ = z/r_s$; q_{Apr} = rate of water loss from the pore, g/gland-hr. q_{Asc} = rate of water loss from the stratum corneum, g/gland-hr.

Results using the foregoing analysis are shown in Figures 5.7 - 5.10. The curves in Figure 5.7 show the rates of total water loss, Q_A (curves 1 and 2), the rates of water loss from pores, Q_{Apr} (curves 3 and 4), and the rates of water loss from surfaces of stratum corneum, Q_{Asc} (curves 5 and 6) as a function of the ambient water vapor content at 32 and 34°C skin surface temperatures. The rates were calculated assuming a total of 3 million glands. Conditions for the calculations are: ambient temperature, T_∞ = 25°C; pore radius, r_s = 7.5 μm; and stratum corneum thickness, Z = 10 μm. The results predict a total water loss rate of between 90 to 260 g/hr at T_s = 32°C. At this particalur T_s, the contribution by the stratum corneum (Q_{Asc}) varies from 41% of the total (Q_A) at 10% RH to 44% of the total at 100% RH. Thus the proportion of Q_{Asc} is moderately greater at higher ambient relative humidity. Similar trends are observed when T_s = 34°C, except that the ratio of Q_{Asc}/Q_A is about 2.5% lower. For a 2°C difference in T_s, Q_A differs by 25 to 30 g/hr. That is, for every °C rise in T_s, Q_A increased by ≈ 10%.

The effect of skin surface temperature (T_s) on water loss rates is shown in Figure 5.8. At T_∞ = 25°C, 60% RH, Q_A increases from 140 g/hr at T_s = 30°C to 230 g/hr at T_s = 35°C, averaging 10% increase for every °C rise. The increase in water loss from the pore is higher than that from the stratum corneum. This results in a change in the ratio of Q_{Apr}/Q_A from ≈56% at T_s = 30°C to ≈58% at T_s = 35°C.

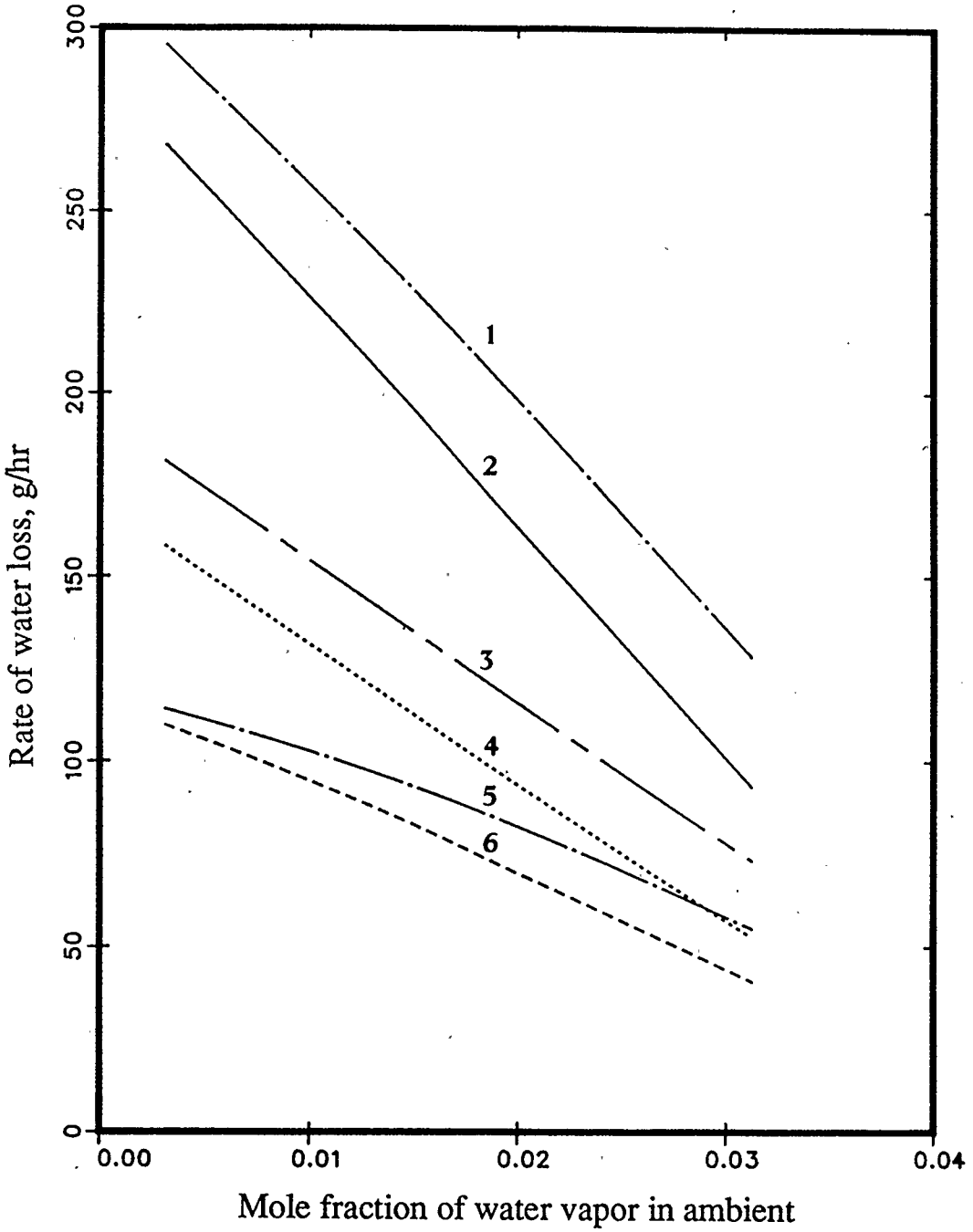

Figure 5.7 : Estimated rates of water loss from 3 million eccrine sweat glands vs. mole fraction of water vapor in ambient when the meniscus is displaced to the skin surface. Curves 1 and 2 are the total losses when the skin surface temperature (T_s) was 34 and 32°C respectively. For curve 1 the loss from the pore and the stratum corneum are shown separately as curves 3 and 5. Similarly curves 4 and 6 are the separate loss from the pore and the stratum corneum for curve 2. Conditions for curves 1 and 2 are : pore radius (r_s) = 7.5 μm, stratum corneum thickness (Z) = 10 μm, ambient temperature (T_∞) = 25°C.

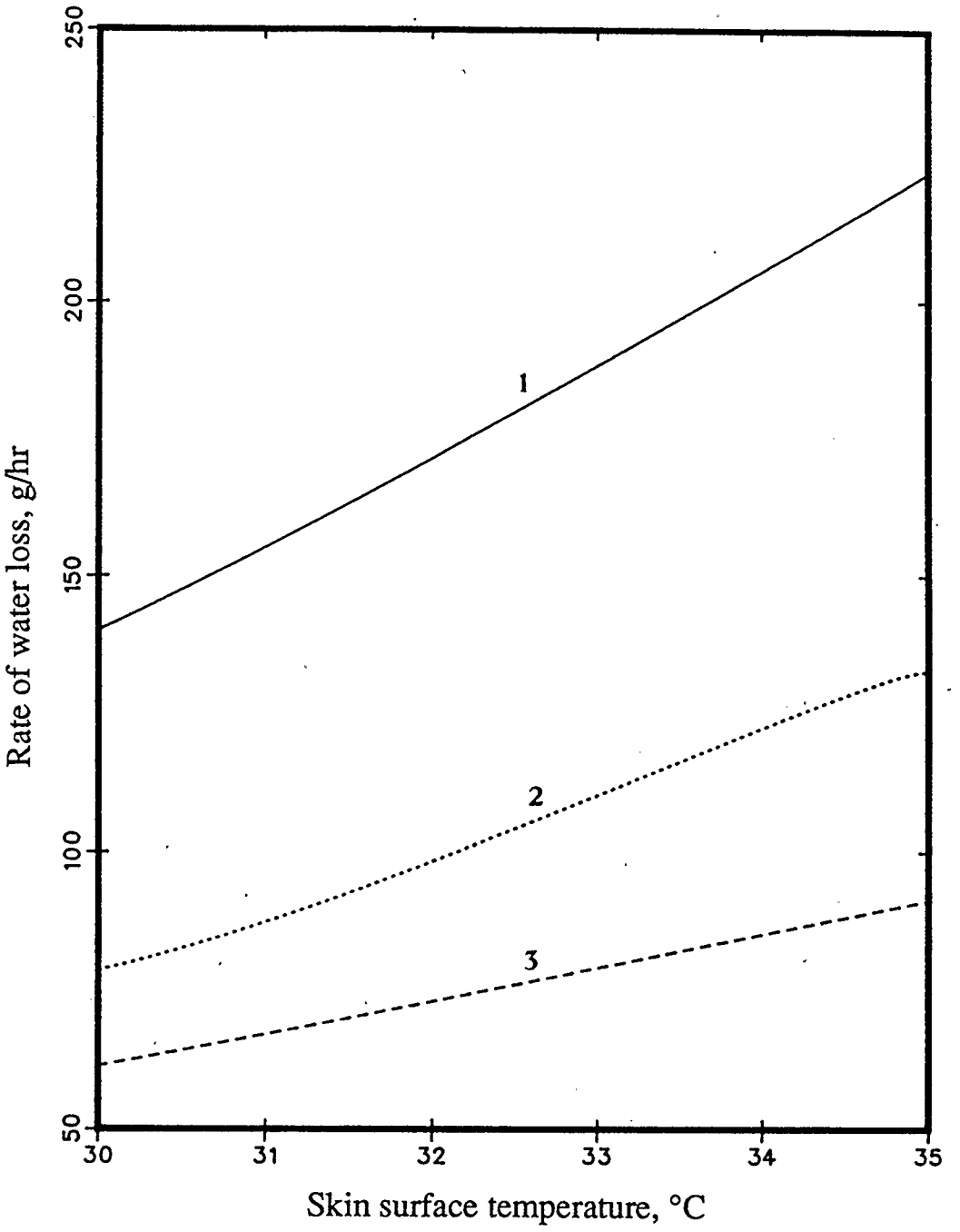

Figure 5.8 : Estimated rates of water loss from 3 million eccrine sweat glands vs. skin surface temperature when the meniscus is displaced near to the skin. Total loss (Q_A) (curve 1), loss due to pores (Q_{Apr}) (curve 2) and loss due to stratum corneum (Q_{Asc}) (curve 3) are shown. The conditions are : r_s = 7.5 μm, Z = 10 μm, T_∞ = 25°C, and ambient relative humidity (RH) = 60%.

The effects of changes in pore radius and stratum corneum thickness were also examined. Figures 5.9 and 5.10 show the corresponding results. For Figure 5.9 the pore radius (r_s) was varied from 5 to 15 μm. The curves for Q_A and Q_{Apr} are approximately linear, while for Q_{Asc} the curve concaves slightly downward. Slopes for the first two curves are approximately 18 and 15 g/hr-μm respectively. The ratio of Q_{Apr}/Q_A increases from 51% at $r_s = 5$ μm to 69% at $r_s = 15$ μm.

Figure 5.10 presents the water loss rates as a function of stratum corneum thickness (Z). Z was varied from 5 to 18 μm, which is a typical range for most body surfaces. For the palms and soles, Z ranges between 400 to 600 μm. To include these two regions an one-dimensional approach would not be justified. Therefore the present analysis does not apply to the palms and soles. As expected, Q_{Asc} increases as the stratum corneum becomes thicker. The relationship is slightly non-linear. Water loss directly from the pore (Q_{Apr}), however, is reduced by the increase in Z. The net effect on Q_A is a moderate rise with an increase in Z.

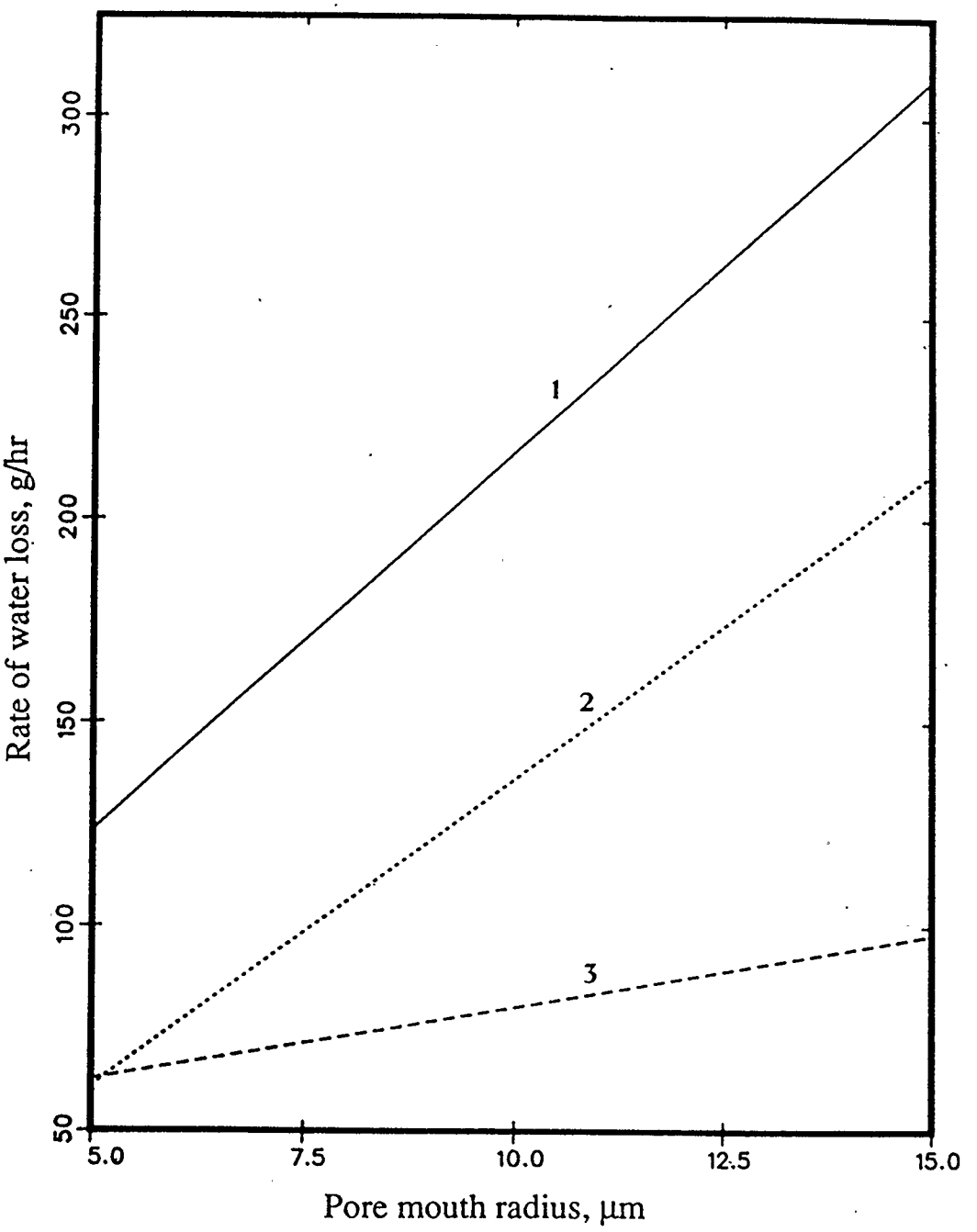

Figure 5.9 : Estimated rates of water loss from 3 million eccrine sweat glands vs. pore mouth radius when the meniscus is displaced to the skin surface. Curve 1 - Q_A; curve 2 - Q_{Apr}; curve 3 - Q_{Asc}; The conditions are : Z = 10 μm, T_s = 32°C, T_∞ = 25°C, and RH = 60%.

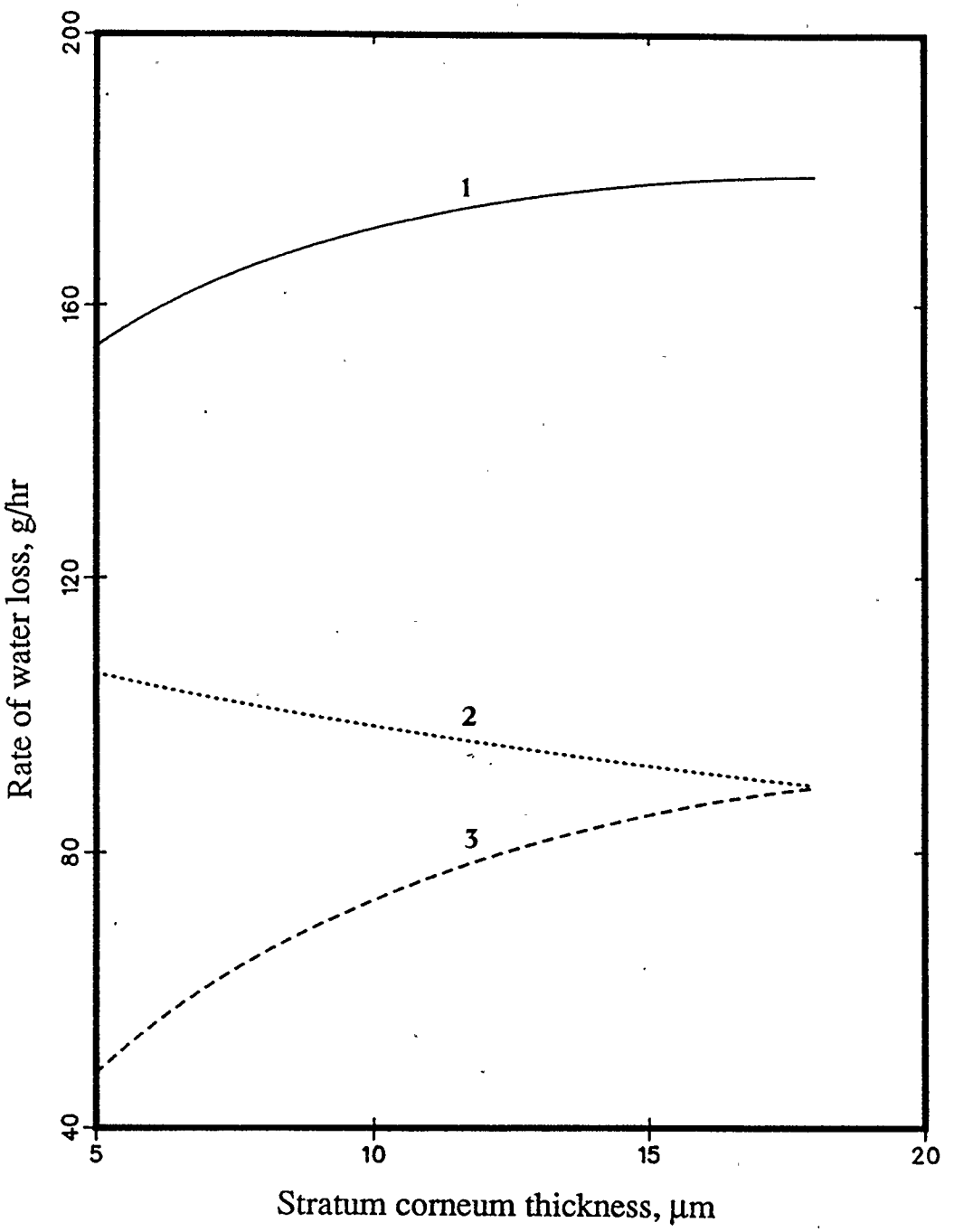

Figure 5.10 : Estimated rates of water loss from 3 million eccrine sweat glands vs. stratum corneum thickness when the meniscus is displaced near to the skin. Curve 1 - Q_A; curve 2 - Q_{Apr}; curve 3 - Q_{Asc}; The conditions are : $r_s = 7.5$ μm, $T_s = 32°C$, $T_\infty = 25°C$ and RH 60%.

CHAPTER SIX

DISCUSSION

The foregoing results demonstrate that direct evaporation of water from the very dilute sweat solutions within eccrine sweat gland ducts could account for most of the insensible water loss through the skin. The analysis provides a rational, physically and physiologically consistent basis for the suggestion advanced earlier by Mali (1956) and others through deductions from experimental observations. The inclusion of anatomical features of the eccrine glands and physiological conditions in the skin into the model served to demonstrate why the numerous attempts to correlate insensible perspiration rates only to the ambient temperature and relative humidity have not been successful. Kerslake's (1972) plot of insensible water loss rates versus vapor pressure difference, as discussed in Chapter 3, shows that a substantial amount of insensible perspiration persists as the vapor pressure difference between water at the skin surface temperature and moisture in ambient air approaches zero. This is consistent with the model that the water evaporates at a temperature higher than at the skin surface and that such water is not bound in a hydrophilic matrix such as the stratum corneum.

The current model, however, is not completely general since heat transfer and insensible water loss from the skin surface have been decoupled in the analysis. The fluxes of water vapor through eccrine ducts embedded in a non-isothermal domain

with a steady temperature profile have been calculated. To effect solutions, temperatures at the site of vapor production had to be specified and the location of the meniscus prescribed. The fact that the free water surfaces within the duct could attain such temperatures were justified with calculations involving the physiological cutaneous temperature profiles and the arrangement of the vessels. In order to predict the water loss rates for living skins, the dynamic characteristics of the secretory coils of the glands, the vascular blood flow and heat transfer rates to the ambient would need to be established. These activities are altered by stimuli such as ambient temperatures, hormonal concentrations and the emotional state of an individual in a complex manner. The heat transfer and water loss rates from exposed surfaces of the body may be higher than would be obtained from the same surfaces were the whole body exposed to the same ambient conditions. Sympathetic and parasympathetic controls are involved for maintaining the core body temperatures, thus reported rates of insensible perspiration exhibit large fluctuations at the same site under similar or slightly different conditions. Reliable computational predictions would have to involve, in addition to the above considerations, the population densities of the sweat glands over the body surfaces, the dimensions and geometry of the glands and the activity levels of the secretory coils.

The foregoing results show a water loss rate of between 1 to 150 g/hr at an ambient temperature of 25°C and a relative humidity of 60%. Experimental values for insensible perspiration range between 1 to 90 g/hr (Kuno, 1956; Lamke et al., 1977; Nilsson, 1977; Grice, 1980). The process of transepidermal water loss

appears relatively insignificant.

Lumped transport properties such as diffusive coefficients or permeability constants (Scheuplein, 1978; Blank et al., 1984) of the stratum corneum were the data estimated for the analysis. The actual magnitude of the transport properties may be different from such estimates based on reported data. The anisotropy of the skin layers has been recognized but reliable measurements of the properties for such domain are rare.

The rate of water loss has been shown to depend largely on the location of meniscus within the eccrine duct (Figure 5.2). For the case of a retracted meniscus the calculations were performed up until the sweat level was at 750 μm along the duct lumen from the dermo-epidermal boundary, approximately the bottom end of the stratum corneum layers. For those so called "active" sweat glands, periodic discharge of sweat droplets has been observed (Randall, 1946; Dole and Thaysen, 1953; Nicolaidis and Savidjian, 1972). These glands may discharge sweat to the skin surface more frequently and therefore contribute more to water loss than "inactive glands" which have lower secretory ability.

It has also been shown that insensible perspiration rates decreased linearly as the ambient water vapor content increased (Figures 5.3 and 5.7). The rates of evaporation of water from the stratum corneum surface appears to increase monotonically with ambient vapor pressure (Figure 5.7). The ambient water vapor content would not significantly alter the hydration of stratum corneum unless the difference

between the skin surface temperature and the ambient temperature is small.

The importance of the size of eccrine glands becomes more apparent when the meniscus is displaced near to the skin surface. In Figure 5.9, the rate of water loss is observed to increase linearly with the pore radius. Loss of water from the stratum corneum surface was also seen to increase slightly. A larger surface area is available for sweat to percolate laterally, but effect of increase in area is partly offset by the fact that local water vapor concentrations in the air next to the skin are elevated. The driving potential is hence reduced. The stratum corneum thickness appears to be a minor factor influencing insensible perspiration rates (Figure 5.10).

The pseudo-steady radial concentration profiles in the stratum corneum are shown in Figure 6.1 at two relative humidities, 60 and 100%, at an ambient temperature of 25°C. Both profiles exhibit the same general trend in that they decrease sharply for the first 2 μm from the pore wall. At about 45 μm from the pore periphery, the difference between the local concentration and the concentration at infinity is less than 1%. The assumption that neighbouring glands do not interfere therefore appears justified. Regarding the effect of the presence of hair follicles, these are distributed non-uniformly over the body surfaces and their population has been estimated at two million (Szabo, 1962). Hair follicles are expected to pose no barriers to the lateral dispersion of water through the stratum corneum in the neighbourhood of the eccrine gland pore mouths.

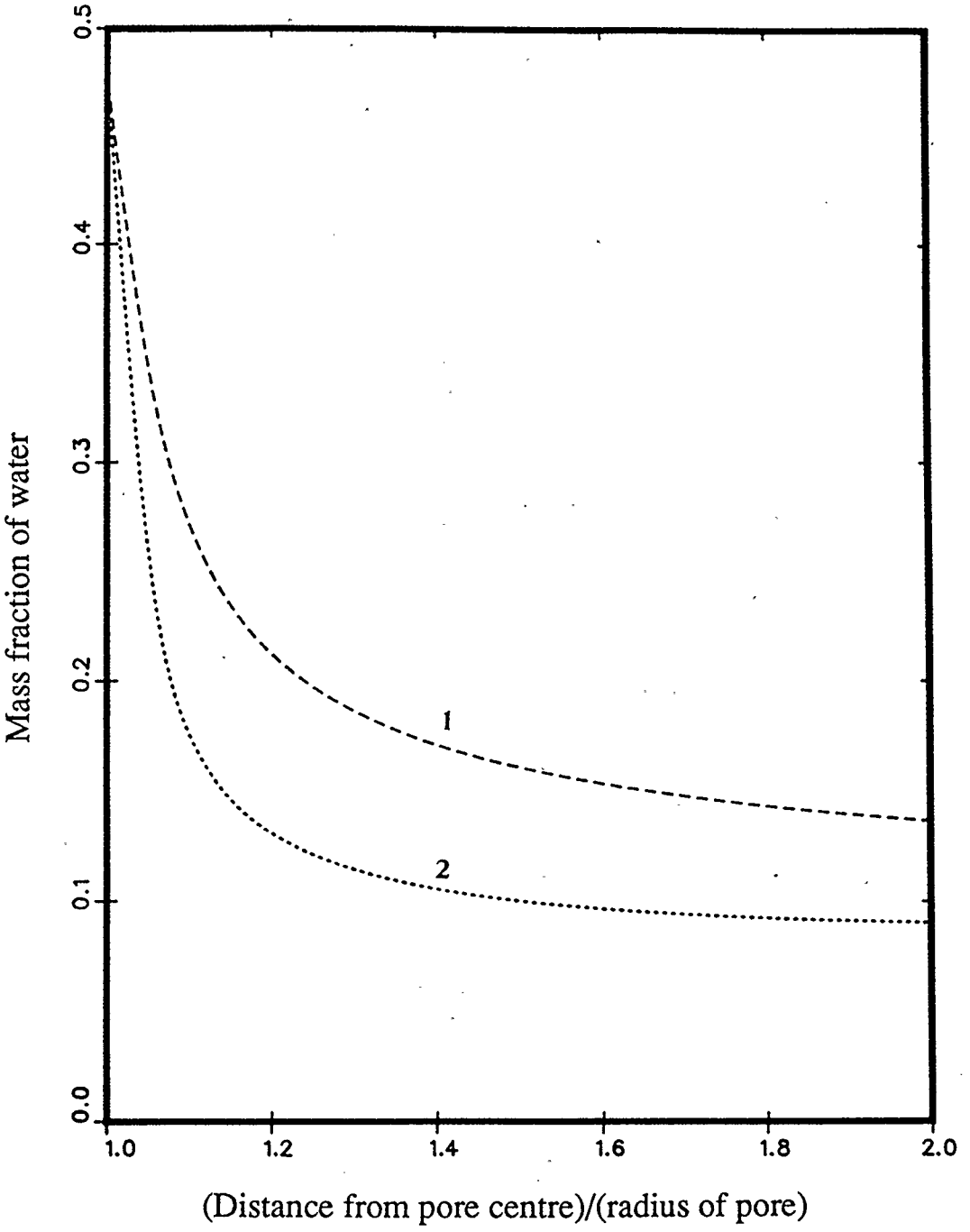

Figure 6.1 : Radial concentration profiles of water in stratum corneum at an ambient relative humidity of 100 (curve 1) and 60% (curve 2). The conditions for both curves are : Z = 10 μm, r_s = 7.5 μm, T_s = 32°C, and T_o = 25°C.

The assumption of a hemispherical surface of the meniscus when it is at the pore mouth should be considered. Brown and Escombe (1900) reported that the diffusion rate of a substance through a large hole was smaller than the total flux through many small holes of equivalent cross-sectional area. Their findings could be explained by the formation of menisci as the aperture of the holes decreases. For a hemispherical geometry, the surface area = $2\pi r^2$, while for a flat circular surface its area = πr^2. Therefore for small holes having hemispherical menisci their total liquid surface area would be double that for a large hole of a equivalent projected area. The concavity or convexity of the meniscus would also be important. For a concave surface, as for water, the average concentration gradient from the meniscus surface would be smaller than that from a flat circular surface of equivalent projected area. Moreover, the equilibrium vapor pressure above a concave surface would be less than that for a flat surface and the flux would be reduced. Of all the three effects, the changes in area appears to be most important to effect the evaporation. The curvature of the surface would not significantly change the vapor pressure until the pore mouth is narrower than ≈0.1 μm. In this study, the rate of water loss was found to increase linearly with the pore mouth diameter. This is in agreement with the experimental findings of Brown and Escombe (1900) for small holes. The concavity becomes important as the meniscus approaches the skin surface. For a meniscus retracted below the skin surface, the diffusion of water vapor is predominantly a one-dimensional problem.

Finally, the results of current calculations show the futility of correlating insensible perspiration rates to the ambient conditions alone without considering the conditions within the skin which contribute to the regulation of water evaporation rates.

CHAPTER SEVEN

CONCLUSIONS

1) Insensible perspiration can solely be explained by evaporation of sweat liquids in the eccrine duct and the process of transepidermal water loss may be relatively insignificant.

2) Insensible perspiration is regulated by conditions internal and external to the skin. These conditions include the temperature profiles within the skin, the flow of warm blood in arterioles surrounding the straight intradermal eccrine duct, the presence of moist microvilli on the periductal surface of the intraepidermal duct, and the ambient temperature and humidity.

3) The microvilli within the intra-epidermal unit may function to regulate both the level of sweat liquids in the duct and the minimum level at which insensible perspiration would occur.

4) Evaporation from the surface of the stratum corneum becomes important when the sweat liquids are displaced to the skin surface. The liquid can then disperse laterally within the layer to function as an extended surface for the evaporative losses. Each gland appears to operate in isolation during insensible perspiration. That is, the vapor concentration fields of neighbouring glands do not interfere. With active production of sweat and flow to the surface, the dispersal of the liquid causes

the skin surface to appear moist and independent activity of the glands would be precluded.

CHAPTER EIGHT

RECOMMENDATIONS

In this work it has been demonstrated by computations that insensible perspiration would be ascribed mainly to the evaporation of sweat in eccrine ducts. A major assumption in the analysis is that the evaporative loss would be supplied continuously and sufficiently from the secretory coil. This still remains to be demonstrated experimentally. Individual eccrine sweat glands has been successfully isolated (Sato and Dobson, 1970; Sato et al., 1971; Sato, 1973; Sato and Sato, 1983) and chemically induced to sweat. These studies focused on the reabsorption process of various ions in the coiled and straight duct and the relation of sweating to gland size. Further studies in this direction, such as inducing sweat with various amounts of chemical agents, may provide information on the secretory rate at rest.

To investigate the relative contributions of transepidermal water loss, the *in vivo* concentration profile of water from the base of stratum corneum to the surface needs to be specified. Simon et al. (1981) have reported that such profiles can be obtained by photoacoustic spectroscopy method. However, no significant results have yet been reported. The transport properties of stratum corneum are also needed. Blank et al. (1984) obtained experimental diffusivity values for the epidermis treated as an anisotropic homogeneous domain at four different ambient conditions. Such studies should be expanded to recognize the anisotropic structures of

the stratum corneum and the malphigii layer.

REFERENCES

Adams, T. and Vaughan, J.A.; 1965 - Human eccrine sweat gland activity and palmer electrical skin resistance, **J. Appl. Physiol. 20,** 980-983.

Adams, T.; 1966 - Characteristics of eccrine sweat gland activity in the footpad of the cat, **J. Appl. Physiol. 21,** 1004-1012.

Albert, R.E. and Palmes, E.D.; 1951 - Evaporative rate patterns from small skin areas as measured by an infrared gas analyzer, **J. Appl. Physiol. 4,** 208-214.

Anderson, R.L., Cassidy, J.M., Hansen, J.R., and Yellin, W.; 1973 - Hydration of Stratum Corneum, **Biopolymers 12,** 2789-2802.

Altman, P.L. and Dittmer, D.S.; 1971 - **Respiration and Circulation,** Federation of American Societies for Experimental Biology.

Baker, H. and Kligman, A.M.; 1967 - Measurement of transepidermal water loss by electrical hygrometry, **Arch. Derm. 96,** 441-452.

Bazett, H.C. and McGlone, B.; 1927 - Temperature gradients in the tissues in man **Am. J. Physiol. 82,** 415-451.

Benedict, F.G. and Root, H.F.; 1926 - Insensible perspiration : its relation to human physiology and pathology, **Arch. Int. Med. 38,** 1-35.

Berenson, G.S. and Burch, G.E.; 1951 - Studies of diffusion of water through dead human skin : the effect of different environmental states and of chemical alterations of the epidermis, **Am. J. Trop. Med. 31,** 842-853.

Bettley, F.R. and Grice, K.A.; 1965 - A method for measuring the transepidermal water loss and a means of inactivating sweat glands, **Br. J. Derm. 77,** 627-635.

Bettley, F.R. and Grice, K.A.; 1967 - The influence of ambient humidity on transepidermal water loss, **British J. Der. 78,** 575-581.

Bickford, R.G.; 1937 - The mechanism of local sweating in response to faradism; **Clinical Science 3,** 337-341.

Bird R.B., Stewart, W.E. and Lightfoot, E.N.; 1960 - **Transport Phenomenon,** J. Wiley & Sons, N.Y.

Blank, I.H.; 1952 - Factors which influence the water content of the stratum corneum, **J. Invest. Derm. 18,** 433-440.

Blank, I.H.; 1953 - Further observations on factors which influence the water content of the stratum corneum, **J. Invest. Derm. 21,** 259-271.

Blank, I.H., Moloney, J., Emslie, A.G., Simon, I., and Apt, C.; 1984 - The diffusion of water across the stratum corneum as a function of its water content **J. Invest. Derm. 82,** 188-194.

Brown, H.T. and Escombe, F.; 1900 - Static diffusion of gases and liquids in relation to the assimilation of carbon and translocation in plants, **Phil. Trans. Roy. Soc. series B 193,** 223-291.

Buettner, K.; 1953 - Diffusion of water and water vapor through human skin, **J. Appl. Physiol. 6,** 220-242.

Buettner, K.; 1959 - Diffusion of liquid water through human skin, **J. Appl. Physiol. 14,** 261-268.

Bullard, R.W.; 1971 - Studies on human sweat gland duct filling and skin hydration, **J. Physiol. 63,** 218-221.

Burch, G.E. and Sodeman, W.A.; 1943 - Regional relationships of rate of water loss in normal adults in a subtropical climate, **Am. J. Physiol. 138,** 603-608.

Burch, G.E. and Winsor, T.; 1944 - Rate of insensible perspiration (diffusion of water) locally through living and through dead human skin, **Arch. Int. Med. 74,** 437-444.

Burch, G.E. and Winsor, T.; 1946 - Diffusion of water through dead plantar, palmar and torsal human skin and through toe nails, **Arch. Derm. Syph. 53,** 39-41.

Cage, G.W. and Dobson, R.L.; 1965 - Sodium secretion and reabsorption in the human eccrine sweat gland, **J. Clin. Invest. 44,** 1270-1276.

Caro, C.G., Pedley, T.J., Schroter, R.C. and Seed, W.A.; 1978 - **The mechanics of the circulation,** Oxford Univ. Press.

Crank, J.; 1979 - **The Mathematics of Diffusion,** Oxford Univ. Press.

Dole, V.P. and Thaysen, J.H.; 1953 - Variation in the functional power of human sweat glands, **J. Exptl. Med. 98,** 129-144.

Dubois, D. and Dubois, E.F.; 1916 - A formula to estimate the approximate surface area if height and weight be known, **Arch. Int. Med. 17,** 863-871.

El-Shimi, A.F. and Princen, H.M.; 1977 - Some aspects of the stratum corneum-organic solvent system, **J. Soc. Cosmet. Chem. 28,** 243-257.

El-Shimi, A.F. and Princen, H.M.; 1978 - Diffusion characteristics of water vapor in some keratins, **Colloid Polymer Sci. 256,** 209-217.

Felsher, Z. and Rothman, S.; 1945 - The insensible perspiration of the skin in hyperkeratotic conditions, **J. Invest. Derm. 6,** 271-278.

Fitch, C.W. and Korones, S.B.; 1984 - Heat shield reduces water loss, **Archives of Disease in Childhood 59,** 886-888.

Goodman, A.B. and Wolf, A.V.; 1969 - Insensible water loss from human skin as a function of ambient vapor concentration, **J. Appl. Physiol. 26,** 203-207.

Grice, K.A. and Bettley, F.R.; 1966 - Inhibition of sweating by poldine

methosulphate - Its use for measuring insensible perspiration, **Br. J. Derm. 77,** 627-640.

Grice, K.A. and Bettley, F.R.; 1967 - Skin water loss and accidental hypothermia in psoriasis, ichthyosis and erythroderma, **Br. Med. J. 4,** 195-199.

Grice, K., Sattar, H., Sharratt, M., and Baker, H.; 1971 - Skin temperature and transepidermal water loss, **J. Invest. Derm. 57,** 108-110.

Grice, K., Sattar, H., and Baker, H.; 1972 - The effect of ambient humidity on transepidermal water loss, **J. Invest. Derm. 58,** 343-346.

Grice, K.A.; 1980 - Transepidermal water loss, **The physiology and pathophysiology of the skin (Jarrett A.,ed) 6,** 2116-2143.

Hammarlund, K., Nilsson, G.E., Oberg, P.A. and Sedin, G.; 1977 - Transepidermal water loss in newborn infants - I. Relation to ambient humidity and site of measurement and estimation of total transepidermal water loss, **Acta Paediatr. Scand. 66,** 553-562.

Hammel, H.T. and Scholander, P.F.; 1976 - **Osmosis and tensile solvent,** Springer-Verlag, Berlin.

Hancock, W., Whitehouse, A.G.R. and Haldane, J.S.; 1929 - The loss of water and salts through the skin, and the corresponding physiological adjustments, **Proc. Roy. Soc. Lond. s.B.105,** 43-59.

Hardy, J.D.; 1934 - The radiation of heat from the human body. II. A comparison of some methods of measurement, **J. Clin. Invest. 13,** 605-614.

Hardy, J.D., Milhorat, A.T. and Dubois, E.F.; 1941 - Basal metabolism and heat loss of young women at temperatures from 22 °C. to 35 °C., **J. Nutrition 21,** 383-404.

Hashimoto, K.; 1978 - The Eccrine Gland, **The Physiology and Pathophysiology of the Skin (Jarrett,A.,ed.) Vol. 5** 1544-1567.

Hattingh, J.; 1972 - The correlation between transepidermal water loss and the thickness of epidermal components, **Comp. Biochem. Physiol. 43A,** 719-722.

Hibbs, R.G.; 1958 - The fine structure of human eccrine sweat glands, **Am. J. Anat. 103,** 201-209.

Holbrook, K.A. and Odland, G.F.; 1974 - Regional differences in the thickness (cell layers) of the human stratum corneum : an ultrastructural analysis, **J. Invest. Derm. 62,** 415-422.

Holmes, K.R. and Adams, T.; 1975 - Epidermal thermal conductivity and stratum corneum hydration in cat footpad, **Am. J. Physiol. 228,** 1903-1908.

Holyoke, J.B. and Lobitz, W.C.; 1952 - Histologic variations in the structure of human eccrine sweat glands, **J. Invest. Derm. 18,** 147-167.

Imokawa, G. and Hattori, M.; 1985 - A possible function of structural lipids in the

water-holding properties of the strtum corneum, **J. Invest. Derm. 84,** 282-284.

Jarrett, A.; 1973 - The epidermis and its relations with the dermis, **The Physiology and Pathophysiology of the Skin (Jarrett, A., ed.) Vol. 1** 3-42.

Jarrett, A.; 1980 - Introduction: The permeability barrier, **The Physiology and Pathophysiology of the Skin (Jarrett, A., ed.) Vol. 6** 2111-2114.

Jeje, A.; 1987 - An analysis on non-equilibrium water fluxes in eccrine ducts, **Abstract, Proc. Physiol. Soc. Lond., J. Physiol. 388,** 40.

Jeje, A. and Koon, D.; 1987 - An analysis on the rates and regulation of insensible water loss through the eccrine sweat glands, **J. Appl. Physiol. (Submitted)**

Jurgensen, E.; 1924 - Mikrobeobachtungen der Schweissekretion der Haut des Menschen unter Kontrastfarbung, **Deutsches Arch. fur klin. Medizin 144,** 193-201 and 257-284.

Kays, W.M. and Crawford, M.E.; 1980 - **Convective Heat and Mass Transfer,** McGraw-Hill, N.Y.

Keenan, J.H.; 1970 - **Thermodynamics,** M.I.T. Press, Cambridge, Mass.

Kerslake, D.McK.; 1972 - **The stress of hot environments,** Cambridge University Press.

Kligman, A.B.; 1964 - The biology of the stratum corneum, **The Epidermis**

(Montagna,W. & Lobitz, Jr.W.C., eds) Ch.20, 387-452 Academic Press, N.Y. and London.

Kuno, Y.; 1956 - **Human Perspiration,** Charles C. Thomas Publ., Springfield, Illn.

Lamke, L.O. and Wedin, B.; 1971 - Water evaporaton from normal skin under different environmental conditions, **Arch. Derm. Vener., Stockh. 51,** 111-119.

Lamke, L.O., Nilsson, G.E. and Reithner, H.L.; 1977 - Insensible perspiration from the skin under standardized environemntal conditions, **Scand. J. Clin. Lab. Invest. 37,** 325-331.

Leider, M. and Buncke, C.M.; 1954 - Physical dimensions of the skin, **Arch. Derm. & Syph. 69,** 563-569.

Lever, W.F. and Lever, G.S.; 1949 - Histology of the Skin, **Histopathology of the Skin** 8-22, J.D. Lippincott Co., Philadelphia.

Lloyd, D.P.C.; 1959 - Secretion and reabsorption in sweat glands, **Proc. Nat. Acad. Sci. 45,** 405-409.

Lloyd, D.P.C.; 1961 - Action potential and secretory potential of sweat glands, **Proc. Nat. Acad. Sci. 47,** 351-362.

Lobitz, Jr.W.C., Holyoke, J.B. and Montagna, W.; 1954 - The epidermal eccrine sweat duct unit: A morphologic and biologic entity, **J. Invest. Derm. 22,** 157-158.

Mali, J.W.H.; 1956 - The transport of water through the human epidermis, **J. Invest. Derm. 27,** 451-469.

Mangos, J.; 1973 - Transductal fluxes of Na, K, and water in the human eccrine sweat gland, **Am. J. Physiol. 224,** 1235-1240.

Mathias, C.G.T., Wilson, D.M. and Maibach, H.I.; 1981 - Transepidermal water loss as a function of skin surface temperature, **J. Invest. Derm. 77,** 219-220.

Mendelson, E.S.; 1936 - Measurement of the superficial temperature gradient in man, **Am. J. Physiol. 114,** 642-647.

Miller, D.L., Brown, A.M. and Artz, E.J.; 1981 - Indirect measures of transepidermal water loss **Bioengineering and the Skin (Marks, R. & Payne, P.A., eds.)** MTP Press Limited, 161-171.

Montagna, W., Ellis, R.A. and Silver, A.F.; 1962 - The Eccrine Sweat Glands, **Advances in the Biology of Skin, Vol 3 ,** Pergamon Press, N.Y.

Montagna, W. and Parakkal, P.F.; 1974 - **The Structure and Function of Skin,** Academic Press, N.Y.

Montgomery, I., Jenkinson, D.M., Elder, H.Y., Czarnecki, D. and MacKie, R.M.; 1984 - The effects of thermal stimulation on the ultrastructure of the human atrichial sweat gland. I. The fundus, **Brit. J. Derm. 110,** 385-397.

Moserova, J. and Behounkova-Houskova, E.; 1979a - Evaporative water loss in partial skin loss in the first 24 hours, **Scand. J. Plast. Reconstr. Surg. 13,** 49-51.

Moserova, J. and Behounkova-Houskova, E.; 1979b - Temporary skin substitutes and evaporative water loss, **Scand. J. Plast. Reconstr. Surg. 13,** 143-145.

Nicolaidis, S. and Sivadjian, J.; 1972 - High-frequency pulsatile discharge of human sweat glands : myoepithelial mechanism, **J. Appl. Physiol. 32,** 86-90.

Nielson, B.; 1969 - Thermoregulation in rest and exercise, **Acta. Physiologica Scandinavia, Suppl. 323,** 1-74.

Nilsson, G.E.; 1977 - Measurement of water exchange through skin, **Med. & Biol. Eng. & Comput. 15,** 209-218.

Odland, G.F.; 1983 - Structure of the Skin, **Biochemistry and Physiology of the Skin (Goldsmith, L.A., ed.) Vol 1** 1-63.

Onken, H.D. and Moyer, C.A.; 1963 - The water barrier in human epidermis, **Arch. Derm. 87,** 584-590.

Perry, R.H. and Chilton, C.H.; 1973 - **Chemical Engineers' Handbook (5th ed.)** McGraw-Hill.

Pinkus, H.; 1939 - Notes on the anatomy and pathology of the skin appendages, **J. Invest. Derm. 2,** 175-186.

Pinson, E.A.; 1942 - Evaporation from human skin with sweat glands inactivated, **Am. J. Physiol. 137,** 492-503.

Prottey, C.; 1977 - Investigation of functions of essential fatty acids in the skin, **Br. J. Derm. 97,** 29-33.

Randall, W.C.; 1946 - Sweat gland activity and changing patterns of sweat secretion on the skin surface, **Am. J. Physiol. 147,** 391-398.

Reader, S.R. and Whyte, H.M.; 1951 - Tissue temperature gradients, **J. Appl. Physiol. 4,** 396-402.

Richardson, H.B.; 1926 - Clinical calorimetry : the effect of the absence of sweat glands on the elimination of water from the skin and lungs, **J. Biol. Chem. 67,** 397-411.

Robbins, C.R. and Fernee, K.M.; 1983 - Some observations on the swelling of human epidermal membrane, **J. Soc. Cos. Chem. 34,** 21-34.

Rothman, S.; 1954 - **Physiology and Biochemistry of the Skin,** Univ. Chicago Press.

Ryan, T.J.; 1973 - Structure, pattern and shape of the blood vessels of the skin, **The physiology and pathophysiology of the skin (Jarrett, A., ed.) Vol 2** 577-625.

Sato, K. and Dobson, R.L.; 1970 - Enzymatic basis for the active transport of

sodium in the duct and secretory portion of the eccrine sweat gland, **J. Invest. Derm. 55,** 53-56.

Sato, K. and Dobson, R.L., and Mali, J.W.H.; 1971 - Enzymatic basis for the active transport of sodium in the eccrine sweat gland. Localization and characterization of Na-K-adenosine triphostase, **J. Invest. Derm. 57,** 10-16.

Sato, K.; 1973 - Sweat induction from an isolated eccrine sweat gland, **Am. J. Physiol. 225,** 1147-1152.

Sato, K., Nishiyama, A. and Kobayashi, M.; 1979 - Mechanical properties and functions of the myoepithelium in the eccrine sweat gland, **Am. J. Physiol. 237,** C177-C184.

Sato, K. and Sato, F.; 1983 - Individual variations in structure and function of human eccrine sweat gland, **Am. J. Physiol.** R203-R208.

Sauer, P.J.J., Dane, H.J. and Visser, H.K.A.; 1984 - Influence of variations in the ambient humidity on insensible water loss and thermoneutral environment of low birth weight infants, **Acta. Paediatr. Scand. 73,** 615-619.

Scheuplein, R. and Blank, I.H.; 1971 - Permeability of the skin, **Physiol. Revs. 51,** 702 -721.

Scheuplein, R.; 1978 - Percutaneous Absorption, **The Physiology and Pathophysiology of the Skin (Jarrett A., ed.) Vol. 5** 1669-1754.

Schwarz, V. and Simpson, I.M.N.; 1985 - Is salt reabsorption in the human sweat duct subject to control ? **Clinical Science 68,** 441-447.

Simon, I.; Emslie, A.G.; Apt, C.M.; Blank, I.H.; and Anderson, R.R.; 1981 - Determination *in vivo* of water concentration profile in human stratum corneum by a photoacoustic method, **Bioengineering and the Skin (Marks, R. and Payne, P.A.; eds.)** 187-195.

Smith, G.D.; 1965 - **Numerical solution of partial differential equations,** Oxford Univ. Press, London.

Sodeman, W.A. and Burch, G.E.; 1944 - Regional variations in water loss from the skin of diseased subjects living in a subtropical climate, **J. Clin. Invest. 23,** 37-43.

Soderstrom, G.F. and Dubois, E.F.; 1917 - Clinical calorimetry : the water elimination through skin and respiratory passages in health and disease, **Arch. Int. Med. 19,** 931-957.

Solomon, E.P. and Davis, P.W.; 1983 - **Human Anatomy and Physiology,** CBS College Publishing.

Spencer, T.S., Linamen, C.E., Akers, W.A. and Jones, H.E.; 1975 - Temperature dependence of water content of stratum corneum, **Brit. J. Derm. 93,** 159-164.

Spruit, D. and Malten, K.E.; 1969 - Humidity of the air and water vapor loss of the skin, **Dermatologica 138,** 418-421.

Stockdale, M.; 1978 - Water diffusion coefficients versus water activity in stratum corneum: a correlation and its implications **J. Soc. Cosmet. Chem. 29,** 625-639.

Stromberg, B., Oberg, P.A. and Sedin, G.; 1983 - Transepidermal water loss in newborn infants : X. Effects of central cold-stimulation and evaporation rate and skin blood flow, **Acta. Paediatr. Scand. 72,** 735-739.

Sunderman, F.W.; 1941 - Persons lacking sweat glands : hereditary ectodermal dysplasia of the anhidrotic type, **Arch. Int. Med. 67,** 846-854.

Szabo, G.; 1962 - The number of eccrine sweat glands in human skin, **Advances in Biology of Skin (Montagna, W., Ellis, R.A. and Silver, A.F., eds.) Vol. 3** 1-5.

Tagami, H., Kanamaru, Y., Inoue, K., Suehisa, S., Inoue, F., Iwatsuki, K., Yoshikuni, K., and Yamada, M.; 1982 - Water sorption-desorption test of the skin *in vivo* for functional assessment of the stratum corneum, **J. Invest. Derm. 78,** 425-428. 65-72.

Thomson, W.; 1871 - On the equilibrium of vapor at a curved surface of liquid, **Philosophical Magazine 42,** 448-452.

Treager, R.; 1966 - **Physical Functions of the Skin,** Academic Press, New York.

Upshaw, B.Y. and Montgomery, H.; 1949 - Hereditary anhidrotic ectodermal dysplasia : a clinical and pathologic study, **Arch. Derm. & Syph. 60,** 1170-1183.

Vasti, A.; 1932 - The insensible water loss through the skin, **Am. J. Physiol. 102,** 60-70.

Vrentas, J.S., Duda, J.L. and Bargeron, K.G.; 1966 - Effect of axial diffusion of vorticity on flow development in circular conduits: part I. numerical solutions **A.I.Ch.E.J. 12,** 837-844.

Wagner, M.H.; 1975 - Developing flow in circular conduits: transition from plug flow to tube flow, **J. Fluid. Mech. 72,** 257-268.

Walkley, K.; 1972 - Bound water in stratum corneum measured by differential scanning calorimetry, **J. Invest. Derm. 59,** 225-227.

Weast, R.C.; 1976 - **CRC Handbook of Chemistry and Physics (5th ed.)**

Wiley, F.H. and Newburgh, L.H.; 1931 - The relationship between the environment and the basal insensible loss of weight, **J. Clin. Invest. 10,** 689-701.

Winsor, T. and Burch, G.E.; 1944 - Differential roles of layers of human epigastric skin on diffusion rate of water, **Arch. Int. Med. 74,** 428-436.

Wu, P.Y.K. and Hodgman, J.E.; 1974 - Insensible water loss in preterm infants: changes with postnatal development and non-ionising radiant energy, **Pediatrics 54,** 704-707.

Wurster, D.E. and Yang, K.H.; 1982 - Water vapor sorption and desorption by

human callus I: Anomalous diffusion, **J. Pharma. Sci. 71,** 1235-1238.

Zelickson, A.S.; 1961 - Electron microscopic study of epidermal sweat duct, **Arch. Derm. 83,** 106-111.

APPENDIX A

A.1. Derivation of the diffusion equation with the meniscus retracted

For the case of a retracted meniscus the one-dimensional steady diffusion equation was given as equation (4.1). Rewrite the equation :

$$S\,N_{Az}|_{z} - S\,N_{Az}|_{z+\Delta z} = 0 \tag{A.1}$$

where

$$N_{Az} = -c\,D_{AB}\,\frac{dx_A}{dz} + x_A\,(N_{Az} + N_{Bz}). \tag{A.2}$$

For stationary B, i.e., $N_{Bz} = 0$,

$$N_{Az} = \frac{-c\,D_{AB}}{1 - x_A}\,\frac{dx_A}{dz}\ . \tag{A.3}$$

The local cross-sectional area (S_z) is given as:

$$S_z = \pi\,r^2 \tag{A.4}$$

where

$$r = r_o\,(1 + (\gamma - 1)\,\frac{z}{L}). \tag{A.5}$$

On substituting equations (A.3) - (A.5) into (A.1) and simplifying, one obtains

$$\frac{d}{dz}\left\{\frac{1}{(1 - x_A)}\,\frac{dx_A}{dz}\left[1 + (\gamma - 1)\,\frac{z}{L}\right]^2\right\} = 0. \tag{A.6}$$

Equation (A.6) may be expanded to:

$$-\left[1+(\gamma-1)\frac{z}{L}\right]^2 \frac{d^2 ln(1-x_A)}{dz^2}$$

$$-\frac{d\, ln(1-x_A)}{dz}\frac{2(\gamma-1)}{L}\left[1+(\gamma-1)\frac{z}{L}\right] = 0. \qquad \text{(A.7)}$$

Equation (A.7) is simplified by adopting the following transformations:

$$\Psi = 1+(\gamma-1)\left(\frac{z}{L}\right) \qquad \text{(A.8)}$$

and

$$\Gamma = \ln(1-x_A). \qquad \text{(A.9)}$$

When equations (A.8) and (A.9) are substituted into (A.7), one obtains:

$$\left[\frac{\gamma-1}{L}\right]^2\left[\Psi^2\frac{d^2\Gamma}{d\Psi^2}+2\Psi\frac{d\Gamma}{d\Psi}\right]=0. \qquad \text{(A.10)}$$

The solution to (A.10) is of the form

$$\Gamma = \frac{C_1}{\Psi}+C_2 \qquad \text{(A.11)}$$

for $\Psi \neq 0$ where C_1 and C_2 are integration constants to be determined from the boundary conditions.

The boundary conditions to the problem are:

(i) at $z = z_o$, $\Psi = \gamma_o$; $x_A = x_{Ao}$ and $\Gamma = \ln(1\text{-}x_{Ao})$

(ii) at $z = L$, $\Psi = \gamma$; $x_A = x_{A\infty}$ and $\Gamma = \ln(1\text{-}x_{A\infty})$

On substituting the two boundary conditions into equation (A.11), one obtains:

$$\ln (1 - x_{Ao}) = \frac{C_1}{\gamma_o} + C_2 \tag{A.12}$$

and

$$\ln (1 - x_{A\infty}) = \frac{C_1}{\gamma} + C_2. \tag{A.13}$$

Equations (A.12) and (A.13) can be combined to give:

$$\ln \left(\frac{1 - x_{A\infty}}{1 - x_{Ao}}\right) = \frac{C_1}{\gamma} - \frac{C_1}{\gamma_o}. \tag{A.14}$$

The constant C_1 is then recovered in an explicit form as:

$$C_1 = \frac{1}{\gamma^{-1} - \gamma_o^{-1}} \ln \left[\frac{1 - x_{A\infty}}{1 - x_{Ao}}\right]. \tag{A.15}$$

To solve for C_2, equation (A.13) may be re-written and combined with equation (A.15) to yield:

$$C_2 = \ln (1 - x_{A\infty}) - \frac{\gamma^{-1}}{\gamma^{-1} - \gamma_o^{-1}} \ln \left[\frac{1 - x_{A\infty}}{1 - x_{Ao}}\right] \tag{A.16}$$

or

$$C_2 = \frac{\gamma^{-1}}{\gamma^{-1} - \gamma_o^{-1}} \ln (1 - x_{Ao}) - \frac{\gamma_o^{-1}}{\gamma^{-1} - \gamma_o^{-1}} \ln (1 - x_{A\infty}). \tag{A.17}$$

Finally, equations (A.15) and (A.17) are incorporated into (A.11) to yield the solution:

$$(1 - x_A)^{\gamma^{-1} - \gamma_o^{-1}} = \frac{(1 - x_{A\infty})^{\Psi^{-1} - \gamma_o^{-1}}}{(1 - x_{Ao})^{\Psi^{-1} - \gamma^{-1}}}. \tag{A.18}$$

On rearranging equation (A.18), one obtains:

$$x_A = 1 - exp\,(Fx) \tag{A.19}$$

where

$$Fx = \frac{(\Psi^{-1} - \gamma_o^{-1}) \ln (1 - x_{A\infty}) - (\Psi^{-1} - \gamma^{-1}) \ln (1 - x_{Ao})}{(\gamma^{-1} - \gamma_o^{-1})}. \tag{A.20}$$

Therefore

$$\frac{dx_A}{dz} = \exp (Fx) \frac{\Psi^{-2}}{\gamma^{-1} - \gamma_o^{-1}} \frac{(\gamma - 1)}{L} \ln \frac{(1 - x_{A\infty})}{(1 - x_{Ao})}. \tag{A.21}$$

The molar flux (N_{Az}) given by (A.3) can thus be evaluated using (A.21). Together with equations (A.4) and (A.5) the rate of water loss at any position can be calculated.

A.2. The Temperature Profile Along The Eccrine Duct

The steady energy equation for blood flow in an arteriole was given as equation (4.14). Rewrite the equation :

$$\frac{\partial^2 T}{\partial r^2} + \frac{1}{r} \frac{\partial T}{\partial r} = \frac{u}{\nu} \frac{\partial T}{\partial z}. \tag{A.22}$$

Equation (A.22) is non-dimensionalized as follows:

$$r^+ = \frac{r}{r_w} \tag{A.23}$$

$$z^+ = \frac{z / r_w}{\mathrm{Re}\, Pr} \tag{A.24}$$

$$\Theta = \frac{T - T_i(z)}{T_e - T_i(z)}. \tag{A.25}$$

For hydrodynamically fully developed laminar flow, the assumption of a parabolic profile is valid, i.e.:

$$u = 2\,\bar{u}\left[1 - \frac{r^2}{r_w{}^2}\right] \tag{A.26}$$

or

$$u^+ = 2\,(1 - r^{+2}). \tag{A.27}$$

On substituting equations (A.23) to (A.25) and (A.27) into (A.23), one would obtain the following partial differential equation:

$$\frac{\partial^2\Theta}{\partial r^{+2}} + \frac{1}{r^+}\frac{\partial\Theta}{\partial r^+} = (1 - r^{+2})\left[\frac{\partial\Theta}{\partial z^+} + \frac{1-\Theta}{T_e - T_t}\frac{\partial T_t}{\partial z^+}\right]. \tag{A.28}$$

Equation (A.28) is to be solved numerically. To permit the use of finite difference discretization, we define the following:

$$r^+ = i\,\Delta r, \qquad i = 0,1,2,...K \tag{A.29}$$

$$z^+ = j\,\Delta z, \qquad j = 0,1,2,...L. \tag{A.30}$$

Equation (A.28) is discretized using standard first and second order central difference approximations. The discretized form of (A.28) is given as:

$$\frac{\Theta_{i+1,j} - 2\Theta_{i,j} + \Theta_{i-1,j}}{(\Delta r)^2} + \frac{1}{i\,\Delta r}\frac{\Theta_{i+1,j} - \Theta_{i-1,j}}{2\Delta r}$$
$$-\left[1 - (i\,\Delta r)^2\right]\left[\frac{\Theta_{i,j+1} - \Theta_{i,j-1}}{2\Delta z} + \frac{1-\Theta_{i,j}}{T_e - T_t}\frac{\partial T_t}{\partial z^+}\right] = 0 \tag{A.31}$$

$$\text{for } i = 1,2,...K-1 \text{ and } j = 1,2,...L-1.$$

T_t is given explicitly as a function of z^+. For the calculations, T_t is given as fol-

lows:

$$T_t = T_\zeta \times 2.8 + 33.45°C \tag{A.32}$$

and

$$T_\zeta = B_1\,\zeta + B_2\,\zeta^2 + B_3\,\zeta^3 + B_4\,\zeta^4 + B_5\,\zeta^5 + B_6\,\zeta^6 + B_7\,\zeta^7 + B_8\,\zeta^8 + B_9\,\zeta^9 + B_{10}\,\zeta^{10} + B_{11}\,\zeta^{11} + B_{12}\,\zeta^{12} + B_{13}\,\zeta^{13} + B_{14}\,\zeta^{14} + B_{15}\,\zeta^{15} + B_{16}\,\zeta^{16} \tag{A.33}$$

where

$$\zeta = \frac{(0.0312 - z)}{0.024} \tag{A.34}$$

and

$$B_1 = 0.8104795862 \tag{A.35}$$

$$B_2 = -0.8931565940 \times 10^1 \tag{A.36}$$

$$B_3 = 0.1720781941 \times 10^2 \tag{A.37}$$

$$B_4 = 0.3096866878 \times 10^3 \tag{A.38}$$

$$B_5 = -0.1996415564 \times 10^4 \tag{A.39}$$

$$B_6 = 0.5497932093 \times 10^4 \tag{A.40}$$

$$B_7 = -0.8511643761 \times 10^4 \tag{A.41}$$

$$B_8 = 0.7653425618 \times 10^4 \tag{A.42}$$

$$B_9 = -0.3207143979 \times 10^4 \tag{A.43}$$

$$B_{10} = -0.9131275894 \times 10^3 \tag{A.44}$$

$$B_{11} = 0.2178100752 \times 10^4 \tag{A.45}$$

$$B_{12} = -0.1466533072 \times 10^4 \tag{A.46}$$

$$B_{13} = 0.5603827989 \times 10^3 \tag{A.47}$$

$$B_{14} = -0.1295281504 \times 10^3 \tag{A.48}$$

$$B_{15} = 0.1695281504 \times 10^2 \tag{A.49}$$

$$B_{16} = -0.9692922774\,. \tag{A.50}$$

Relevant boundary conditions are:

(i) at r = 0 or $r^+ = 0$,

$$\frac{\partial T}{\partial r}\Big|_{r=0} = 0 \tag{A.51}$$

or

$$\frac{\partial \Theta}{\partial r^+}(0, z^+) = 0. \tag{A.52}$$

We have

$$\lim_{r^+ \to 0}\left[\frac{1}{r^+}\frac{\partial \Theta}{\partial r}\right] = \frac{\partial^2 \Theta}{\partial r^{+2}} \tag{A.53}$$

by L'Hospital's rule. Therefore equation (A.28) becomes:

$$2\frac{\partial^2 \Theta}{\partial r^{+2}} = \frac{\partial \Theta}{\partial z^+} + \frac{1-\Theta}{T_e - T_t}\frac{\partial T_t}{\partial z^+} \tag{A.54}$$

and its finite difference form is given as:

$$4\frac{\Theta_{1,j} - \Theta_{0,j}}{\Delta r^2} - \frac{\Theta_{0,j+1} - \Theta_{0,j-1}}{2\Delta z} - \frac{1-\Theta_{0,j}}{T_e - T_t}\frac{\partial T_t}{\partial z^+} = 0. \tag{A.55}$$

(ii) at r = r_w or $r^+ = 1$,

$$-k_B \frac{\partial T}{\partial r}\Big|_{r=r_w} = h_w\,(T_w - T_t) \tag{A.56}$$

or

$$-\frac{\partial \Theta}{\partial r^+}(1,z^+) = Bi\ \Theta(1,z^+) \tag{A.57}$$

where

$$Bi = \frac{h_w r_w}{k}. \tag{A.58}$$

Equation (A.57) can be discretized as follows:

Let

$$\frac{\Theta_{K-1,j} - \Theta_{K+1,j}}{2\Delta r} = Bi\ \Theta_{K,j} \tag{A.59}$$

where $\Theta_{K+1,j}$ is a fictitious point. On rearranging (A.59), one obtains:

$$\Theta_{K+1,j} = \Theta_{K-1,j} - 2\Delta r\ Bi\ \Theta_{K,j}. \tag{A.60}$$

Equation (A.31) can therefore be applied with the term $\Theta_{K+1,j}$ replaced everywhere using expression (A.60).

(iii) at z = 0 or $z^+ = 0$,

$$T|_{z=0} = T_e \tag{A.61}$$

or

$$\Theta(r^+,0) = 1 \tag{A.62}$$

and hence

$$\Theta_{i,0} = 1. \tag{A.63}$$

In addition, to permit the use of the numerical procedure, at j = L, the first order partial derivative with respect to z^+ in equation (A.28) is discretized using backward difference approximation. The finite difference equation is given as:

$$\frac{\partial \Theta}{\partial z^+} = \frac{\Theta_{i,L-2} - 4\Theta_{i,L-1} + 3\Theta_{i,L}}{2\Delta z}. \tag{A.64}$$

Equation (A.31) can then be applied with the appropriate replacement using expression (A.64).

As a result of the above discretization scheme, we end up with (K+1)×(L+1) finite difference equations. These equations can be solved by the method of Newton-Raphson.

Let

$$k = i \times (L+1) + j$$

then for

$$k = 0,1,2,...K \times (L+1) + L,$$

define

$$J_{k,l} = \frac{\partial F_k}{\partial \Theta_{i,j}} \tag{A.65}$$

for

$$i = 0,1,2,...K$$

and

$$j = 0,1,2,...L$$

and

$$l = i \times (L+1) + j$$

where F_k is the finite difference equation at point (i,j).

In matrix form, the following set of linear equations is obtained,

$$\left[J \right] \left[\Delta\Theta \right] = - \left[F \right] \tag{A.66}$$

The Jacobian matrix J is evaluated by numerical differentiation. Since both J and F are known, the matrix $\Delta\Theta$, which is the change or increment in Θ at every iteration, can subsequently be calculated. To obtain values of $\Delta\Theta$, equations resulting from the matrix representation of (A.66) are solved by the method of successive-over-relaxation (SOR). The form of equations to be solved is given as:

$$d\Theta_k^{\,*} = (1-\omega)\, d\Theta_k + \frac{\omega \left[-\sum_{l=0}^{k-1} J_{k,l}\, d\Theta_l - \sum_{l=k+1}^{K\times(L+1)+L} J_{k,l}\, d\Theta_l - F_k \right]}{J_{k,k}} \tag{A.67}$$

where ω is the relaxation factor.

For successful convergence, the stopping criterion is given as:

$$\left| d\Theta_k^{\,*} - d\Theta_k \right| \le 1 \times 10^{-8} \tag{A.68}$$

for every point (i,j). Once satisfactory convergence is achieved for SOR. The calculated values, $d\Theta$'s, are checked whether another operation of Newton-Raphson is required. In this case the criterion is given as:

$$\left| \frac{d\Theta_k}{d\Theta_k + \Theta_k} \right| \le 1 \times 10^{-6} \tag{A.69}$$

for every point (i,j). Once the criterion is fulfilled, results are considered satisfactory. The bulk or mixed-cup temperature for the blood at any longitudinal distance (z) can be calculated using the following equation:

$$T_b = \frac{1}{A\bar{u}} \int_A u(r)\, T(r,z)\, dA \tag{A.70}$$

where A is the cross-sectional area of the blood vessel. For a parabolic profile, equation (A.70) can be written as:

$$T_b = \frac{2}{A} \int_A \left[1 - (\frac{r}{r_w})^2 \right] T(r,z)\, dA. \tag{A.71}$$

The solution to equation (A.71) is approximated by numerical integration using composite trapezoidal scheme.

Let

$$f(r,z) = \left[1 - (\frac{r}{r_w})^2 \right] T(r,z)\, dA \tag{A.72}$$

then, for any distance z, the composite trapeizoidal scheme is given as:

$$\int_0^{r_w} f(r,z)\, dr = \frac{r_w\, \Delta r}{2} \left[f(0,z) + f(r_w,z) + 2 \sum_{i=1}^{K-1} f(r_i,z) \right]. \tag{A.73}$$

The bulk temperature (T_b) can therefore be estimated.

Temperature, °C	Vapor pressure, mmHg
25	23.756
26	25.209
27	26.739
28	28.349
29	30.043
30	31.824
31	33.695
32	35.663
33	37.729
34	39.898
35	42.175

Table A.1 : Vapor pressure of liquid water (Perry and Chilton, 1973).

APPENDIX B

B.1. Case when meniscus is displaced to skin surface

For the case when the meniscus is at the pore rim, the governing diffusion equation was given as equation (4.23). Rewrite the equation :

$$\frac{1}{r\,(x_A-1)}\frac{\partial x_A}{\partial r}+\frac{1}{(x_A-1)}\frac{\partial^2 x_A}{\partial r^2}-\frac{1}{(x_A-1)^2}\left[\frac{\partial x_A}{\partial r}\right]^2 + \frac{1}{(x_A-1)}\frac{\partial^2 x_A}{\partial z^2}-\frac{1}{(x_A-1)^2}\left[\frac{\partial x_A}{\partial z}\right]^2=0 \qquad \text{(B.1)}$$

$$\text{for } 0\le r\le\infty,\ 0\le z\le\infty.$$

Equation (B.1) is to be solved numerically by finite difference approximations. It is necessary to split the domain into three regions, with a different co-ordincate system for each region. The form of equation (B.1) as applied to each region and the appropriate boundary conditions are now described.

Region 1 : $0\le \mathrm{r}\le f_r, f_z\le \mathrm{z}\le r_s$;

where

$$f_r{}^2+(r_s-f_z)^2=r_s{}^2. \qquad \text{(B.2)}$$

The functions f_r and f_z describe the curved boundary. For this region equation (B.1) can be directly applied. The finite difference equation is given as:

$$\frac{1}{i\Delta r(X_{i,j}-1)}\frac{X_{i+1,j}-X_{i-1,j}}{2\Delta r}+\frac{1}{(X_{i,j}-1)}\frac{X_{i+1,j}-2X_{i,j}+X_{i-1,j}}{\Delta r^2}$$
$$-\frac{1}{(X_{i,j}-1)^2}\left[\frac{X_{i+1,j}-X_{i-1,j}}{2\Delta r}\right]^2+\frac{1}{(X_{i,j}-1)}\frac{X_{i,j+1}-2X_{i,j}+X_{i,j-1}}{\Delta z^2}$$
$$-\frac{1}{(X_{i,j}-1)^2}\left[\frac{X_{i,j+1}-X_{i,j-1}}{2\Delta z}\right]^2=0 \qquad \text{(B.3)}$$

where

$$\Delta r=\frac{r_s}{K} \qquad \text{(B.4)}$$

and

$$\Delta z=\frac{r_s}{L} \qquad \text{(B.5)}$$

where K and L are the number of intervals in the r- and z- directions respectively.

The curved surface remains to be defined properly. The key is to find $imax_j$, the column subscript of the rightmost grid point in each row j, and $jmin_i$, the row subscript of the bottom-most grid point in each column i. i.e.,

$$r=i\Delta r, \quad i=0,1,2,...imax_j \qquad \text{(B.6)}$$

and

$$z=j\Delta z, \quad j=jmin_i,...L-2,L-1,L \qquad \text{(B.7)}$$

where

$$imax_j=\sqrt{L^2-(L-j)^2} \qquad \text{(B.8)}$$

raised to the next higher integer, and

$$jmin_i=K-\sqrt{K^2-i^2} \qquad \text{(B.9)}$$

truncated to the next lower integer. Equation (B.3) can be generally applied to any grid point in the region $1 \le i \le (imax_j\text{-}2)$ and $(jmin_i\text{+}2) \le j \le L$. For grid points $(imax_j\text{-}1,j)$ or $(i,jmin_i\text{+}1)$, an alternative treatment has to be applied. The approach is now described.

Referring to Figure B.1, in which point A is located adjacent to the boundary points C and E, we write out the appropriate Taylor's expansions for points B, C, D, and E, neglecting third order terms or higher:

$$X_B = X_A + \Delta z\, X_z + \frac{(\Delta z)^2}{2} X_{zz}. \tag{B.10}$$

$$X_C = X_A - q\,\Delta z\, X_z + \frac{(q\,\Delta z)^2}{2} X_{zz}. \tag{B.11}$$

$$X_D = X_A - \Delta r\, X_r + \frac{(\Delta r)^2}{2} X_{rr}. \tag{B.12}$$

$$X_E = X_A + p\,\Delta r\, X_r + \frac{(p\,\Delta r)^2}{2} X_{rr}. \tag{B.13}$$

X_r, X_{rr}, X_z, and X_{zz} are the first and second order partial derivatives with respect to r and z respectively. Equations (B.10) and (B.11) can be combined to give:

$$X_z = \frac{1}{\Delta z}\left[\frac{q}{q+1} X_B - \frac{q-1}{q} X_A - \frac{1}{q(q+1)} X_C\right] \tag{B.14}$$

and

$$X_{zz} = \frac{2}{(\Delta z)^2}\left[\frac{X_B}{q+1} - \frac{X_A}{q} + \frac{X_C}{q(q+1)}\right]. \tag{B.15}$$

Again, by manipulating equations (B.15) and (B.16), one would obtain the

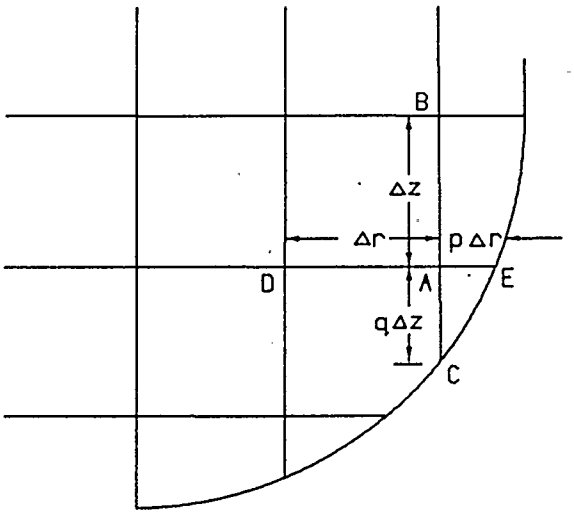

Figure B.1 : Schematic diagram illustrating the treatment of irregular boundaries in discretization.

following expressions:

$$X_r = \frac{1}{\Delta r}\left[\frac{1}{p(1+p)}X_E - \frac{1-p}{p}X_A - \frac{p}{1+p}X_D\right] \tag{B.16}$$

and

$$X_{rr} = \frac{2}{(\Delta r)^2}\left[\frac{X_E}{p(1+p)} - \frac{X_A}{p} + \frac{X_D}{1+p}\right]. \tag{B.17}$$

Equation (B.1) together with expressions (B.14) to (B.17) are applied to all boundary points such as A. A similar treatment can be applied to the interface between region 1 to 2 and between region 2 to 3. The details would not be given here.

The boundary condition at the centre-line can be approached as follows:

$$at\ r = 0, \qquad \frac{\partial x_A}{\partial r} = 0.$$

By L'Hospital's rule, we have:

$$\lim_{r\to 0}\left[\frac{1}{r}\frac{\partial x_A}{\partial r}\right] = \frac{\partial^2 x_A}{\partial r^2} \tag{B.18}$$

and equation (B.1) becomes:

$$\frac{2}{(x_A-1)}\frac{\partial^2 x_A}{\partial r^2} + \frac{1}{(x_A-1)}\frac{\partial^2 x_A}{\partial z^2} - \frac{1}{(x_A-1)^2}\left[\frac{\partial x_A}{\partial z}\right]^2 = 0. \tag{B.19}$$

On discretizing equation (B.19), one obtains:

$$\frac{4}{(X_{0,j}-1)}\frac{X_{1,j}-X_{0,j}}{(\Delta r)^2} + \frac{1}{(X_{0,j}-1)}\frac{X_{0,j+1,}-2X_{0,j}+X_{0,j-1}}{(\Delta z)^2}$$

$$-\frac{1}{(X_{0,j}-1)^2}\left[\frac{X_{0,j+1}-X_{0,j-1}}{2\Delta z}\right]^2=0. \tag{B.20}$$

Region 2 : $0 \le r \le r_s, r_s \le z \le \infty$;

Let

$$\beta = \tanh(bz) \tag{B.21}$$

then

$$\frac{\partial x_A}{\partial z} = b(1-\beta^2)\frac{\partial x_A}{\partial \beta} \tag{B.22}$$

and

$$\frac{\partial^2 x_A}{\partial z^2} = b^2(1-\beta^2)^2\frac{\partial^2 x_A}{\partial \beta^2} - 2b^2\beta(1-\beta^2)\frac{\partial x_A}{\partial \beta} \tag{B.23}$$

$$\text{for} \quad tanh(br_s) \le \beta \le 1.$$

Standard central difference approxiamtions can be applied to the transformed co-ordinate β-. The grid sizes are defined as:

$$\Delta r = \frac{r_s}{K} \tag{B.24}$$

or

$$r = i\,\Delta r \qquad i = 0,1,2,...K \tag{B.25}$$

and

$$\Delta\beta = \frac{1-tanh(br_s)}{M} \tag{B.26}$$

or

$$\beta = j\,\Delta\beta + tanh(br_s) \quad j = L, L+1, ...L+M. \tag{B.27}$$

The boundary condition at r = 0 can be treated the same way as for region 1. For z = ∞, we have

$$X_{i,L+M} = x_{A\infty}. \tag{B.28}$$

Region 3 : $r_s \le r \le \infty$, $r_s \le z \le \infty$;

For this region, both the r- and z- co-ordinates need to be transformed. The procedure is the same for the transformation of the z- co-ordinate in region 2. For completeness, the transformation of the r- co-ordinate is now described.

Let

$$\alpha = tanh(ar) \tag{B.29}$$

therefore

$$\frac{\partial x_A}{\partial r} = a(1-\alpha^2)\frac{\partial x_A}{\partial \alpha} \tag{B.30}$$

and

$$\frac{\partial^2 x_A}{\partial r^2} = a^2(1-\alpha^2)^2\frac{\partial^2 x_A}{\partial \alpha^2} - 2a^2\alpha(1-\alpha^2)\frac{\partial x_A}{\partial \alpha}. \tag{B.31}$$

The grid sizes are defined as:

$$\Delta\alpha = \frac{1 - tanh(ar_s)}{N} \tag{B.32}$$

or

$$\alpha = i\,\Delta\alpha + tanh(ar_s) \quad \text{for } i = K, K+1, \ldots K+N \tag{B.33}$$

and

$$\Delta\beta = \frac{1 - tanh(br_s)}{M} \tag{B.34}$$

or

$$\beta = j\,\Delta\beta + tanh(br_s) \quad \text{for } j = L, L+1, \ldots L+M. \tag{B.35}$$

The boundary condition at j = K, the surface of the stratum corneum, expressed in equation (4.32) is given as:

$$\frac{1}{r}\frac{\partial(rn_{Ar})}{\partial r} + \frac{n_{Az}}{Z} = 0. \tag{B.36}$$

On expanding the equation, one obtains:

$$\rho_s D_s \left\{ \frac{1}{r(1-\omega_{As})}\frac{\partial \omega_{As}}{\partial r} + \frac{1}{(1-\omega_{As})^2}\left[\frac{\partial \omega_{As}}{\partial r}\right]^2 + \frac{1}{(1-\omega_{As})}\frac{\partial^2 \omega_{As}}{\partial r^2}\right\}$$
$$+ \frac{MW_A\, c\, D_{AB}}{Z\,(1-x_A)}\frac{\partial x_A}{\partial z} = 0 \tag{B.37}$$

where both ρ_s and D_s are functions of ω_{As}. The discretized form of the equation is given as:

$$\frac{a^2(1-\alpha^2)}{(1-W_{i,L})}\left\{\left[\frac{1}{\tanh^{-1}(\alpha)} - 2\alpha\right]\rho_{si}\, D_{si}\,\frac{W_{i+1,L} - W_{i-1,L}}{2\Delta\alpha}\right.$$
$$+ \frac{(1-\alpha^2)}{(1-W_{i,L})}\rho_{si}\, D_{si}\left[\frac{W_{i+1,L} - W_{i-1,L}}{2\Delta\alpha}\right]^2$$
$$+ (1-\alpha^2)\left[\rho_{si+1/2}\, D_{si+1/2}\,\frac{W_{i+1,L} - W_{i,L}}{(\Delta\alpha)^2}\right.$$
$$\left.\left. + \rho_{si-1/2}\, D_{si-1/2}\,\frac{W_{i-1,L} - W_{i,L}}{(\Delta\alpha)^2}\right]\right\}$$
$$- \frac{MW_A\, c\, D_{AB}}{Z\,(1-X_{i,L})}\, b(1-\beta^2)\,\frac{3X_{K,L} - 4X_{K,L+1} + X_{K,L+2}}{2\Delta\beta} = 0. \tag{B.38}$$

where for values of ρ_s and D_s the subscript i+1/2 denotes an arithmetic mean between interval i and i+1, i for the mean between i-1 and i+1, and i-1/2 for the mean between i-1 and i.

The mass fraction of water in stratum corneum, ω_{As}, as a function of mole fraction of water vapor in the ambient, $x_{A\infty}$, is given as:

$$\omega_{As} = B_1 x_{A\infty} + B_2 x_{A\infty}^2 + B_3 x_{A\infty}^3 + B_4 x_{A\infty}^4 + B_5 x_{A\infty}^5 + B_6 x_{A\infty}^6. \quad \text{(B.39)}$$

At $T_s = 30°C$

$$B_1 = 0.1034068387 \times 10^{-3} \quad \text{(B.40)}$$

$$B_2 = 0.1476339588 \times 10^{-2} \quad \text{(B.41)}$$

$$B_3 = -0.1516669269 \times 10^{-2} \quad \text{(B.42)}$$

$$B_4 = 0.6485702778 \times 10^{-3} \quad \text{(B.43)}$$

$$B_5 = -0.1335676134 \times 10^{-3} \quad \text{(B.44)}$$

$$B_6 = 0.1156279760 \times 10^{-4}. \quad \text{(B.45)}$$

At $T_s = 35°C$

$$B_1 = -0.4093281817 \times 10^{-2} \quad \text{(B.46)}$$

$$B_2 = 0.7920811667 \times 10^{-2} \quad \text{(B.47)}$$

$$B_3 = -0.5178442552 \times 10^{-2} \quad \text{(B.48)}$$

$$B_4 = 0.1600164520 \times 10^{-3} \quad \text{(B.49)}$$

$$B_5 = -0.2353842991 \times 10^{-3} \quad \text{(B.50)}$$

$$B_6 = 0.1215036977 \times 10^{-4}. \quad \text{(B.51)}$$

The other two boundary conditions for region 3 are:

$$At\ r=\infty, \qquad \alpha=1; \qquad X_{K+N,j}=x_{A\infty} \tag{B.52}$$

$$At\ z=\infty, \qquad \beta=1; \qquad X_{i,L+M}=x_{A\infty} \tag{B.53}$$

As a consequence, a set of (K+N+1)×(L+M+1) equations is developed for the whole domain. The equations are solved by the method of Newton-Raphson in conjunction with SOR iteration scheme.

Once the results for all grid points are successfully calculated. The rates of water loss from the pore and the stratum corneum surface can be determined.

The rate of water loss from the pore is determined by calculating the rate of water passing through the projected surface at skin surface level. i.e.,

$$Q_{Apr}=2\pi\int_{0}^{r_s} n_{Az}|_{z=r_s}\ r\ dr. \tag{B.54}$$

The amount of water evaporating from the stratum corneum surface is given as:

$$Q_{As}=2\pi\int_{r_s}^{\infty} n_{Az}|_{z=r_s}\ r\ dr. \tag{B.55}$$

Alternatively, Q_{As} is estimated by calculating the amount of water dispersing into the stratum corneum from the pore. This is given as:

$$Q_{As}=2\pi\, r_s\, Z\, n_{Ar}|_{r=r_s}. \tag{B.56}$$

Equations (B.54) to (B.56) are estimated numerically using composite trapeizoidal scheme, as described in appendix A.